Lateral condylar fractures in Thoroughbred racehorses: Investigation of premonitory radiographic changes in distal metacarpal III

Tariq Bin Mohammed Al Zidjali. 2107776
DVet Med, MSc

Submitted in fulfilment of the requirement for

the Degree of Doctor in Philosophy

School of Veterinary Medicine

College of Medical, Veterinary and Life Science

(MVLS)

University of Glasgow
May 2018

Abstract

Reasons for performing this study: Metacarpal/metatarsal III condylar fractures are the most common type of fracture associated with Thoroughbred horseracing in the UK, and the most common reason for euthanasia on the racecourse. Prediction of fracture through quantification of exercise-related radiographic changes could enable modification of horse management to prevent this injury, improving animal welfare and reducing wastage.

Objectives: The general aims were to validate objective radiographic measurement of exercise-related modelling in distal metacarpal III of Thoroughbred racehorses and to explore their utility for fracture prediction by comparing measurements from horses that sustained a fracture of the lateral condyle of distal metacarpal III with those from controls. The initial objective was to establish methods to measure objectively the following variables in distal metacarpal III: condyle opacity, cortical thickness and metaphyseal angle. Radiographic measurements were correlated with equivalent measurements derived from computed tomography (CT) to determine their accuracy. The second objective was to explore the ability of the radiographic measurements to identify horses at risk of fracture. This was done initially by comparing measurements made from radiographs taken at a single time point between Thoroughbred racehorses with and without a lateral condylar fracture, and subsequently by analysis of measurements from series of radiographs obtained prior to and at diagnosis of lateral condylar fracture as part of routine clinical practice. For the final objective, the maximum density of the palmar condyles of distal metacarpal III was determined using a quantitative CT-based technique. Maximum density was compared between horses with fractures and those without, and comparison made with the maximum opacity measured from radiographs, to investigate whether these measurements could be used to identify horses at risk of fracture.

Materials and Methods: Fifty-five metacarpal III bones obtained from Thoroughbred racehorses euthanized on UK racecourses (age range 3-11 years) were divided in to three groups: control (no distal limb fracture, n=30), non-fractured (contralateral limb lateral condylar fracture, n=11) and fractured (lateral condylar fracture, n=14). All limbs were subjected to radiography and computed tomography for measurement of diaphyseal cortical thickness 2.5cm distal to the nutrient foramen (expressed as dorsal cortex:medulla width) and metaphyseal angle (deviation of the metaphysis relative to the diaphysis). Measurement of radiopacity of the medial and lateral condyles was calibrated using an aluminium phantom

(condyle:phantom ratio). Correlation between radiography and CT measurements and comparison of radiography measurements between groups was performed.

For the longitudinal study, medical records of the Singapore Turf Club were reviewed. Thoroughbred racehorses diagnosed with a lateral condylar fracture that had also been radiographed in the previous 24 months were identified and placed in the 'high risk' group (n=16). Horses radiographed and then raced for a minimum of 2 years without suffering a fracture were placed in the 'low risk' group (n=15).

Twenty-seven metacarpal III bones obtained from Thoroughbred racehorses euthanized on UK racecourses (age range 3-10 years) were used in the investigation of maximum density of the palmar condyles. They were divided in to three groups: control (no distal limb fracture, n=10), non-fractured (contralateral limb lateral condylar fracture, n=8), and fracture (lateral condylar fracture, n=9). Computed tomography measurement of condyle density was calibrated using a potassium phosphate phantom to enable comparison between age-matched bones.

Results: Diaphyseal cortical thickness and metaphyseal angle measurements made by radiography and CT were significantly correlated (r=0.74, 0.73; p=0.007, 0.004) but there was no significant difference in measurements between groups. Radiopacity of medial and lateral condyles was significantly greater in non-fracture (0.67±0.04, 0.68±0.04) and fracture (0.82±0.07, 0.68±0.09) groups than the control (0.59±0.08, 0.57±0.09) group (p=0.003). The medial condyle (0.82±0.07) was significantly more radiopaque than the lateral condyle (0.68±0.09) in the fracture group only (p=0.001).

In the longitudinal study, the dorsal cortex was thicker in high risk than low risk horses, the mean ± SD cortical thickness ratio of the high and low risk groups was 1.36 ± 0.26 and 1.08 ± 0.19 respectively (p=0.008). Metaphyseal angle measurement displayed a similar pattern and the difference was statistically significant, the mean ± SD metaphyseal angle of the high and low risk groups was 9.65° ± 2.21 and 6.95° ± 1.65 respectively (p=0.000).

Computed tomography measurement of maximum density of distal metacarpal III, found no significant difference in maximum density of the lateral and medial palmar condyle between groups. There was a significant correlation between age and maximum density of the lateral condyle (r=0.44, p=0.019) and medial condyle (r=0.54, p=0.003).

Conclusions: Objective measurement of dorsal cortical thickness and metaphyseal angle of distal metacarpal III can be performed accurately and precisely using radiography in Thoroughbred horses. Radiographic measurement of condyle opacity was precise but conclusions about the accuracy of this measurement await comparison with an appropriate reference standard.

Increased radiopacity of the distal condyles was identified in horses that sustained lateral condylar fracture. However, this finding was not reflected by data from the horses represented by the clinical radiographs, suggesting that this measurement may not be useful in identifying horses at risk of fracture. Evidence supportive of this conclusion was provided by maximum density measurements made by CT.

Significant differences in dorsal cortical thickness and metaphyseal angle were found between horses that sustained a lateral condylar fracture and horses that underwent radiography for clinical reasons but subsequently raced without fracture, suggesting that these variables could be of value in determining the risk of fracture and merit further investigation.

Acknowledgements

In the name of Allah the most Gracious, the dispenser of grace, “Read in the name of your Lord who created’’ The Holy Quran , Iqra verse (96:1).

There are many people who deserve thanks for their substantial and varied contribution to this PhD thesis, as completion of this PhD was not possible without the guidance and support of several people. Firstly, I would like to express my sincere appreciation of Dr. John Marshall, my primary supervisor for the patient guidance and encouragement he has provided throughout my time as his PhD student. I have been extremely lucky to have a supervisor who has inspired me and cared so much about my work as well as responding to any questions and meeting on a once weekly basis for the first 3 years of my PhD. Similarly I would like to acknowledge Dr. Lance Voute, my secondary supervisor, for his valuable support, guidance and encouragement he has provided throughout to draw the entire thesis hypothesis and objectives together. I would like also to thank Professor Sandy Love for his continuous support. I would also like Professor Tim Parkin who has provided metacarpal III cadaver bones and similarly Dr. Bronte Forbes of the Singapore Turf Club who actively supported this this study by supplying clinical radiographs ofr Thoroughbred horses. Additionally gratitude goes to Mrs. Nicola Brannan who gave me technical support regarding the Computed Tomography scanning and also many thanks to Mr Karol Lewandowski who from the School of Engineering who provided assistance for computed tomography related software analysis. Finally, thanks to Clare Welsh for her initial statistics advice.

I would like to thank the Omani government which provided a PhD scholarship and funded me and this study via the embassy of the Sultanate of Oman in London. This not only for providing the funding which allowed me to under take this research, but also for the continued technical guidance and support.

I must express my gratitude to my parents, who spent their time in looking after me, for their continuous support and encouragement until my father passed away during the last year of this study. My uncle Al Waleed deserve deepest appreciation for his outstanding concern about me. I must express my gratitude to my family in Oman for constant inspiration and support as well as looking after my children Al Waleed and Omar, who experienced all of the up and downs throughout my research time.

Declaration

I hereby declare that this thesis represents my own work that has been done after registration for the degree of PhD in Veterinary Clinical Studies and has not been included in any other thesis previously submitted to this institution.

Signature _____

Printed Name: Tariq Mohamed Al Zidjali

Table of Contents

List of Figures

List of Tables

List of Abbreviations

CT:	Computed Tomography
DP:	Dorsopalmar Projection
DICOM:	Digital Imaging and Communications in Medicine
DC:	Dorsal Cortex
HAL:	Hip Axis Length
LC:	Lateral Condyle
LM:	Lateromedial Projection
MCIII:	Third Metacarpal Bone
MTIII:	Third Metatarsal Bone
MC:	Medial Condyle
MRI:	Magnetic Resonance Imaging (MRI)
M:	Medulla
NSA:	Femoral Neck Shaft Angle
RD:	Radiography
ROI:	Region of Interest
SPSS:	Statistical Package for the Social Sciences
TB:	Thoroughbred

Chapter 1: Investigation of the premonitory radiographic changes in the distal metacarpal III of Thoroughbred racehorses related to lateral condylar fracture

1.1 Introduction

Exercise-related injury to the musculoskeletal system is the most prevalent health problem of Thoroughbred racehorses, resulting in 25%, or more, of horses annually being withdrawn from training for a period (Cogger *et al.*, 2008; Ramzan and Palmer, 2011). In addition, over 75% of the horse deaths that occur as a result of racing are attributed to musculoskeletal injury (Allen *et al.*, 2017; Rosanowski *et al.*, 2017). Injuries to the bony or soft tissue components of the musculoskeletal system occur, and may affect a range anatomical sites although distal limb locations predominate (Cogger *et al.*, 2008; Ramzan and Palmer, 2011; Hill *et al.*, 2015).

Despite the apparent variety of injury type, the accumulation of microdamage in musculoskeletal tissues as a consequence of the high loads and repeated loading cycles produced by training at speed and racing is a feature of the pathogenesis of many of the injuries, for example, fracture of the condyles of distal metacarpal or metatarsal III (Riggs, 1999; Radtke *et al.*, 2003; Stepnik *et al.*, 2004; Parkin *et al.*, 2006), suspensory apparatus failure (Hill *et al.*, 2015) and superficial digital flexor tendonitis (Smith *et al.*, 2002).

Current knowledge of the epidemiology of racehorse musculoskeletal injury is derived predominantly from study of injuries sustained during racing, which lead to the destruction of the animal because of a poor prognosis for treatment (Parkin *et al.*, 2004a). This inclusion criterion therefore means that the injuries recorded are severe. An additional characteristic of these studies is the use of post mortem examination to reach a precise diagnosis. Fewer epidemiological studies of the non-fatal musculoskeletal injuries sustained by racehorses have been performed; these use veterinary examination on the racecourse or during training to obtain data and therefore diagnosis is frequently less precise than can be achieved by post-mortem examination (Peloso, Mundy and Cohen, 1994; Cogger *et al.*, 2008; Ramzan and Palmer, 2011; Reed *et al.*, 2013; Hill *et al.*, 2015).

Articular fractures of the metacarpophalangeal joint (i.e. fractures of the proximal phalanx, condyles of distal metacarpal III or proximal sesamoid bones) are the most common diagnoses for fatal musculoskeletal injuries sustained by Thoroughbred racehorses during racing. This reflects the magnitude of energy generation and dissipation in the region, which is related to soft tissue biomechanics (Clayton *et al.*, 1998), as well as the greater loads experienced by the forelimb compared to the hindlimb. The most frequent specific fracture type differs between racing discipline, racecourse surface and country of jurisdiction. Proximal phalanx fractures are the most common type in UK flat racing on turf, fractures of the lateral condyle of distal metacarpal III in UK National Hunt racing, and biaxial proximal sesamoid bone fractures in UK all weather surface flat racing but when data from all racing disciplines are combined, distal metacarpal III lateral condylar fractures are the most common fatal musculoskeletal injury in UK Thoroughbred racing (Parkin *et al.*, 2004b). Fractures of the lateral condyle of distal metacarpal III or metatarsal III are also the most common serious musculoskeletal injury in flat and jump racing on turf in Victoria, Australia (Boden, *et al*. 2006), and in flat racing on turf and dirt in Japan (Maeda, Hanada and Oikawa, 2016). Metacarpal III fractures (all types) are the most frequent fracture category flat racing on turf and dirt in New York (Mohammed, Hill and Lowe, 1991) and on the same surfaces in Ontario, Canada (Cruz *et al.*, 2007). Proximal sesamoid bone fractures are the most frequent fracture, and metacarpal III fractures (all types) the second most frequent, in racing at Californian racecourses in North America (Johnson *et al.*, 1994).

The prevalence of fractures of the condyles of distal metacarpal III sustained by Thoroughbred racehorses, which are not sufficiently severe to warrant euthanasia of the animal is poorly documented in comparison to fatal fractures. Data from the epidemiological studies performed have ranked this category of metacarpal III fracture as the 5th (Hill *et al.*, 2015) or 6th most common (Ramzan and Palmer, 2011) non-fatal musculoskeletal injury or concluded that the injury occurred at a low incidence (Cogger *et al.*, 2008; Dyson *et al.*, 2008). Further, but indirect, evidence suggesting that non-fatal fractures of the condyles of distal metacarpal III are an important injury in the Thoroughbred racehorse is the numerous journal articles, book chapters, conference presentations in the literature describing their diagnosis and treatment (Rick *et al.*, 1983; Zekas *et al.*, 1999; Richardson, 2012).

The frequency of metacarpal III fractures relates to this bone being the most intensely loaded in the appendicular skeleton (Richardson, 2012). Both single event catastrophic fractures and stress fractures resulting from repeated cyclic loading occur, with the latter being the more common in racehorses. Fractures commonly originate at the articular surface of distal metacarpal III, specifically at the palmar aspect of the parasagittal groove of a condyle because of coalescence of subchondral bone microcracks and failure of repair mechanisms to keep pace with the rate of injury (cumulative adaptive failure) may result in weakness and stress concentration at this location (see pathogenesis section for further discussion). Based on descriptions of fracture morphology from cases submitted to veterinary clinics for treatment, lateral condylar fractures typically extend proximally in the same sagittal plane as the articular defect initially and then deviate laterally towards, and potentially, through the lateral cortex (complete fractures) of the diaphysis of distal metacarpal III (Rick *et al.*, 1983; Ellis, 1994; Bassage and Richardson, 1998; Zekas *et al.*, 1999). Lateral condylar fractures may be short or long.

However, recent careful analysis of radiographs of lateral condylar fractures of distal metacarpal III in a series of Thoroughbred racehorses found that the configuration of a significant proportion did not correspond to the accepted description (Jacklin and Wright, 2012). These fractures originated abaxial to the parasagittal groove, rather than from the groove, suggesting an alternate pathogenesis to cumulative adaptive bone failure for this subset of fractures.

The only published study describing the morphology of fatal lateral condylar fractures of distal metacarpal III in Thoroughbred racehorses found broad similarities to the less severe fractures represented by clinical cases series, although the frequency and severity of comminution and the frequency of concurrent fracture of either the proximal sesamoid bones or the proximal phalanx was greater (Parkin *et al.*, 2006). This is expected given that these injury features are associated with prognosis. All the fractures reported by Parkin *et al* (2006) originated at the parasagittal groove of distal metacarpal III.

Lateral condylar fractures also occur in the hindlimb but are less common than in the forelimb (Rick *et al.*, 1983; Ellis, 1994; Bassage and Richardson, 1998; Zekas *et al.*, 1999). Fractures of the medial condyle of distal metacarpal III or metatarsal III are less common than lateral condylar fractures; they occur at similar frequency in fore and hindlimbs (Rick *et al.*, 1983; Ellis, 1994; Bassage and Richardson, 1998; Zekas *et al.*, 1999). Their length and configuration is different to lateral condylar fractures: medial condylar fractures either

spiral proximally from the articular defect or extend proximally in the same sagittal plane as the defect to the middle third of the diaphysis, where they may then assume an oblique or spiral course; they made extend to the proximal extremity of metatarsal III (Rick *et al.*, 1983; Ellis, 1994; Bassage and Richardson, 1998; Zekas *et al.*, 1999).

Lateral condylar fractures of distal metacarpal III were the focus of the research project described in this thesis. The overall aim of the project was to investigate whether premonitory radiographic or computed tomographic changes related to lateral condylar fracture occur in the distal metacarpal III of Thoroughbred racehorses. Such changes could be used to identify horses at increased risk of fracture and therefore form part of a risk reduction strategy. This would have the potential for significant welfare and economic benefit given the prevalence, and absolute numbers, of metacarpal III lateral condylar fractures in the Thoroughbred racehorse.

1.2 Diagnosis and treatment of lateral condylar fractures of distal metacarpal III

The typical clinical presentation of lateral condylar fractures of distal metacarpal III in the Thoroughbred racehorse is sudden onset of severe lameness when exercising at high speed during training or racing and the concurrent development of metacarpophalangeal joint distension (Richardson, 2012). Lameness may be less severe and take longer to develop when the fracture is short and incomplete. Axial stability of the limb is not compromised unless fracture instability and trauma to the supporting soft tissues is sufficient to result in joint luxation.

Diagnosis is confirmed by radiography, although non-standard view are necessary to examine the palmar aspect of the condyle for comminution and may be necessary to define the main fracture fully (Butler *et al.*, 2011).

Conservative treatment is appropriate for short, incomplete lateral condylar fractures whereas internal fixation using screws inserted using the lag technique is recommended for long incomplete fractures (Zekas *et al.*, 1999), and is required when displacement is present. The prognosis for return to racing in Thoroughbreds following lateral condylar fracture is 70-80% (Richardson, 2012), although it is reduced for complete compared to incomplete fractures (Bassage and Richardson, 1998; Zekas *et al.*, 1999) and when a proximal sesamoid bone fracture is also present (Bassage and Richardson, 1998). The prognosis is more

favourable for metatarsal III lateral condylar fractures compared to metacarpal fractures (Bassage and Richardson, 1998).

The duration of convalescence following fracture before return to racing is prolonged; Zekas et al (, 1999) found that the mean time to return to racing in 118 horses with lateral condylar fractures was 9.4 months. Following return to racing, performance (as measured by earnings) is reduced in the majority of horses (Bassage and Richardson, 1998; Zekas *et al.*, 1999), particularly when metacarpophalangeal joint osteoarthritis is present, the fracture was complete and displaced or articular fragmentation was identified (Bassage and Richardson, 1998).

Although the prognosis for Thoroughbred racehorses to return to racing following metacarpal III lateral condylar fracture is good, the frequency at which the injury occurs means that wastage for the industry is considerable. Additionally, the lengthy convalescence for affected horses and the reduction in performance level for recovered horses contribute to impact of the injury.

1.3 Risk factors for lateral condylar fracture of distal metacarpal III in Thoroughbred racehorses

The design of most epidemiological studies of musculoskeletal injury in Thoroughbred racehorses has limited the conclusions to the incidence or risk factors for injuries in general. Consequently, there are few data on risk factors specific to lateral condylar fractures of distal metacarpal III in Thoroughbred racehorses.

Risk factors for lateral condylar fractures of distal metacarpal III and metatarsal III in Thoroughbred racehorses include training which does not feature galloping exercise, the first year of racing, racing for the first time as a 3 or 4-year-old, longer races, firm or hard going, races with bigger fields and being ridden by an amateur rider (Parkin *et al.*, 2005). The importance of the interaction between the foot and the ground was emphasised by Kane *et al's* study (1996) which found that the use of horseshoes with toe grabs increased the risk of fatal musculoskeletal injury in general in horses racing on dirt in California, and of suspensory apparatus failure and metacarpal III lateral condylar fractures specifically. These findings also suggest a possible association between lateral condylar fracture and injury to the suspensory apparatus. Supporting evidence for this association is provided by the results of post mortem examination of the suspensory ligament of Thoroughbred horses used for

flat racing on turf or dirt on Californian racecourses, which died as a consequence of lateral condylar fracture or suspensory apparatus failure (Hill *et al.*, 2016). Further circumstantial evidence for one musculoskeletal injury predisposing to another is the association between previous identification of a musculoskeletal injury at a veterinary examination and catastrophic musculoskeletal injury (which included lateral condylar fracture) identified in a study of Thoroughbred horses racing on the flat on turf and dirt in Kentucky (Cohen *et al.*, 1999).

Training intensity, stage of racing career and age at first race will affect bone modelling and remodelling and therefore the likelihood of cumulative adaptive bone failure, which is a key feature of the pathogenesis of lateral condylar fractures. Firm or hard going increases the forces experienced by the distal limbs compared to softer going and hence the chance of bone overload and fracture. Race length and size of field reflect time at risk and the amateur rider effect may be the result of reduced proficiency compared to professionals in detecting the early signs of lateral condylar fracture during a race. The association between suspensory ligament branch injury and lateral condylar fracture may relate to the effect of these soft tissue injuries on the forces experienced by the distal metacarpal condyles (Le Jeune *et al.*, 2003) but could be coincidental (i.e. metacarpophalangeal joint hyperextension causes both).

Other risk factors for Thoroughbred racehorse musculoskeletal injury which may be relevant to fracture of the lateral condyle of distal metacarpal III include conformation (Anderson *et al*., 2004), duration of convalescence from injury prior to return to racing (Carrier *et al.*, 1998) and chronic, low grade contralateral limb lameness, although none has been associated specifically with lateral condylar fracture. Conformational abnormalities of the feet and limbs could predispose to fracture by altering the biomechanics of the musculoskeletal system (Harrison *et al.*, 2014). Convalescence is likely to be important in relation to the time required for complete remodelling following bone injury, and chronic, low grade lameness important by causing asymmetrical loading of the forelimbs (Peloso *et al*., 2015).

1.4 Pathogenesis of lateral condylar fractures of distal metacarpal III in Thoroughbred racehorses

Although single event (monotonic) metacarpal III fractures due to extreme overload occur in Thoroughbred racehorses, e.g. caused by a kick, fatigue fractures resulting from repeated cyclic loading is the more common pathogenesis. In the instance of lateral condylar fractures of distal metacarpal III, consistency of origin at the parasagittal groove of the distal palmar

condyle and the identification of pre-fracture pathology is circumstantial evidence for this pathogenesis (Riggs, 1999).

Failure of skeletal adaptation is central to the theory of the pathogenesis of fatigue fractures (Muir *et al.*, 2006, 2008; Martig *et al.*, 2014). Adaptation describes the process by which modelling results in changes in the shape and volume of bones in response to changes in stress to maintain strains at a safe level. In distal metacarpal III, the most obvious evidence of adaptation is progressive sclerosis of the epiphysis in Thoroughbred racehorses entering training (Firth *et al*., 2005) but the process also involves changes to the subchondral bone and overlying articular cartilage (Muir *et al.*, 2006).

If skeletal adaptation is inadequate, bone and cartilage damage result at sites subjected to high loads. Sclerosis of distal metacarpal III does not develop uniformly across the epiphysis, producing a transitional region in the distal palmar condyle between abaxial more dense bone and axial less dense bone (Riggs, Whitehouse and Boyde, 1999a). The change in bone stiffness in this region, which corresponds to the parasagittal groove, will result in a concentration in shear stress during loading leading to high strain. The cartilage over the parasagittal groove is relatively thin compared to other areas of the condyles, which may compound the vulnerability of this site to damage (Muir *et al.*, 2008). Differences in geometry of the lateral and medial condyles are likely to influence the stress experienced by the condyles and could be a reason for the greater prevalence of lateral fractures (Kawcak *et al.*, 1999). Similarly, the effect of suspensory ligament injury on lateral condyle stress (Le Jeune *et al.*, 2003; Merritt *et al.*, 2010) may explain the epidemiological association between suspensory apparatus injury and lateral condylar fracture (Hill *et al.*, 2016).

Concentrations of microcrack arrays have consistently been identified in the calcified cartilage and subchondral bone of the parasagittal grooves of distal metacarpal III of Thoroughbred racehorses with contralateral limb lateral condylar fractures suggesting that these represent an early feature of bone injury at this site (Radtke *et al.*, 2003; Muir *et al.*, 2006, 2008). Coalescence of microcracks is thought to lead to the development of a dominant crack, which then propagates as the result of micromotion induced by the high stress created by high speed running. Thirty mm^2 has been identified as a threshold for a microcrack array to promote the formation of a dominant crack (Dubois *et al.*, 2014). Extension of the dominant crack through the subchondral bone plate renders distal metacarpal III vulnerable to catastrophic failure because the orientation of epiphyseal trabeculae predominantly in the sagittal plane offers limited resistance to fracture in the same plane (Currey, 2003).

Repair of subchondral bone microcracks is likely to be ineffective without a rest from high speed running because of rate of damage accumulation will overwhelm the remodelling response (Martig *et al.*, 2014). The effects of chronic repetitive injury on blood supply to the subchondral bone of the palmar condyles of distal metatarsal III may also limit healing (Santschi, 2008). In the early stages of remodelling, localised resorption of damaged bone may promote fracture development as a consequence of increased subchondral bone porosity (Riggs, Whitehouse and Boyde, 1999b); in the later stages, subchondral bone sclerosis resulting in increase in stiffness may have a similar effect (Muir *et al.*, 2006).

1.5 Diagnostic imaging of lateral condylar fractures of distal metacarpal III - radiography, scintigraphy, computed tomography, MRI

Reducing exposure to risk factors is clearly an important strategy in the reduction in the incidence of lateral condylar fractures in Thoroughbred racehorses. Fracture detection at an early, reversible, stage of their pathogenesis however, would make an important contribution both at the individual horse level and at the population level through guiding the design of effective prevention measures, for example, training regimens which represent an appropriate compromise between the development of fitness and fracture risk (Verheyen *et al.*, 2006).

Currently, diagnostic imaging offers the best prospects for early fracture detection. Radiography however, is limited by the effects of tissue superimposition when imaging in two-dimensions, which prevent visualisation of pathology at the subchondral microcrack stage (Morgan *et al.*, 2006; O'Brien *et al.*, 2011; Gaschen and Burba, 2012). The poor resolution of scintigraphy means that this modality is ineffective at discriminating between developing fractures and other subchondral bone disease, such as palmar osteochondral disease (Trope, Anderson and Whitton, 2011).

The three-dimensional skeletal imaging modalities, computed tomography (CT) and MRI, have both shown the potential to detect early fracture pathology (O'Brien *et al.*, 2011; Gaschen and Burba, 2012). Computed tomography has been extensively used in *ex vivo* studies, in which it consistently demonstrated the ability to detect features indicative of inadequate distal metacarpal III bone adaptation and subchondral microcracks, especially when high resolution systems were used (Dubois *et al.*, 2014). Similarly, MRI is theoretically capable of identifying features of inadequate distal metacarpal III bone

adaptation which would be useful for fracture prevention (Tranquille, Parkin and Murray, 2012).

Significant disadvantages of CT and MRI are high cost and limited availability, and that most CT systems and higher field strength MRI require the patient to be anaesthetised. Recovery from general anaesthesia of a horse at risk of lateral condylar fracture would require special precautions to avoid catastrophic bone failure. Whilst radiography does not suffer from these disadvantages, it has been assumed that the sensitivity and specificity of radiography is insufficient for this imaging modality to be suitable for the detection of early fracture pathology. However, improved knowledge of the bone changes stimulated by exercise in Thoroughbred horses, and the image analysis techniques currently available, are reasons to test this assumption.

Radiography-based techniques with the potential for detection of fracture of the lateral condyle at an early stage of pathology include analysis of the radiopacity of distal metacarpal III epiphysis, measurement of the thickness of the dorsal cortex of metacarpal III and measurement of the angle of the metaphysis of distal metacarpal III relative to the diaphysis.

Sclerosis of distal metacarpal III in Thoroughbred racehorses entering training, which reflects adaption of this bone to the stress produced by high speed running, is seen radiographically as increased opacity. Although a general measurement of radiopacity may not be informative, measurement of change in opacity in the region of the distal palmar parasagittal groove would be if it mirrored a critical change material properties.

Change in the thickness of the cortices of metacarpal III in young Thoroughbred racehorses has been recognised as adaptive response, reflecting the loading pattern of the bone (Davies, 2002). The facility with which cortical thickness can be measured radiographically and its apparent sensitivity to alteration in training load (Firth *et al.*, 2011), makes this parameter a potential indicator of the status of metacarpal III adaptation.

The geometrical configuration of the proximal phalanx, proximal sesamoid bones and metacarpal III at the metacarpophalangeal joint affect how these bones are loaded (Merritt and Davies, 2010), with deviation from the ideal likely to have consequences for joint health. This is illustrated in the human by the association between morphological features of the proximal femur, e.g. neck-shaft angle, and femoral neck fracture risk in osteoporotic patients (Gnudi *et al.*, 2004; Dinçel *et al.*, 2008; Muir *et al.*, 2008; Maeda *et al.*, 2011). In a similar

way, measurement of aspects of metacarpophalangeal joint geometry may allow identification of Thoroughbred racehorses at risk of lateral condylar fracture.

1.6 Project outline

This project aimed to investigate whether x-radiation based diagnostic techniques (namely, radiography and computed tomography) could be used to identify Thoroughbred racehorses at particular risk of lateral condylar fracture of distal metacarpal III.

Novel aspects of the work were the use of objective image analysis techniques for radiography, the availability of a longitudinal radiographic dataset for a population of Thoroughbred racehorses and the approach used to measure density in CT images of distal metacarpal III.

The *overall hypothesis* for this project was that specific radiographic changes in metacarpal III of Thoroughbred racehorses relating to lateral condylar fracture could be monitored to predict fracture. In initial experiments, radiographic measurements of opacity, cortical thickness and angle of the metaphysis of distal metacarpal III relative to the diaphysis from Thoroughbred racehorse cadavers were compared with computed tomographic measurements to determine the correlation between the techniques in order to validate the radiographic technique.

Specific hypotheses were that condyle radiopacity, cortical thickness and metaphyseal angle of the distal metacarpal III could be used to predict lateral condylar fracture. These were investigated in experiments that measured the parameters in bones with and without fractures and in clinical radiographs prior to and at diagnosis of lateral condylar fracture. In a final experiment, the density of the palmar condyles of distal metacarpal III specimens with and without lateral condylar fracture were measured using a computed tomography based technique to explore the hypothesis that maximum density is altered in fractured bones.

The experiments designed to test the specific hypotheses are described in three chapters in the thesis:

Objective analysis of distal metacarpal III of Thoroughbred racehorses using radiography and computed tomography. Radiographic measurement of condyle opacity, cortical thickness and metaphyseal angle were validated by comparison with the same variables

measured by computed radiography. These measurements were then used to analyse differences in the radiographic appearance of distal metacarpal III in horses with lateral condylar fracture and controls without.

A longitudinal study evaluating the measurement of condyle opacity, cortical thickness and metaphyseal angle of distal metacarpal III of Thoroughbred racehorses from clinical radiographs for the prediction of lateral condylar fracture. Changes in these variables were monitored to identify differences between horses which developed lateral condylar fractures and control horses which did not.

Evaluation of measurement of density from computed tomography images at the palmar distal condyles of metacarpal III of Thoroughbred racehorses for prediction of lateral condylar fracture. Maximum density in the region of the origin lateral condylar fractures was compared between horses with lateral condylar fracture and controls without.

Chapter 2: Validation of radiographic measurement of condyle opacity, cortical thickness and metaphyseal angle of the equine distal metacarpal III bone

2.1 Introduction

Fractures continue to be a serious problem for the horse racing industry, as both a significant cause of fatality and a common cause of days lost from training (Ramzan and Palmer, 2011). Condylar fractures of the distal metacarpal III bone are a leading cause of fatality in Thoroughbred (TB) racehorses (Trope *et al.*, 2015). This type of fracture is considered to be a fatigue fracture that disseminates from a region of pre-existing pathology within the parasagittal groove (Muir *et al.*, 2006). Evidence from post-mortem and diagnostic imaging studies support the existence of pre-existing pathological defects (Tranquille, Parkin and Murray, 2012).

Early detection of existing fatigue lesions could greatly contribute to prevention of condyle fracture, reducing the mortality rate at racetracks and improving equine welfare. Diagnostic methods that are capable of predicting fracture prior to occurrence have been investigated in the human and veterinary literature. Worldwide, radiography is by far the most common diagnostic imaging method routinely performed to investigate lameness and poor performance. Previous studies have investigated methods of predicting fracture using advanced imaging techniques such as magnetic resonance imaging (MRI) (Tranquille, Parkin and Murray, 2012) and quantitative computed tomography (CT) (Trope *et al.*, 2015). However, only a very small minority of horses worldwide are examined clinically using MRI due to limited availability of equipment and prohibitive costs. Quantitative CT is currently not in clinical use in the horse and is limited to cadaver studies. Furthermore, a recent study demonstrated that even in a clinic with access to MRI, the majority of condylar fractures are diagnosed using radiography (Ramzan, Palmer and Powell, 2015). The widespread availability, simplicity and low cost of radiography make it an ideal screening tool for fracture risk. Digital radiography is now the industry standard, making software that can analyse digitised radiographs a rapid and efficient approach to identifying horses at increased risk of fracture.

The morphology of the equine metacarpal III bone has been described using cadaver bones (Dymock and Pauwels, 2012) and the use of radiography to quantify changes in bone

morphology in response to exercise in Thoroughbred racehorses has been previously described (Davies, Gale and Baker, 1999). The use of geometrical measures including hip axis length (HAL), femoral neck shaft angle (NSA), and femoral neck width were demonstrated to be associated with the risk of proximal femoral fractures in humans (Maeda *et al.*, 2011; Ripamonti, Lisi and Avella, 2014). The overall goal of this study was to develop and validate objective radiographic methods of describing the distal condyle of the equine metacarpal III bone.

2.2 Aims and objectives

The hypothesis for this work was that measurement of radiopacity, cortical thickness and metaphyseal angle from radiographs of the distal metacarpal III bone of Thoroughbred racehorses is precise and accurate.

The principal aim of the study was to determine the precision and accuracy of radiographic measurement of opacity, cortical thickness and metaphyseal angle of the distal metacarpal III bone of Thoroughbred racehorses.

The following targeted objectives were set to accomplish this aim:

i. Use cadaver bones to establish methods to measure objectively the following variables in the distal metacarpal III bone: condyle radiopacity; cortical thickness; and metaphyseal angle.

ii. Determine the intra-observer variability of radiographic measurement of radiopacity, cortical thickness and metaphyseal angle of the distal metacarpal III bone of Thoroughbred racehorses made from cadaver specimens: bones with lateral condylar fracture; non-fractured bones from the contralateral limbs; and normal control bones (from horses euthanized for reasons unrelated to distal limb fracture).

iii. Determine the accuracy of the measurements by comparing the radiographic measurements with measurements derived from computed tomography.

2.3 Materials and methods

2.3.1 Cadaver bones

Cadaver metacarpal III bones (n=55) with the distal carpus but without soft tissues that were obtained from a previous study were used for this study (Parkin *et al.*, 2006). The bones were classified into three groups based on the presence or absence of a lateral condylar fracture. Bones in the control group (n=30) were obtained from horses euthanized on racecourses as a result of injuries unrelated to fracture of the distal limb (including fracture of the neck or back and cardiovascular pathology); non-fractured group (n=11) bones were obtained from the contralateral limb of horses that sustained a lateral condylar fracture of the metacarpal bone III; fracture group (n=14) bones were obtained from the fractured limb of horses that sustained a lateral condylar fracture of the metacarpal III bone.

2.3.2 Aluminium radiography phantom

To perform measurement of radiopacity an aluminium phantom was developed as a radiographic reference. In a pilot study, an aluminium step wedge phantom of 1mm, 2mm, 3mm, 4mm, and 5mm thickness was constructed. The step wedge phantom was placed on a radiographic cassette (AGFA, CR35-X, 3.0mm) and radiographs were obtained at using 10mAs and a kV range of 53-74kV. The radiopacity of the phantom was measured using commercially available software (Osirix Lite 2, Pixmeo SARL) by placing a 1cm^2 region of interest (ROI) over each section and measuring the brightness. The relationship between kV, aluminium thickness and radiopacity was described graphically.

2.3.3 Radiography

The cadaveric bones (n=55) were removed from -20C storage and thawed at room temperature for 24 hours before radiography. Each limb was positioned on a radiographic cassette (AGFA, CR35-X, 3.0mm) so that the palmar surface was on the cassette and the long axis of the metacarpal III was parallel with the cassette and a 2mm aluminium radiographic phantom was placed laterally. The lateral side was identified using the anatomy of the carpus. Using a clamp for positioning a dorsopalmar (DP) and lateromedial (LM) projection was obtained for each specimen using exposure factors of 62kV/10mAs and 60kV/10mAs respectively. All radiography was performed using a film focus distance of 80 cm. The images were stored as DICOM files for subsequent analysis.

2.3.4 Computed tomography

A computed tomography (CT) study of each bone was performed following radiography using a clinical CT machine (Somatom Spirit, Siemens) with settings of 130kV/30mAs, 2 x 1.5mm detector collimation and 3mm slice thickness (reduced to 1.5mm in the reconstructed images). Field of view was 12cm, image matrix size was 512*512, and average voxel size was 0.24mm^3 (0.28x0.28x3.0mm). The images were stored as DICOM files for subsequent analysis.

2.3.5 Image processing

Radiographic and CT images were stored in DICOM format. Processing, which included image manipulation, overlay of reference lines and shapes, and measurement of bone opacity, lengths and angles was performed using commercially available software (Osirix Lite 2, Pixmeo SARL).

2.3.6 Radiopacity measurement from radiographs and CT images

The opacity ratios (arbitrary units) calculated from the radiographs were used as a proxy for bone radiopacity. In the case of the CT, measurements were made directly from the images (Hounsfield units).

2.3.6.1 Radiographic opacity ratio measurement

The standardised radiopacity of the distal metacarpal was described using a ratio of the bone radiopacity and the phantom radiopacity. The dorsopalmar radiographs were used to calculate bone radiopacity ratios for each distal metacarpal III. Specifically, a rectangular ROI of set size (8mm X 6.3mm) was drawn over the subchondral bone of the lateral and the medial condyle (X, Fig 2.1). A further identical ROI was drawn over the phantom so that its boundaries were within the those of the portion of the phantom corresponding to 2mm thick aluminium (Y, Fig 2.1). The distal metacarpal III ROIs were positioned with their axial border aligned with the intersection of the sloping surface of the sagittal ridge and the more horizontal surface of the condyle and their distal border outlined the subchondral bone surface. These ROIs therefore included the parasagittal groove region of the condyles. The radiographic opacity of the condyle ROIs was determined from the opacity measurements made with Osirix Lite 2 (Fig 2.1):

Condyle radiopacity ratio = lateral or medial condyle ROI opacity (X)/phantom ROI (Y) opacity

The condyle radiopacity ratio was measured independently by a single observer three times for each radiograph and CT.

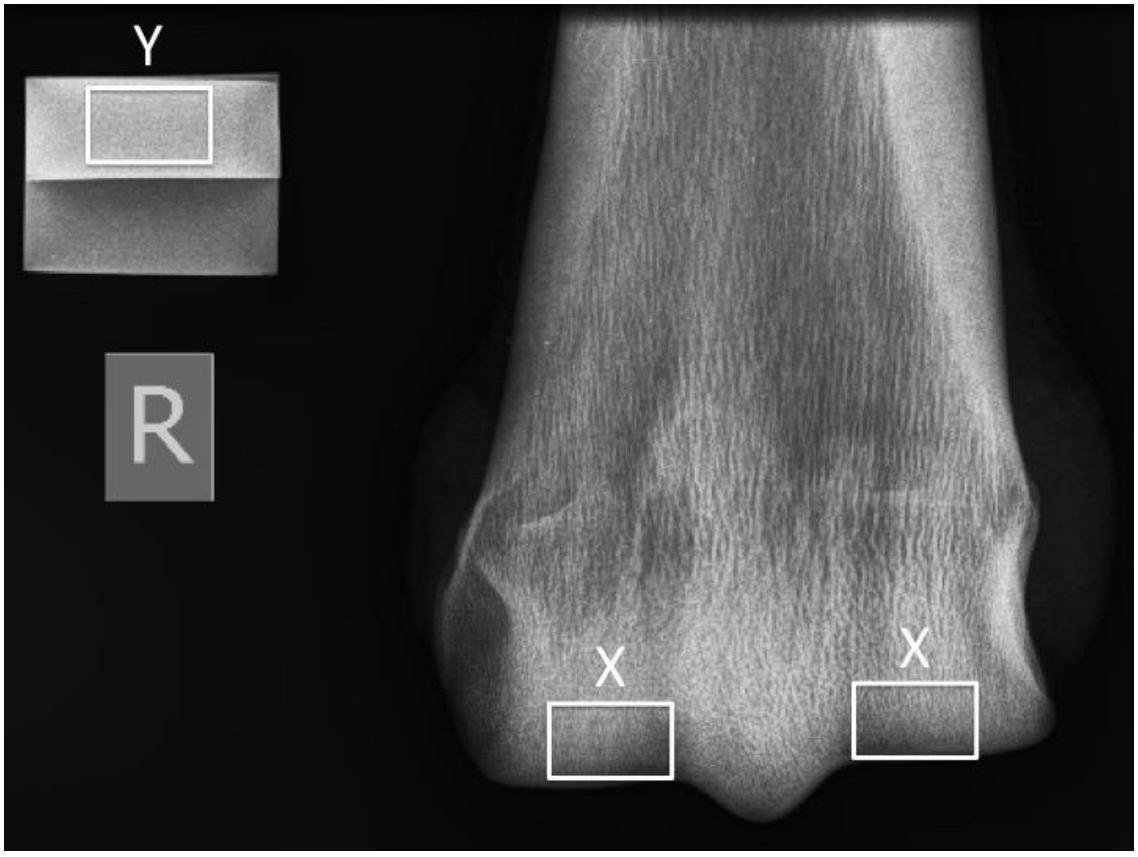

Figure 2.1: Dorsopalmar radiograph of distal metacarpal III with ROIs (X) overlaid to illustrate where opacity measurements were made when calculating lateral and medial condyle radiopacity ratios. Condyle measurements were normalised using the radiopacity measurement from an aluminium phantom placed on the radiographic cassette (Y). The marker is lateral.

2.3.6.2 Computed tomography radiopacity ratio measurement

Technical difficulties prevented the use of the aluminium phantom for computed tomography. Radiopacity was measured using dorsal slice computed tomography images from midway between dorsal and palmar cortices. ROIs of set size (8mm X 6.3mm) were drawn over the subchondral bone of the lateral and medial condyle as described for radiography. These measurements were normalised using the measurement from a ROI positioned over lateral diaphysis 4.5cm proximal to the sagittal ridge of distal metacarpal III.

2.3.7 Cortical thickness ratio measurements

2.3.7.1 Radiography measurement

The dorsal cortical thickness ratio was measured using a previously described method (Davies, Gale and Baker, 1999). Briefly, a point 2.5 cm distal to the nutrient foramen was identified on each lateromedial radiograph with the aid of a dorsopalmar view radiograph. The width of the dorsal cortex (DC) and medulla (M) were measured on the lateromedial radiographs before calculating the ratio of DC/M (Fig 2.2). The dorsal cortical thickness ratio was measured independently by a single observer three times for each radiograph and CT.

2.3.7.2 Computed tomography measurement

Distal metacarpal III cortical thickness ratios were calculated in a similar way as previously described for radiography using a mid-sagittal CT image (Fig 2.2).

Figure 2.2: Mid-sagittal CT image (left) and lateromedial radiograph (right) of an equine metacarpal III bone. Measurement of the dorsal cortical ratio (DC/M) was performed on CT (A) and radiography (B) as previously described (Davies, Gale and Baker, 1999).

2.3.8 Metaphyseal angle measurement

2.3.8.1 Radiographic and computed tomography

The metaphyseal angle refers to the deviation of distal metacarpal condyle III against its diaphysis in degrees. It objectively describes the relationship between metaphysis and diaphysis and is based upon previous descriptions of the human femur (Maeda *et al*., 2011; Ripamonti, Lisi and Avella, 2014). Metaphyseal angle was measured using a method similar to the measurement of carpal valgus (Baker *et al.*, 2015). The metaphyseal angle was measured using lateromedial radiographs and mid-sagittal CT images. Firstly, a line parallel to the dorsal diaphysis was drawn through the middle of the diaphysis (Fig 2.3A). The metaphysis was identified as the narrow section of bone between the epiphysis and diaphysis. A second line was drawn parallel to the dorsal metaphysis through the middle of the metaphysis (Fig 2.3B). The angle formed between the diaphyseal and metaphyseal lines was measured to yield the metaphyseal angle (Fig 2.3C). The metaphyseal angle was measured independently by a single observer three times for each radiograph and CT.

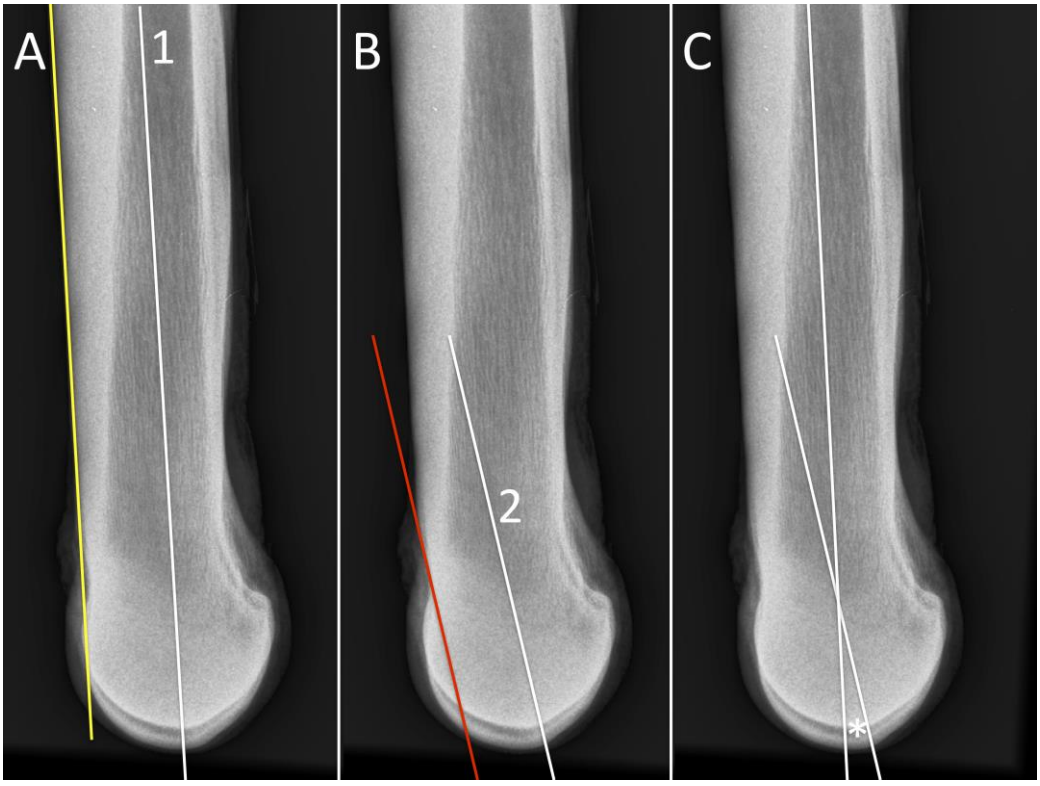

Figure 2.3A-C: Lateromedial radiographs demonstrating the method of metaphyseal angle measurement. A line was drawn in the centre of the diaphysis (1) parallel to the dorsal surface (yellow, Fig 2.3A), before a line was drawn in the centre of the metaphysis (2) parallel to the dorsal surface of the diaphysis (red, Fig 2.3B). The angle formed at the intersection of the two lines (*) was measured (Fig 2.3C).

2.3.9 Statistical Analysis

A Shapiro-Wilk normality test was performed prior to data analysis.

2.3.9.1 Comparison between medial and lateral condyles

The radiopacity of the medial and lateral condyles were compared using a paired t-test.

2.3.9.2 Comparison between radiography and computed tomography

The mean measurements obtained by radiography and CT of radiopacity, dorsal cortical thickness ratio, and metaphyseal angle were compared by performing a t-test and Pearson product moment correlation. Statistical significance was set at $P<0.05$.

2.3.9.3 Intra-observer agreement

A group of 20 bones [Control (n=10), non-fractured (n=5) and fractured (n=5)] were selected by random number and used for the analysis of intra-observer agreement. The agreement between measurements was determined using the Bland-Altman method (Bland and Altman, 1999). The measurements were compared in pairs by calculating the mean value of each pair and the difference between each pair. To determine whether there was a significant difference between pairs of measurements a one-sample T-test was performed on the differences between each pair. Where there was no significant difference between measurements a Bland-Altman plot was constructed to describe agreement between two observer measurements. To further identify and describe any proportional bias linear regression was performed using SPSS software.

2.4 Results

2.4.1 Cadaver bones

The horses that were the source of the cadaver bones used in this study are described in Table 2.1.

Group	Control	Non Fractured	Fractured
Sample No	30	11	14
Male (intact)	0	0	1
Male (Gelding)	28	9	10
Female	2	2	3
Age Range (years)	4-11	3-10	3-9

Table 2.1: Describing the sex and age distribution of the horses from which the cadaver bones used in this study were collected (Parkin *et al.*, 2006).

2.4.2 Aluminium radiography phantom

The pilot study revealed that the 2mm thick aluminium phantom had the most linear relationship between exposure (kV) and radiopacity over the required kV range (Fig 2.4). A 2mm thick aluminium phantom was used for all further experiments.

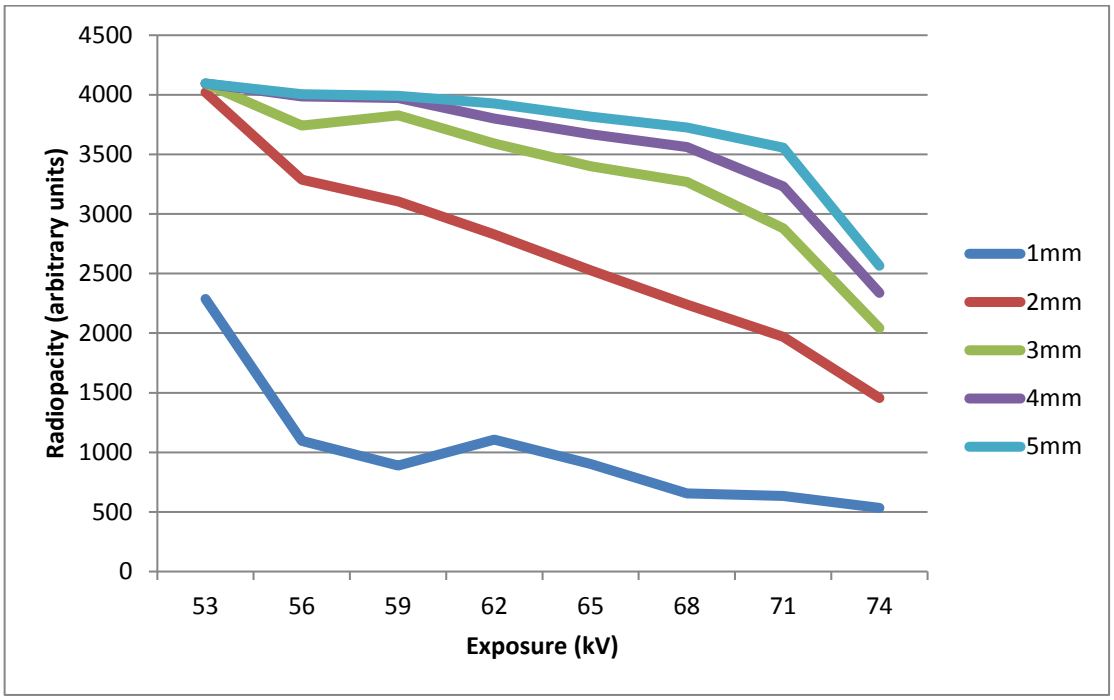

Figure 2.4: Line graph showing the relationship between aluminium phantom thickness (mm) and radiopacity across a range of exposures (53-74kV). The constant exposure of 10mA was used.

2.4.3 Radiopacity measurements

The mean ± SD of the radiopacity ratio measured by radiography of the lateral and medial condyles were 0.61 ± 0.10 and 0.67 ± 0.12 respectively. The radiopacity ratio of the medial condyle was significantly greater than the lateral condyle (p=0.002).

The mean ± SD of the radiopacity ratio measured by CT of the lateral and medial condyles were 0.66 ± 0.12 and 0.71 ± 0.12 respectively. The radiopacity ratio of the medial condyle was significantly greater than the lateral condyle (p=0.001).

There was no significant correlation between radiopacity ratios measured by radiography and CT for either the lateral or medial condyle.

2.4.4 Cortical thickness ratio measurements

The mean ± SD of the cortical thickness ratio measured by radiography and CT were 1.10 ± 0.22 and 1.12 ± 0.23 respectively. There was no significant difference between methods. There was a significant correlation between cortical thickness ratio measurements obtained by radiography and CT (r=0.74, p=0.007, Fig 2.5).

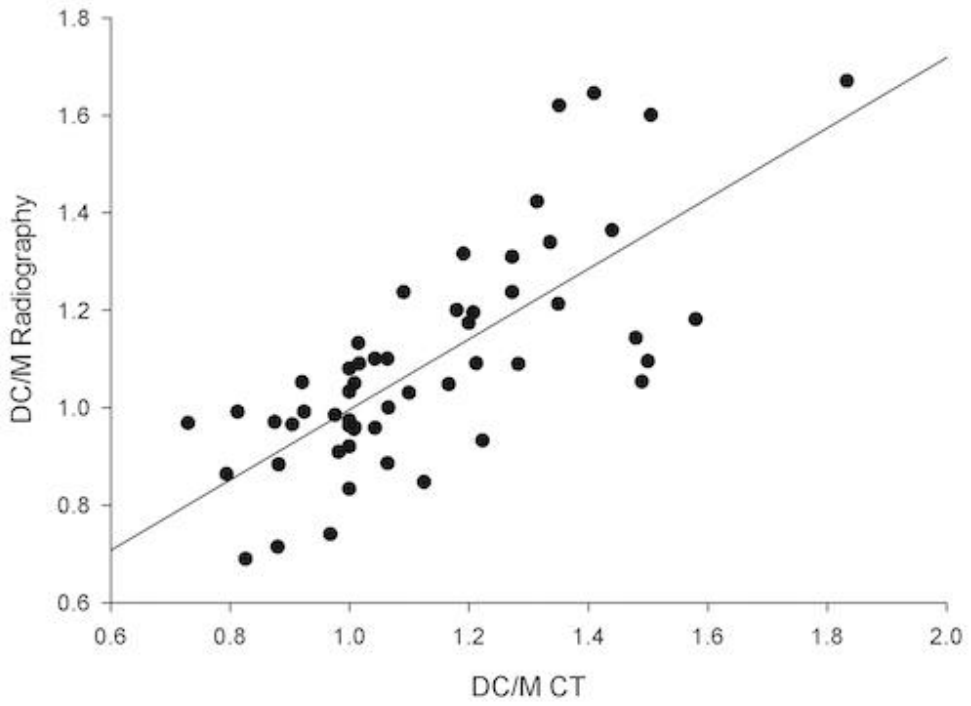

Figure 2.5: Scatter plot describing the relationship between the dorsal cortical ratio (DC/M) measured by radiography and CT. Linear regression revealed a significant correlation between the methods (r=0.74, p=0.007).

2.4.5 Metaphyseal angle measurement

The mean ± SD of the metaphyseal angle measured by radiography and CT were 6.92 ± 1.82° and 7.14 ± 2.14° respectively. There was no significant difference between methods. There was a significant correlation between metaphyseal angle measurements obtained by radiography and CT (r=0.732, p=0.004, Fig 2.6).

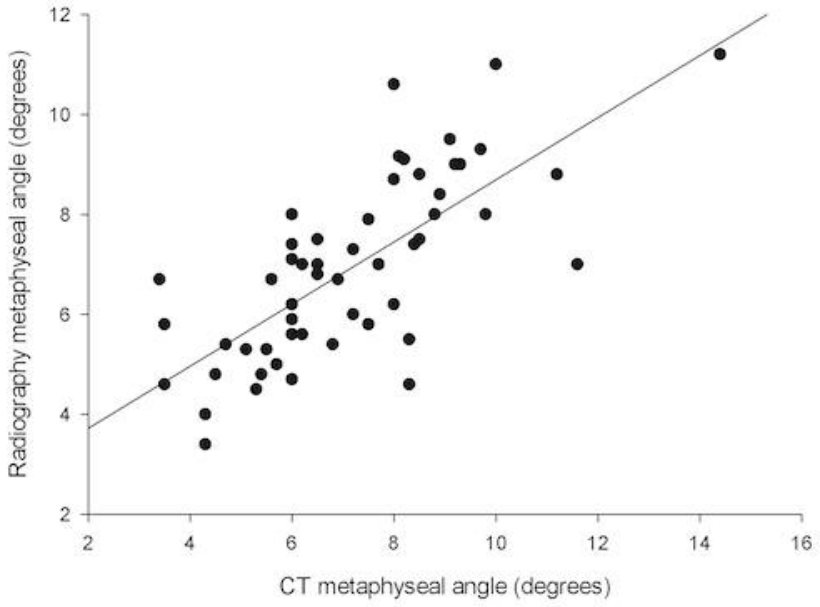

Figure 2.6: Scatter plot describing the relationship between the metaphyseal angle measured by radiography and CT. Linear regression revealed a significant correlation between the methods (r=0.732, p=0.004).

2.4.6 Intra-observer agreement

2.4.6.1 Radiopacity measurement from radiographs

The differences between the first and second, first and third, and second and third measurements of radiopacity ratio for the lateral condyle were not significantly different from zero (p=0.781, 0.684, and 0.467) (Table 2.2). The limits of agreement (95% CI) for the mean difference between the 1st and 2nd measurements were -0.03-0.02, for 1st and 3rd measurements 0.03-0.04 and 2nd and 3rd measurements were -0.032-0.038 (Fig 2.7). Bland-Altman plots revealed no evidence of proportional bias (p=0.128, 0.490 and 0.636) (Fig 2.7).

	Test Value = 0					
					95% Confidence Interval of the Difference	
Difference	T	df	Sig. (2-tailed)	Mean Difference	Lower	Upper
1-2	-0.282	19	.781	-0.001	-0.008	0.006
1-3	0.413	19	.684	0.002	-0.008	0.012
2-3	0.742	19	.467	0.003	-0.006	0.012

Table 2.2: Results of a one-sample t test of the difference between observer measurements of lateral condyle radiopacity ratio.

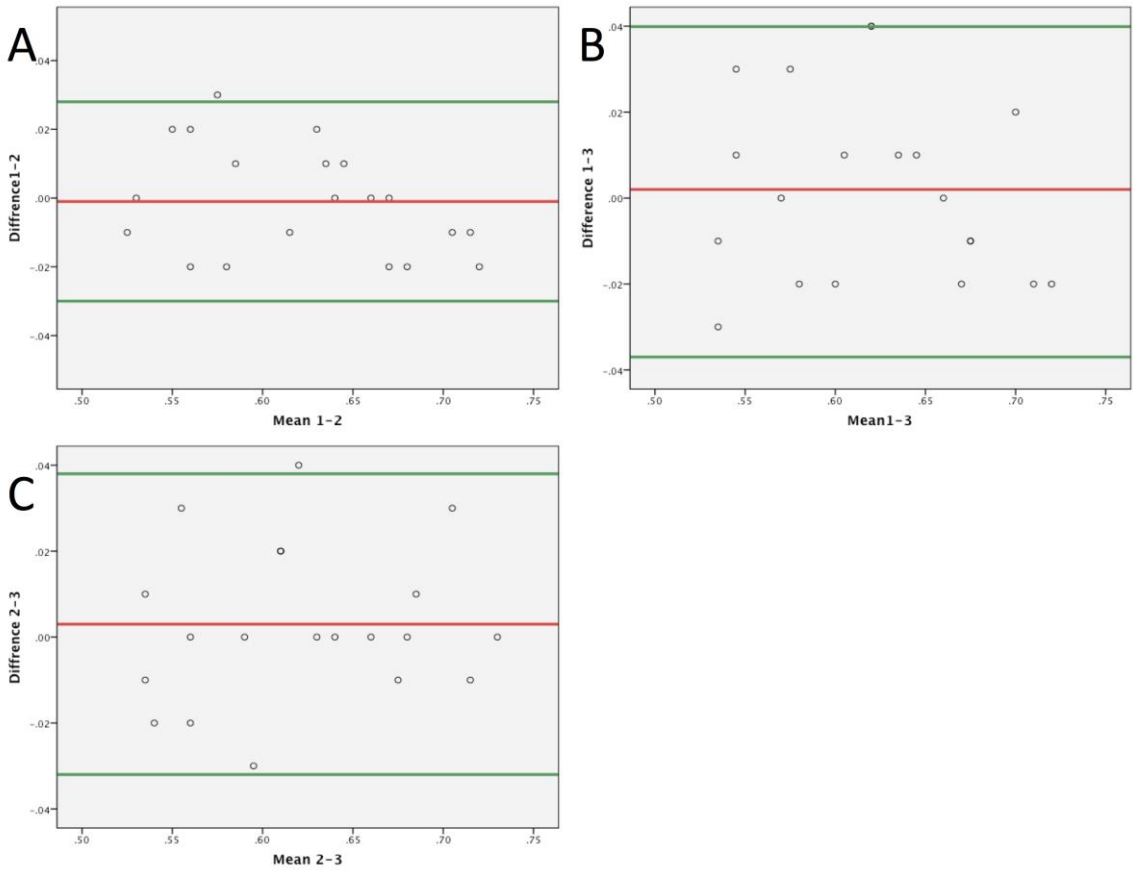

Figure 2.7: Bland-Altman plots of lateral condyle radiopacity ratio measurements. The difference versus average of paired values measured with 95% limits of agreement (green lines). A: Measurements 1 and 2, B: Measurements 1 and 3, C: Measurements 2 and 3.

The differences between the first and second, first and third, and second and third measurements of radiopacity ratio for the medial condyle were not significantly different from zero (p=0.351, 0.472 and 0.933) (Table 2.3). The limits of agreement (95% CI) for the mean difference between the 1st and 2nd measurements were -0.12-0.15, for 1st and 3rd measurements -0.17-0.20 and 2nd and 3rd measurements were -0.09-0.09 (Fig 2.8). Bland-Altman plots revealed no evidence of proportional bias (p =0.175, 0.297 and 0.869) (Fig 2.8).

	Test Value = 0					
					95% Confidence Interval of the Difference	
Difference	t	Df	Sig. (2-tailed)	Mean Difference	Lower	Upper
1-2	0.956	19	.351	0.017	-0.02	0.05
1-3	0.733	19	.472	0.016	-0.03	0.06
2-3	-0.086	19	.933	-0.001	-0.03	0.02

Table 2.3: Results of a one-sample t test of the difference between observer measurements of medial condyle radiopacity ratio.

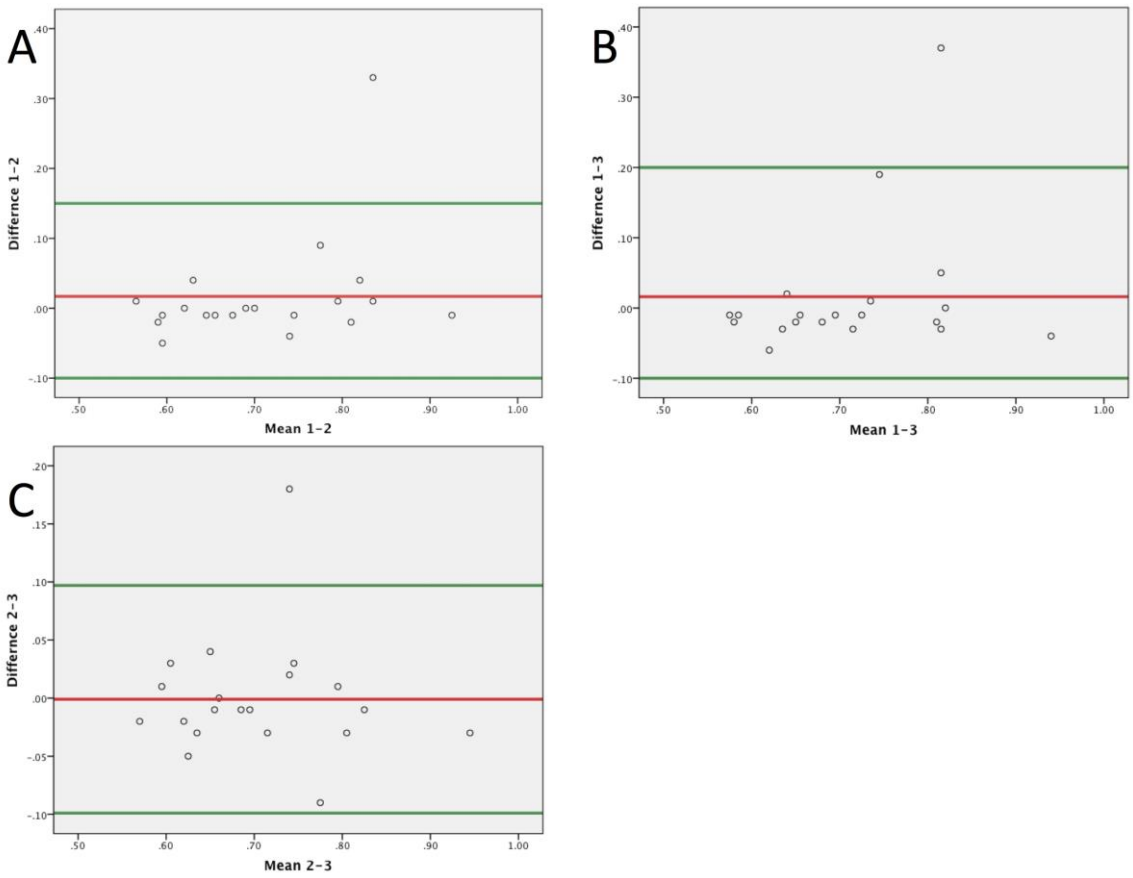

Figure 2.8: Bland-Altman plots of medial condyle radiopacity ratio measurements. The difference versus average of paired values measured with 95% limits of agreement (green lines). A: Measurements 1 and 2, B: Measurements 1 and 3, C: Measurements 2 and 3.

2.4.6.2 Cortical thickness ratio

The differences between the first and second, first and third, and second and third measurements of cortical thickness ratio were not significantly different from zero (p= 0.186, 0.729 and 0.328) (Table 2.4). The limits of agreement (95% CI) for the mean difference between the 1st and 2nd measurements were -0.05-0.06, for 1st and 3rd measurements -0.08-0.08 and 2nd and 3rd measurements were -0.07-0.06 (Fig 2.9). Bland-Altman plots revealed no evidence of proportional bias (p=0.632, 0.905 and 0.736 (Fig 2.9).

Difference	Test Value = 0					
	t	Df	Sig. (2-tailed)	Mean Difference	95% Confidence Interval of the Difference	
					Lower	Upper
1-2	1.373	19	0.186	0.011	-0.01	0.03
1-3	0.352	19	0.729	0.004	-0.02	0.02
2-3	-1.004	19	0.328	-0.008	-0.02	0.01

Table 2.4: Results of a one-sample t test of the difference between observer measurements of cortical thickness ratio.

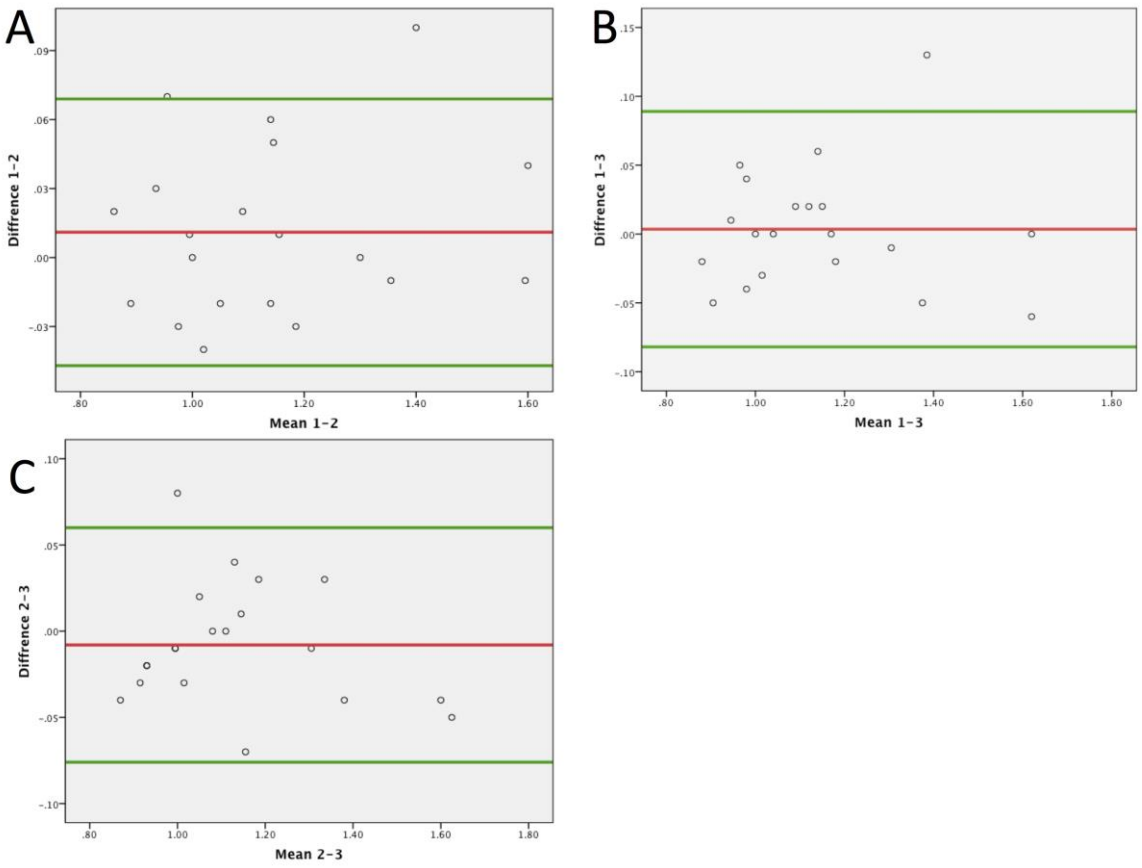

Figure 2.9: Bland-Altman plots of dorsal cortical ratio measurements. The difference versus average of paired values measured with 95% limits of agreement (green lines). A: Measurements 1 and 2, B: Measurements 1 and 3, C: Measurements 2 and 3.

2.4.6.3 Metaphyseal angle measurements

The differences between the first and third and second and third measurements of metaphyseal angle were not significantly different from zero (p= 0.345, and 0.580) (Table 2.5). The differences between the first and second measurements of metaphyseal angle were significantly greater than 0 (p=0.028, Table 2.5), therefore Bland-Altman analysis was not performed on this pair. The limits of agreement (95% CI) for the mean difference between the 1st and 3rd measurements were -2.0°-2.5° and 2nd and 3rd measurements were –2.56°-2.25°

(Fig 2.10). Bland-Altman plots revealed no evidence of proportional bias (p=0.928 and 0.994) (Fig 2.10).

Difference	Test Value = 0					
	T	Df	Sig. (2-tailed)	Mean Difference	95% Confidence Interval of the Difference	
					Lower	Upper
1-2	2.373	19	.028	0.41	0.05	0.76
1-3	0.969	19	.345	0.25	-0.29	0.79
2-3	-0.563	19	.580	-0.16	-0.73	0.42

Table 2.5: Results of a one-sample t test of the difference between observer measurements of metaphyseal angle.

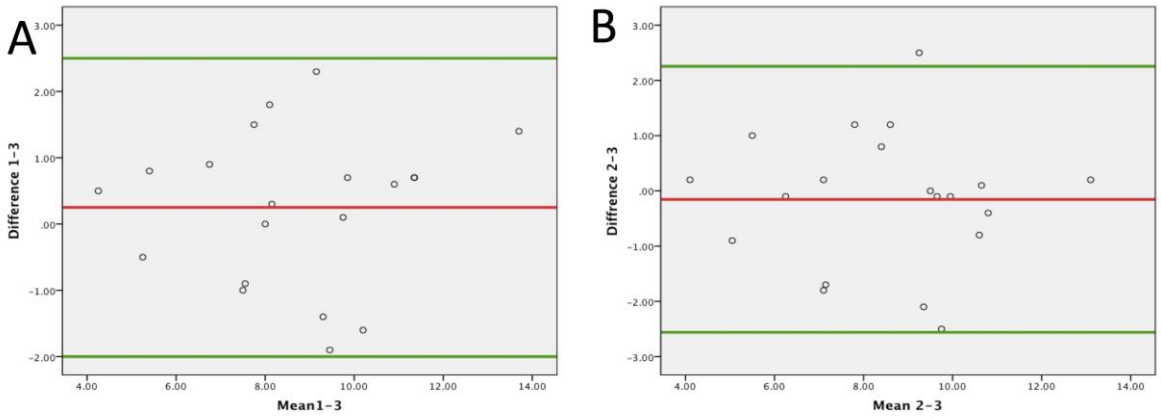

Figure 2.10: Bland-Altman plots of metaphyseal angle measurements. The difference versus average of paired values measured with 95% limits of agreement (green lines). A: Measurements 1 and 3, B: Measurements 2 and 3

2.5 Discussion

The overall purpose of this study was to develop and validate novel objective geometrical measurements of the equine metacarpal III bone, and validate the dorsal cortical ratio measurement that has previously been described. A range of radiographic voltages were applied to determine the phantom with the most linear relationship with exposure. The 2mm phantom was found to have the most linear relationship with exposure and was used for all further experiments. The use of the ratio of the dorsal cortex to the medulla measured using radiography has previously been described as a method of assessing the change in metacarpal bone geometry in response to exercise (Davies, Gale and Baker, 1999). However, radiography is liable to magnification, positioning error and variation in the number and energy of photons therefore a study comparing measurement to a 'gold standard', in this case computed tomography, is required. In addition, this study aimed to determine the repeatability of the dorsal cortical ratio measurement by an observer. This study found that there was no significant difference in measurements obtained by radiography and CT, and there was a strong correlation between methods. It is likely that since this method uses a ratio rather than an absolute measurement, the effect of magnification is eliminated. There were no significant differences between repeated measures and the limits of agreement were extremely small for dorsal cortical ratio measurement. Therefore, this method is very repeatable, likely aided by the well-defined measurement site and accurate digital radiography measurement tools. A limitation of this study is the lack of inter-observer validation, particularly since the observer in this study was very familiar with the method and study. The mean dorsal cortical ratio reported in this study (1.1) was similar to that previously reported in a group of racehorses (1.18) (Davies, Gale and Baker, 1999).

Previous studies have shown that lateral condylar fractures occur in remodelled areas of low bone density, often adjacent to areas of higher bone density. This has been demonstrated in cadaver bones and using advanced imaging techniques such as quantitative computed tomography (qCT) (Riggs, Whitehouse and Boyde, 1999). However, the limited availability of advanced imaging means that a simple, low cost alternative for screening horses is warranted. This study examined the possibility of using densitometry to measure radiopacity in the parasagittal groove and standardise this using a simple aluminium phantom to create a ratio. A number of limitations meant that simple comparison with CT was not possible in this study. The flat 2mm phantom was unsuitable for use in CT images. Therefore, a reference site in the diaphysis of the metacarpal III bone was used instead to create a ratio for comparison with radiography. There was no significant correlation between the

radiopacity measurements from radiography and CT. This likely reflects the difference in methods or the fact that radiographs and CT images are fundamentally different, with a 2D radiograph representing a summation of a 3D structure while a CT image is an individual 3mm slice. Interestingly, both radiography and CT methods were in agreement that the radiopacity ratio was significantly lower in the lateral condyle than the medial condyle. This suggests that the region of interest was incorporating the area of porous subchondral bone at the parasagittal groove that has previously been described by qCT (Riggs, Whitehouse and Boyde, 1999).

Anecdotal evidence suggests that the shape of the distal condyle in horses with fetlock disease can change in the sagittal plane (J Marshall, personal communication). A previous study of the equine metacarpal III was limited to the description of the relationship between the diaphysis and metaphysis in the dorsal plane (Dymock and Pauwels, 2012). In human studies, there has been interest in the measurement of femoral neck shaft angle (NSA), a geometrical measurement of the relationship between the diaphysis, metaphysis and epiphysis of the femur (Ripamonti, Lisi and Avella, 2014). The NSA is the angle measured at the intersection of the axis of the femoral diaphysis and the axis of the metaphysis and epiphysis (neck). It changes during growth and development; initially it is approximately 150° and becomes more acute in the adult (120°) (Dobbs and Morcuende, 1986). NSA has been linked to the risk of osteoporotic fracture; biomechanically a more obtuse angle results in a higher bending moment at the femoral neck in the event of an impact on the femur (Ripamonti, Lisi and Avella, 2014). To allow further description of the geometry of the distal metacarpal III, this study aimed to define measurement of the angle between the axis of the diaphysis and the axis of the metaphysis/epiphysis. This angle, referred to as the metaphyseal angle, was approximately 7° when measured by radiography and CT; there was no significant difference in measurements by these methods and the measurements showed good correlation. Metaphyseal angle was the only measurement performed where a significant difference was found between repeated measurements (Measurements 1 and 2). However, although significant the mean difference between these sets of measurements was small at 0.41°. There was good agreement between the other two pairs of measurements. It is possible that this geometrical measure of the relationship between the diaphysis and metaphysis of the metacarpal III could be applied to the future study of condylar fractures, growth and development, the effect of training, and osteoarthritis of the fetlock.

2.6 Conclusion

The overall goal of this study to develop and validate objective methods of measuring radiopacity, cortical thickness and metaphyseal angle from radiographs of the distal metacarpal III bone of Thoroughbred racehorses was achieved. Interestingly, the measurement of radiopacity identified significant differences between the lateral and medial condyle similar to those reported by studies using more complex methods (Loughridge *et al*., 2017). However, this study was limited to the use of cadaver materials from a small population of horses. Further validation and application of these methods in the assessment of clinical radiographs and fracture risk is warranted.

Chapter 3: Comparison of radiographic measurements of metacarpal III between horses with and without lateral condylar fracture

3.1. Introduction

Previous studies have described the pre-existing gross and microscopic pathology in the distal third metacarpal condyle of racehorses that have suffered a lateral condylar fracture (Parkin *et al.*, 2006). Pre-existing bone modelling and remodelling has been visualised using radiography of thin bone sections (Parkin *et al.*, 2006), computed tomography (CT) (Loughridge *et al.*, 2017), quantitative computed tomography (qCT) (Whitton *et al.*, 2010; Trope *et al.*, 2015), and magnetic resonance imaging (MRI) (Tranquille, Parkin and Murray, 2012).These workers hypothesized that diagnostic imaging offers the possibility of identifying pre-existing pathology and intervening through treatment including rest and rehabilitation to prevent subsequent fracture. However, to date no study has demonstrated the ability of diagnostic imaging to identify those horses at increased risk of fracture (Dubois *et al.*, 2014). Furthermore, previous studies have focused on advanced imaging techniques such as CT and MRI, which although increasingly available in the clinic, are still only accessible to a very small minority of racehorses worldwide (Tranquille, Parkin and Murray, 2012; Trope *et al.*, 2015; Loughridge *et al.*, 2017).

Radiography is the most commonly employed diagnostic imaging technique in equine practice, even in hospitals that have MRI facilities (Ramzan, Palmer and Powell, 2015). It is inexpensive, widely available, technically simple to perform and the technique of choice for the diagnosis of the majority of lateral condylar fractures. The use of radiography to determine the risk of subsequent fracture has not been investigated in the horse. However, the ability of radiography to quantify the changes in dorsal metacarpal cortical thickness that occurs in response to exercise has been demonstrated (Davies, Gale and Baker, 1999). In human medicine, radiography has been widely explored as a method of predicting femoral fractures, particularly in patients with osteoporosis (Maeda *et al.*, 2011; Ripamonti, Lisi and Avella, 2014). Simple geometric parameters such as femoral neck angle (FNA) have been shown to relate to the risk of fracture in humans, as they reflect the biomechanical stresses on the bone (Ripamonti, Lisi and Avella, 2014). However, the use of geometrical parameters to determine the risk of fracture in the horse has not been explored.

In Chapter 2, objective methods of quantifying the radiopacity and geometric parameters of the equine metacarpal III bone were validated. In this chapter, these methods were applied

to determining whether there are significant differences in radiopacity and geometrical measures between horses that have suffered a lateral condylar fracture, and a control population of horses euthanized for other reasons. Where differences exist, the value of these measurements as diagnostic tests will be determined.

3.2. Aims and objectives

The hypothesis for this work was that there are significant differences in radiopacity, dorsal cortical thickness, and metaphyseal angle between Thoroughbred racehorses that have sustained a lateral condylar fracture and those that are euthanized for other reasons.

The principal aim of this study was to identify differences in condylar radiopacity, dorsal cortical thickness and metaphyseal angle of the distal metacarpal III bone between horses that sustained a lateral condylar fracture and horses that were euthanized for other reasons.

The following targeted objectives were set to accomplish this aim:

i. Objectively measure condyle opacity, dorsal cortical thickness, and metaphyseal angle of cadaver bones from racehorses that have sustained a lateral condylar fracture and those euthanized on the racecourse for other reasons.
ii. Compare these measures to identify differences between racehorses that have sustained a lateral condylar fracture and those euthanized on the racecourse for other reasons.
iii. Determine the sensitivity and specificity of objective measures of distal metacarpal III to identify horses that sustained a lateral condylar fracture of distal metacarpal III.

3.3 Material and Methods

3.3.1 Cadaver bones

Cadaver metacarpal III bones (n=55) with the distal carpus but without soft tissues that were obtained from a previous project were used for this study (Parkin *et al.*, 2006). The bones were classified in to three groups based on the presence or absence of a lateral condylar fracture. Bones in the control group (n=30) were obtained from horses euthanized on racecourses as a result of injuries unrelated to fracture of the distal limb (including fracture of the neck or back and cardiovascular pathology); non-fractured group (n=11) bones were obtained from the contralateral limb of horses that sustained a lateral condylar fracture of the metacarpal bone III; fracture group (n=14) bones were obtained from the fractured limb of horses that sustained a lateral condylar fracture of the metacarpal III bone.

3.3.2 Radiography

The cadaveric bones (n=55) were removed from -20°C storage and thawed at room temperature for 24 hours prior to radiography. Each limb was positioned on a radiographic cassette (AGFA, CR35-X, 3.0mm) so that the palmar surface was on the cassette and the long axis of the metacarpal III was parallel to the cassette, with a 2mm aluminium radiographic phantom placed laterally. The lateral side was identified using the anatomy of the carpus. Using a clamp for positioning, a dorsopalmar (DP) and a lateromedial (LM) projection were obtained for each specimen using exposure factors of 62kV/10mAs and 60kV/10mAs respectively. All radiography was performed using a film focus distance of 80 cm. The images were stored as DICOM files for subsequent analysis.

3.3.3 Radiographic opacity ratio measurement

The standardised radiopacity of the distal metacarpal was described using a ratio of the bone radiopacity and the phantom radiopacity as previously described in Chapter 2. The dorsopalmar radiographs were used to calculate bone radiopacity ratios for each distal metacarpal III. Specifically, a ROI of set size (8mm X 6.3mm) was drawn over the subchondral bone of the lateral and the medial condyle. A further identical ROI was drawn over the phantom so that its boundaries were within the area of 2mm thick aluminium. The distal metacarpal III ROIs were positioned with the axial border aligned with the intersection of the sloping surface of the sagittal ridge and the more horizontal surface of the condyle and their distal border outlined the subchondral bone surface. These ROIs therefore included

the parasagittal groove region of the condyles. The radiographic opacity of the condyle ROIs was determined from the opacity measurements made with Osirix Lite 2:

Condyle radiopacity ratio = lateral or medial condyle ROI opacity (X)/phantom ROI (Y) opacity

A single observer blinded to the identity of the horse measured the condyle radiopacity ratio independently three times and the mean calculated.

3.3.4 Cortical thickness ratio measurements

The dorsal cortical thickness ratio was measured using a the method described in Chapter 2 (Davies, Gale and Baker, 1999). Briefly, a point 2.5 cm distal to the nutrient foramen was identified on each lateromedial radiograph with the aid of a dorsopalmar view radiograph. The width of the dorsal cortex (DC) and medulla (M) were measured on the lateromedial radiographs before calculating the ratio of DC/M. A single observer blinded to the identity of the horse measured the dorsal cortical thickness ratio three times independently for each radiograph and the mean value calculated.

3.3.5 Metaphyseal angle measurement

Metaphyseal angle was measured using the method previously described in Chapter 2. The metaphyseal angle was measured using lateromedial radiographs. Firstly, a line parallel to the dorsal diaphysis was drawn through the middle of the diaphysis. The metaphysis was identified as the narrow section of the between the epiphysis and diaphysis. A second line was drawn parallel to the dorsal metaphysis through the middle of the metaphysis (Fig 2.3). The angle formed between the diaphyseal and metaphyseal lines was measured to yield the metaphyseal angle. A single observer blinded to the identity of the horse measured the metaphyseal angle three times independently for each radiograph and the mean value was calculated.

3.3.6 Statistical Analysis

A Shapiro-Wilk normality test was performed prior to data analysis. The effect of group (control, non-fractured, fractured) on the age of the horses was compared using a one-way ANOVA. The proportion of horses of each sex (stallion, gelding, mare) was compared between groups using a chi-squared test. The effect of group (control, non-fractured,

fractured) on the radiopacity ratio, dorsal cortical thickness, and metaphyseal angle of the horses was compared using a one-way ANOVA. Statistical significance was set at $p<0.05$.

Receiver-operator curves (ROC) were generated for radiopacity ratio of the medial and lateral condyles to identify values for each parameter that would represent cut-off values differentiating between those horses that suffered a lateral condylar fracture (non-fracture and fracture groups), and those that were euthanized for other reasons (control group).

3.4. Results

3.4.1 Cadaver bones

The horses that were the source of the cadaver bones used in this study are described in Table 3.1. The mean ± SD age of all horses was 6.44 ± 2.25 years. There was no significant difference in age ($p=0.326$) or sex ($p=0.287$) between groups.

Group	No	Male (intact)	Gelding	Female	Age (Mean ± SD) (years)
Control	30	0	28	2	6.73 ± 1.89
Non Fractured	11	0	9	2	5.55 ± 3.01
Fractured	13	1	10	3	6.54 ± 2.25

Table 3.1: Describing the sex and age distribution of the horses from which the cadaver bones used in this study were collected (Parkin *et al.*, 2006). There was no significant difference in age or sex distribution between groups.

3.4.2 Radiopacity measurements

The overall mean ± SD of the radiopacity ratio measured by radiography of the lateral and medial condyles were 0.61 ± 0.10 and 0.67 ± 0.12 respectively. The mean ± SD radiopacity ratio of the lateral condyle of the control, non-fractured, and fractured groups were 0.57 ± 0.08, 0.68 ± 0.04, and 0.67 ± 0.09 respectively. The mean ± SD radiopacity ratio of the medial condyle of the control, non-fractured, and fractured groups were 0.59 ± 0.08, 0.67 ± 0.04, and 0.82 ± 0.07 respectively (Table 3.2). Overall, the radiopacity ratio of the medial condyle was significantly greater than the lateral condyle ($p=0.002$). The mean radiopacity ratios of the medial and lateral condyles were significantly greater in both the non-fracture and fracture groups than the control group ($p=0.003$). The medial condyle had a significantly greater radiopacity ratio than the lateral condyle in the fracture group only ($p=0.001$).

Group	N	Condyle	Mean	Std. Dev	Min.	Max.
Control	30	Lateral	0.57	0.08	0.41	0.72
		Medial	0.59	0.08	0.40	0.75
Non-fractured	11	Lateral	0.68[a]	0.04	0.60	0.74
		Medial	0.67[a]	0.04	0.60	0.73
Fractured	13	Lateral	0.67[a]	0.09	0.55	0.82
		Medial	0.82[ab]	0.07	0.72	0.93

Table 3.2: Describing the radiopacity ratio of the medial and lateral condyles of the control, non-fractured and fractured group horses. a Significantly different compared to control group ipsilateral condyle; b Significantly different compared to fractured group lateral condyle.

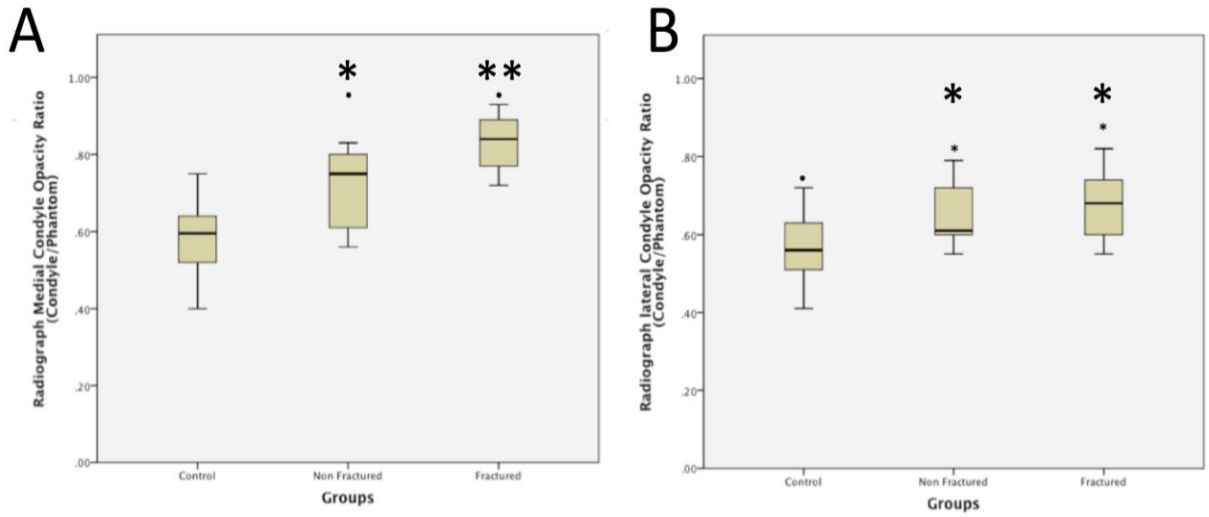

Figure 3.1: Box and whisker plot describing the distribution of the radiopacity ratio of the medial (A) and lateral (B) condyles of control, non-fracture, and fracture groups. * Significantly different compared to control group, ** significantly different compared to control and non-fracture groups (p=0.001).

3.4.3 Cortical thickness ratio measurements

The overall mean ± SD of the cortical thickness ratio measured by radiography was 1.10±0.22. The mean ± SD cortical thickness ratio of the control, non-fractured, and fractured groups were 1.04 ± 0.16, 1.19 ± 0.3, 1.07 ± 0.25 (Table 3.3). There was no significant difference in cortical thickness ratio between groups (Fig 3.2).

Group	N	Mean	Std. Dev	Min.	Max.
Control	30	1.04	0.16	0.71	1.36
Non Fractured	11	1.19	0.30	0.90	1.67
Fractured	13	1.07	0.25	0.68	1.61

Table 3.3: Describing the dorsal cortical thickness ratio measurements of the control, non-fractured and fractured group horses.

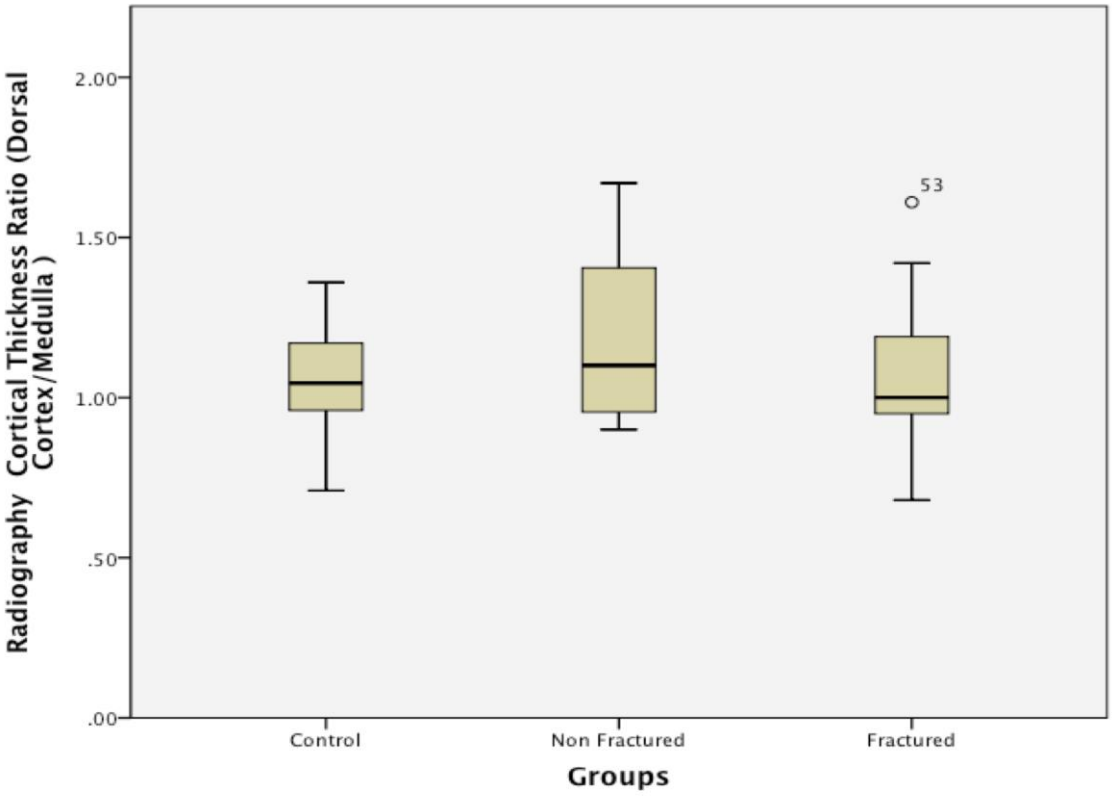

Figure 3.2: Box and whisker plot describing the distribution of the dorsal cortical ratio of metacarpal III condyles of control, non-fracture, and fracture groups.

3.4.4 Metaphyseal angle measurements

The mean ± SD of the metaphyseal angle measured by radiography was 6.92 ± 1.82°. The mean ± SD metaphyseal angle of the control, non-fractured, and fractured groups were 6.64 ± 1.85°, 6.67 ± 2.01°, 7.75 ± 1.41° (Table 3.4). There was no significant difference in metaphyseal angle between groups (Fig 3.3).

Group	N	Mean (°)	Std. Dev (°)	Min. (°)	Max. (°)
Control	30	6.64	1.84	4.32	9.82
Non Fractured	11	6.67	2.01	4.61	11.64
Fractured	13	7.74	1.41	5.35	11.65

Table 3.4: Describing the metaphyseal angle measurements of the control, non-fractured and fractured group horses.

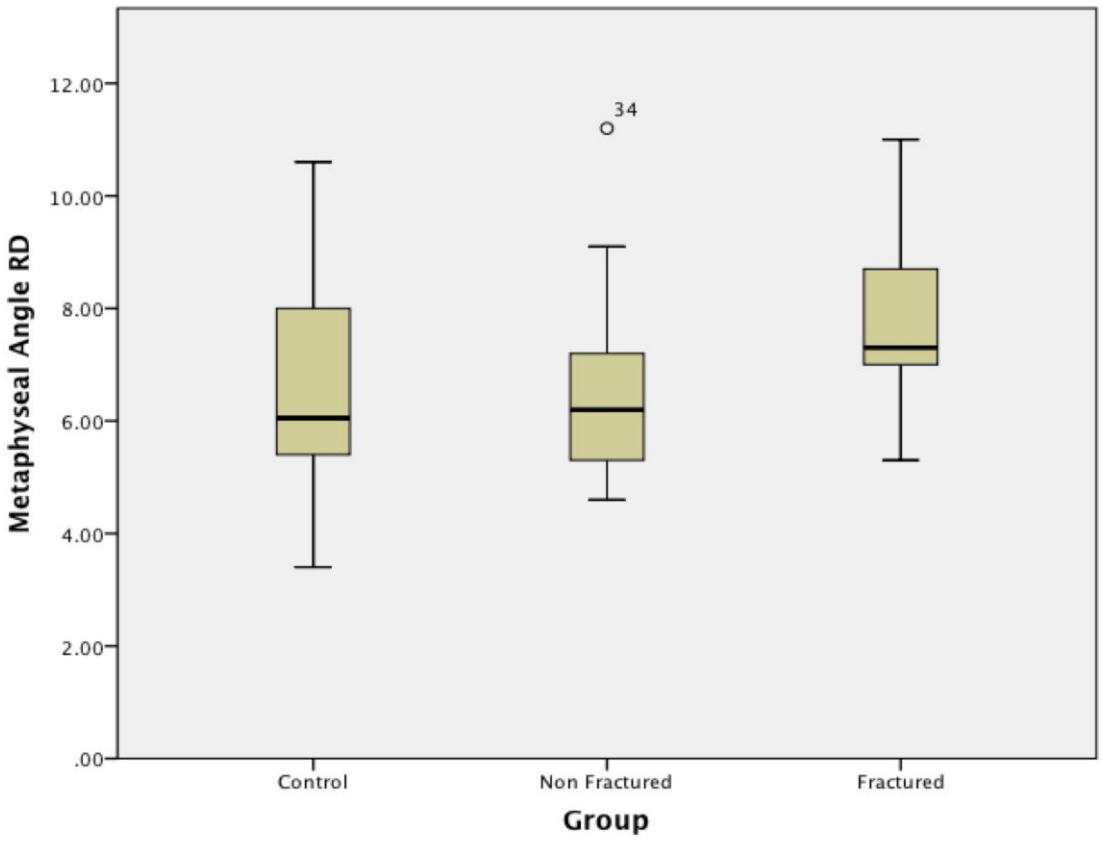

Figure 3.3: Box plot and whisker plot describing the distribution of the metaphyseal angle of control, non-fracture, and fracture groups. There are no significant differences between groups.

3.4.5 Receiver-operator characteristic curve analysis

Receiver-operator characteristic curve analysis determined that the radiopacity ratios of the lateral and medial condyles are good diagnostic tests with areas under the curve (AUC) of 0.83 and 0.91 respectively (Fig 3.4 A & B). A lateral condyle radiopacity ratio of 0.64 was determined to have a sensitivity of 75% and specificity of 83% for distinguishing those horses that suffered a lateral condylar fracture from control horses. A medial condyle radiopacity ratio of 0.65 was determined to have a sensitivity of 83% and specificity of 80% for distinguishing those horses that suffered a lateral condylar fracture from control horses.

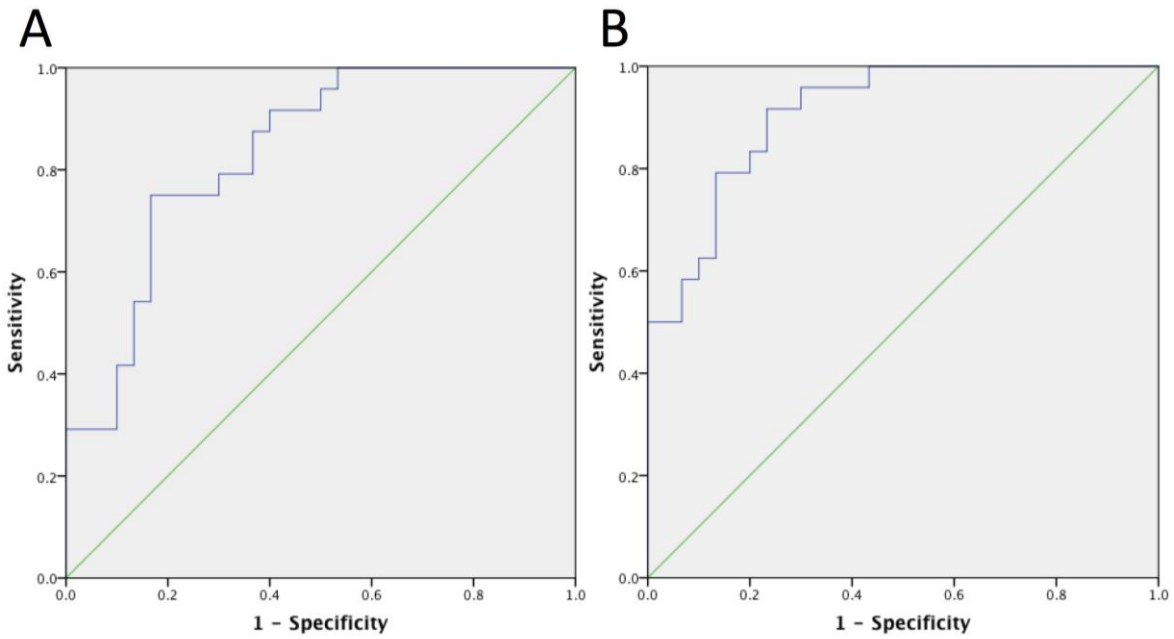

Figure 3.4: Receiver-operator characteristic curves describing the sensitivity and specificity of a range of radiopacity ratio values of the lateral (A) and medial (B) condyle to identify a horse that had sustained a lateral condylar fracture. The area under the curve of A=0.83 and B=0.91. A lateral condyle radiopacity ratio of 0.64 was determined to have a sensitivity of 75% (0.75) and specificity of 83% (1-0.17=0.83) for distinguishing those horses that suffered a lateral condylar fracture from control horses. A medial condyle radiopacity ratio of 0.65 was determined to have a sensitivity of 83% (0.83) and specificity of 80% (1-0.2=0.8) for distinguishing those horses that suffered a lateral condylar fracture from control horses.

3.5 Discussion

This study examined the cadaver bones of three groups of horses (Parkin *et al.*, 2006). The control population consists of a group bones from horses that were euthanized on UK racecourses for reasons unrelated to fracture of the distal limb. The second group of bones were the contralateral limbs of horses that suffered a lateral condylar fracture. Previous studies suggest that it is likely these bones have the pre-existing pathology observed in bones that had suffered a lateral condylar fracture (Whitton *et al.*, 2010). Lastly, the third group of bones have sustained a lateral condylar fracture. Unfortunately, specific details about the training, racing, and medical histories of these horses were not available and only limited analyses could be performed. No significant differences in the age or proportion of different sexes, the information that was available for analysis, were identified between groups. However, this study could not control for the many other factors that are known to affect the risk of fracture, such as exercise history or track surface (Parkin *et al.*,2004a). Future studies that incorporate this information into analyses are therefore warranted.

This study compared simple geometric measurements of the distal metacarpal III bone between groups. The dorsal cortical thickness ratio measurements reported in this study are similar to those previously reported in horses undergoing exercise (Davies, Gale and Baker, 1999). However, there were no significant differences in the dorsal cortical thickness between groups. As this measurement has been shown to change with exercise due to a periosteal response, this may suggest that there was no significant difference in duration of exercise history between groups (Davies, Gale and Baker, 1999). However, as this measurement did not differentiate between groups it was not investigated as a potential diagnostic test for horses at risk of fracture.

The metaphyseal angle of the distal metacarpal III bone was measured as it was hypothesized that it may be altered in response to bone development and loading, which may relate to fracture risk. The biomechanical effect of metaphyseal angle on the fetlock joint has not been previously investigated. Similar to dorsal cortical thickness ratio there was no significant difference in metaphyseal angle between groups and this was not investigated further.

The radiopacity ratio is an indirect measurement of bone density. A higher radiopacity ratio would represent more sclerotic, denser bone while a lower radiopacity radio would represent a more radiolucent, less dense area of bone. In this study, the radiopacity ratio of the lateral condyle was significantly greater in horses that had suffered a fracture (fracture and non-

fracture groups), than the control horses; this was also true of the medial condyle. This result suggests that the bone of both the distal condyles is more sclerotic, and therefore denser in those horses at risk of fracture. The findings of this study are in agreement with previous work that used CT to demonstrate higher bone volume in the lateral condyle of horses that suffered a lateral condylar fracture (Loughridge *et al.*, 2017). It also suggests that this method is quantifying the dense, modelled bone of the articular surface rather than the less dense, re-modelled bone of the parasagittal groove. Future studies could investigate the value of measuring both sites independently. Interestingly, in this study the medial condyle had a higher radiopacity ratio, and was therefore significantly denser, than the lateral condyle in the fracture group only. The medial condyle of the fracture group was the most radiodense condyle of any group. The reason for this difference is not clear. The measurement site was designed to allow measurement without interference from the fracture itself, and it is unlikely that this is the reason for this difference.

The possibility of using the radiopacity ratios as diagnostic tests to differentiate between control horses, and those that suffered a fracture was investigated using receiver-operator characteristic curve analyses. Both the lateral and medial condyle radiopacity ratios were found to be good diagnostic tests, with areas under the curve of 0.83 and 0.91 respectively. The sensitivity and specificity of measurement of the lateral condyle radiopacity ratio were reasonable at 75% and 83% respectively; the sensitivity and specificity of measurement of the medial condyle radiopacity ratio were greater at 83% and 80% respectively. While this analysis is simplistic and has significant limitations, it does demonstrate the possibility that objective radiographic measurements have the potential to differentiate between horses that suffered a fracture and those that did not. In practice, it would not be possible to perform a dorso-palmar radiograph of the distal metacarpus without superimposition of the first phalanx and proximal sesamoid bones. However, a dorsoproximal-palmarodistal oblique radiograph may limit superimposition and allow assessment of the subchondral bone of the condyle. Ultimately, more sophisticated techniques could be developed to quantify the risk of fracture in a horse and therefore prevent injury.

Chapter 4: Retrospective objective analysis of the metacarpal III bone of Thoroughbred racehorses

4.1 Introduction

Lateral condylar fractures are associated with a complex process of bone modelling and remodelling that can be identified at post mortem, and using diagnostic imaging techniques. Previous studies have attempted to determine whether it is possible to use diagnostic imaging to distinguish between horses with and without fracture, and ultimately to identify those horses at risk of fracture. In the previous chapter, it was demonstrated that using a simple radiopacity ratio it is possible to distinguish between horses that have sustained a lateral condylar fracture, and those that were euthanized for reasons unrelated to distal limb fracture with reasonable sensitivity and specificity. However, to date these studies have all used cadaver bones from horses that were euthanized on the racecourse (Tranquille, Parkin and Murray, 2012). The use of cadaver material presents significant limitations when trying to develop methods of predicting fracture. First, in this population of horses the fracture has already occurred (obviously), therefore any pre-existing changes will be advanced and may not be identifiable early enough to institute an intervention. Second, the control population in these studies is a group of horses that were euthanized on the racecourse for reasons unrelated to distal limb fracture. However, the true risk of lateral condylar fracture in these horses is unknown, as it is not possible to know whether they would have suffered a fracture in the future. Radiography of the Thoroughbred racehorse is routinely performed for a number of reasons including pre- and post-purchase assessment, and investigation of lameness or poor performance. The Singapore Turf Club purchases and imports horses in training from overseas, for the purpose of racing at Singapore Racecourse. Horses arriving at the Singapore Turf Club routinely have a series of radiographs taken including four standard fetlock projections to check for existing pathology prior to commencing training. Therefore, this radiographic resource offers the potential to compare a group of horses that have suffered a condylar fracture with a appropriate control group of horses that have raced without developing a fracture. Furthermore, by comparing radiographs taken prior to fracture with those taken at the time of fracture it may be possible to determine if there are any early radiographic indicators that distinguish horses at high and low risk of fracture. Ultimately the goal of this work would be to allow all trainers and veterinarians to implement strategies to reduce the risk of fracture.

4.2 Aims and Objectives

The hypothesis for this work was that there are significant differences in radiopacity, dorsal cortical thickness, and metaphyseal angle between Thoroughbred racehorses that have sustained a lateral condylar fracture (high risk) and those that race without sustaining a fracture (low risk). Furthermore, it was hypothesised that radiopacity, dorsal cortical thickness, and metaphyseal angle will change over time in Thoroughbred racehorses.

The principal aim of this study was to retrospectively identify differences in condylar radiopacity, dorsal cortical thickness and metaphyseal angle of the distal metacarpal III bone between horses that sustained a lateral condylar fracture, and horses that raced successfully for a further 2 years after routine radiography.

The following targeted objectives were set to accomplish this aim:

i. Objectively measure condyle opacity, dorsal cortical thickness, and metaphyseal angle of the metacarpal III bone in radiographs of racehorses that have subsequently sustained a lateral condylar fracture (high risk group) and those that raced successfully for a further 2 years (low risk group).

ii. Compare objective measures of the distal metacarpal III to identify differences between high and low risk groups.

iii. Compare objective measures of the distal metacarpal III to identify differences over time, i.e. within the high risk group.

4.3 Material and methods

4.3.1 Horses and radiography

Medical records of the Singapore Turf Club were retrospectively reviewed to identify horses that had radiography of the fetlock performed during a 12-year period between 2004 and 2016. Horses that were diagnosed with a lateral condylar fracture and had also been radiographed in the previous 24 months were identified and placed in the 'high risk' group. Horses that had fetlock radiography performed and then raced for a minimum of 2 years without suffering a fracture were placed in the 'low risk' group. Horses for which dorsoproximal-palmarodistal oblique and lateromedial radiographic views were not available were excluded. All lifetime fetlock radiographs were acquired for all horses.

4.3.2 Radiographic opacity ratio measurement

A modified method was used to measure a standardised radiopacity ratio of the distal metacarpal. Dorsoproximal-palmarodistal (20°) oblique radiographs were used to calculate bone radiopacity ratios for each distal metacarpal III to minimise superimposition of the first phalanx and sesamoid bones over metacarpal III. Specifically, a ROI of set size (8mm X 6.3mm) was drawn over the subchondral bone of the lateral and the medial condyle. A further identical ROI was drawn over an area of the lateral cortex of the distal diaphysis 4.5cm proximal to the lateral condyle. The distal metacarpal III ROIs were positioned with the axial border aligned with the intersection of the sloping surface of the sagittal ridge and the more horizontal surface of the condyle and the distal border outlined the subchondral bone surface. These ROIs therefore included the parasagittal groove region of the condyles. The radiographic opacity of the condyle ROIs was determined from the opacity measurements made with Osirix Lite 2:

Condyle radiopacity ratio = lateral or medial condyle ROI opacity/diaphysis ROI opacity

A single observer blinded to the identity of the horse measured the condyle radiopacity ratio independently three times and the mean was calculated.

4.3.3 Cortical thickness ratio measurement

The dorsal cortical thickness ratio was measured using a modified method as the nutrient foramen was not always present on the radiographs. Briefly, the mean distance between the

articular surface of the distal condyle and the nutrient foramen was calculated using the radiographs of cadaver bones (n=54) previously described in Chapter 2. This mean ± SD distance was 17.7 ± 0.68cm. To find a point approximately 2.5 cm distal to the nutrient foramen (Davies, Gale and Baker, 1999), a point was identified on each lateromedial radiograph 17.7-2.5=15.2cm proximal to the articular surface of the distal condyle. The width of the dorsal cortex (DC) and medulla (M) were measured on the lateromedial radiographs before calculating the ratio of DC/M as previously described. A single observer blinded to the identity of the horse measured the dorsal cortical thickness ratio three times independently for each radiograph and the mean value was calculated.

4.3.4 Metaphyseal angle measurement

Metaphyseal angle was measured using the method previously described in Chapter 2. The metaphyseal angle was measured using lateromedial radiographs. Firstly, a line parallel to the dorsal diaphysis was drawn through the middle of the diaphysis. The metaphysis was identified as the narrow section of the between the epiphysis and diaphysis. A second line was drawn parallel to the dorsal metaphysis through the middle of the metaphysis. The angle formed between the diaphyseal and metaphyseal lines was measured to yield the metaphyseal angle. A single observer blinded to the identity of the horse measured the metaphyseal angle three times independently for each radiograph and the mean value was calculated.

4.3.5 Statistical Analysis

A Shapiro-Wilk normality test was performed prior to data analysis. The effect of group (high risk, low risk) on the radiopacity ratio, dorsal cortical thickness, and metaphyseal angle of the horses was compared using a one-way ANOVA. The effect of time on the radiopacity ratio, dorsal cortical thickness, and metaphyseal angle of the horses was determined by comparing pre-fracture and post-fracture radiographs using a paired T-test. Statistical significance was set at $p<0.05$.

4.4 Results

4.4.1 Horses and Radiography

Sixteen gelding horses were identified that met the inclusion criteria for the high-risk group. The median age of the high-risk group at the time of fracture was 5.0 years (range 3.2-7.7 years). The median number of radiography episodes per horse was 2 (range 1-6) and the median number of days between radiography and fracture was 253 days (range 10-1183 days). The median number of career race starts for the high-risk group was 33 (range 10 – 52) (Table 4.1).

Fifteen gelding horses were identified that met the inclusion criteria for the low risk group. The median age of the low-risk group was 5.2 years at the time of radiography (range 3.3-7.0 years). The median number of radiography episodes per horse was 2 (range 1-2) and the median number of days for radiography was 369 days (range 85-1068 days). The median number of career race starts for the low risk group was 46 (range 18 – 75). (Table 4.2).

There was no significant difference in age at the time of radiography between the high- and low-risk groups (p=0.291).

4.4.2 Condyle opacity ratio measurement

4.4.2.1 Comparison between high and low risk groups

Radiographs were available for analysis of condyle opacity ratio for 16 high risk and 12 low risk group horses. The overall mean ± SD of the radiopacity ratio measured by radiography of the lateral and medial condyles were 1.02 ± 0.15 and 1.03 ± 0.16 respectively. The mean ± SD radiopacity ratio of the lateral condyle of the high and low risk groups were 1.05 ± 0.18 and 1.00 ± 0.12 respectively. The mean ± SD radiopacity ratio of the medial condyle of the high and low risk groups were 1.07 ± 0.18 and 1.00 ± 0.13 respectively (Table 4.3). There was no significant difference in radiopacity ratio between the lateral and medial condyles (Table 4.3). There was no significant difference in ratiopacity ratio between the high and low-risk groups (Table 4.3).

						High risk versus low risk analyses			Pre- & Post-fracture analyses		
Number	Date of birth	Age at fracture	Career races	No of radiographs	Days between radiographs	Radiopacity ratio	Cortical ratio	Metaphyseal angle	Radiopacity ratio	Cortical ratio	Metaphyseal angle
1	19/10/07	5.5	15	6	1183	Yes	Yes	Yes	Yes	Yes	Yes
2	10/09/17	4.6	33	2	185	Yes		Yes	Yes		Yes
3	17/08/07	6.8	52	1	0	Yes					
4	04/10/09	5.4	17	2	253	Yes	Yes	Yes	Yes	Yes	Yes
5	14/10/08	4	17	2	43	Yes	Yes	Yes	Yes	Yes	Yes
6	27/11/04	3.2	20	2	262	Yes	Yes	Yes	Yes	Yes	Yes
7	22/08/11	4.9	10	2	10	Yes		Yes	Yes		Yes
8	14/11/03	3.6	20	5	570	Yes		Yes			Yes
9	25/11/04	7.3	44	2	635	Yes		Yes			Yes
10	01/01/01	7.2	34	2	523	Yes	Yes	Yes		Yes	Yes
11	20/10/05	7.7	46	2	166	Yes	Yes		Yes	Yes	
12	26/09/06	3.7	43	2	165	Yes		Yes	Yes		Yes
13	31/10/06	5	18	2	483	Yes		Yes	Yes		Yes
14	25/11/06	7.1	49	2	162	Yes		Yes	Yes		Yes
15	23/09/05	5.2	10	2	146	Yes		Yes			Yes
16	05/08/07	4.2	36	3	254	Yes		Yes	Yes		Yes
17	01/01/04	4.0	17	2	319		Yes			Yes	

Table 4.1: Describes high risk horses history data and measurement of condyle opacity, cortical thickness and metaphyseal angle were taken pre-post fractured.

						High risk versus low risk analyses		
Number	Date of birth	Age at radiography	Career races	No of radiographs	Days between radiographs	Radiopacity ratio	Cortical ratio	Metaphyseal angle
1	17/10/08	5.4	56	1	N/A	Yes	Yes	Yes
2	31/08/06	3.9	50	1	N/A	Yes		Yes
3	08/10/06	3.7	27	1	N/A	Yes	Yes	Yes
4	25/09/07	6.3	46	1	N/A	Yes	Yes	Yes
5	05/10/07	3.4	26	1	N/A	Yes	Yes	Yes
6	19/10/07	3.3	14	1	N/A	Yes		Yes
7	06/09/08	5.4	41	1	N/A	Yes	Yes	Yes
8	25/04/04	3.7	75	2	378	Yes	Yes	Yes
9	04/08/01	5.7	43	2	85		Yes	Yes
10	07/09/02	5.7	52	2	861		Yes	Yes
11	25/02/02	7	5	2	1068		Yes	Yes
12	14/08/07	5.2	58	2	416	Yes		Yes
13	17/09/03	5.4	55	2	216	Yes	Yes	Yes
14	03/09/06	3.3	18	2	110	Yes	Yes	Yes
15	13/09/06	5	33	2	361	Yes	Yes	Yes

Table 4.2: Describes low risk horses history data and measurement of condyle opacity, cortical thickness and metaphyseal angle.

		Radiopacity ratio				
Group	N	Condyle	Mean	Std. Dev	Min.	Max.
High risk	16	Lateral	1.05	0.18	0.86	1.50
		Medial	1.07	0.18	0.90	1.60
Low risk	12	Lateral	1.00	0.12	0.71	1.24
		Medial	1.00	0.13	0.72	1.31

Table 4.3:Describing the radiopacity ratio of the medial and lateral condyles of the high and low-risk group horses.

4.4.2.2 Comparison pre- and post-fracture

Dorsoproximal-palmarodistal (20°) oblique radiographs of high-risk group horses (n=11) acquired pre- and post- fracture were available for examination to determine whether the condylar opacity ratio had changed over time. The pre-fracture radiographs were acquired a median of 265 days (range 9-262) prior to fracture.

The mean ± SD condylar opacity ratio of the lateral condyle of the high-risk group horses pre- and post-fracture were 0.98 ± 0.28 and 1.05 ± 0.14 respectively (Table 4.4). The mean ± SD condylar opacity ratio of the medial condyle of the high-risk group horses pre- and post-fracture were 0.99 ± 0.28 and 1.05 ± 0.12 respectively (Table 4.4). There was no significant difference in either lateral or medial condylar opacity ratio pre- and post-fracture.

		Radiopacity ratio				
Condyle	N	Condyle	Mean	Std. Dev	Min.	Max.
Lateral	11	Pre-fracture	0.98	0.28	0.59	1.66
		Post-fracture	1.05	0.14	0.90	1.31
Medial	11	Pre-fracture	0.99	0.28	0.54	1.69
		Post-fracture	1.05	0.12	0.92	1.22

Table 4.4: Describing the radiopacity ratio measurements of the high-risk group horse pre-and post-fracture.

4.4.3 Cortical thickness ratio measurement

4.4.3.1 Comparison between high and low risk groups

Lateromedial radiographs that included the diaphysis to a point 2.5cm distal to the nutrient foramen were available for seven high-risk horses and 12 low-risk horses. The high risk and low risk groups had median ages of 6.0 (range 3-8 years) and 4.5 (range 3-8 years) years respectively. There was no significant difference in age between groups (p=0.291).

The mean ± SD cortical thickness ratio of the high and low risk groups were 1.36 ± 0.26 and 1.08 ± 0.19 respectively (Table 4.5). The dorsal cortical thickness was significantly greater in the high risk than the low risk group (p=0.008).

	Dorsal cortical thickness ratio				
Group	N	Mean	Std. Dev	Min.	Max.
High risk	7	1.36	0.26	1.06	1.74
Low risk	12	1.08	0.19	0.72	1.38

Table 4.5: Describing the dorsal cortical thickness ratio measurements of the high and low risk groups of horses. The mean cortical thickness of the high-risk group was significantly greater than the low risk group (p=0.008).

In order to reduce the potential influence of age on dorsal cortical thickness, the analysis was repeated with six high-risk horses and six age-matched control low-risk horses. The mean ± SD cortical thickness ratio of the age-matched high and low risk groups were 1.41 ± 0.24 and 0.98 ± 0.17 respectively (Table 4.6). The dorsal cortical thickness was significantly greater in the high risk than the low risk group (p=0.005).

	Dorsal cortical thickness ratio				
Age-matched Groups	N	Mean	Std. Dev	Min.	Max.
High risk	6	1.41	0.24	1.17	1.74
Low risk	6	0.98	0.17	0.72	1.22

Table 4.6: Describing the dorsal cortical thickness ratio measurements of age-matched high and low risk groups of horses. The mean cortical thickness of the high-risk group was significantly greater than the low risk group (p=0.005).

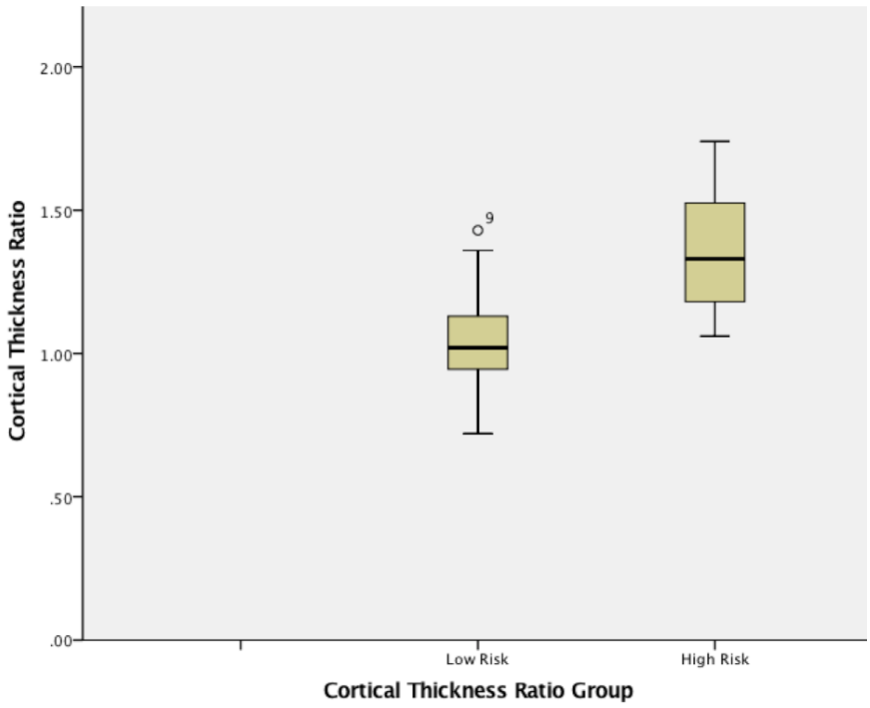

Figure 4.1: Box and whisker plot describing the distribution of the dorsal cortical thickness ratio of the low and high risk groups. The dorsal cortical thickness was significantly greater in the high risk group than the low risk group (p=0.008).

4.4.3.2 Comparison pre- and post-fracture

Radiographs of the high-risk group horses acquired pre- and post- fracture were examined to determine whether the dorsal cortical thickness ratio had changed over time. The pre-fracture radiographs were acquired a median of 253 days (range 43-523) prior to fracture.

The mean ± SD cortical thickness ratio of the high group horses pre- and post-fracture were 1.09 ± 0.16 and 1.36 ± 0.26 respectively (Table 4.7, Fig 4.2). The dorsal cortical thickness was significantly greater in the post-fracture than the pre-fracture group (p=0.006).

	Dorsal cortical thickness ratio				
Group	N	Mean	Std. Dev	Min.	Max.
Pre-fracture	7	1.09	0.16	0.88	1.39
Post-fracture	7	1.36	0.26	1.06	1.74

Table 4.7:Describing the dorsal cortical thickness ratio measurements of the high-risk group horse pre-and post-fracture (p=0.006).

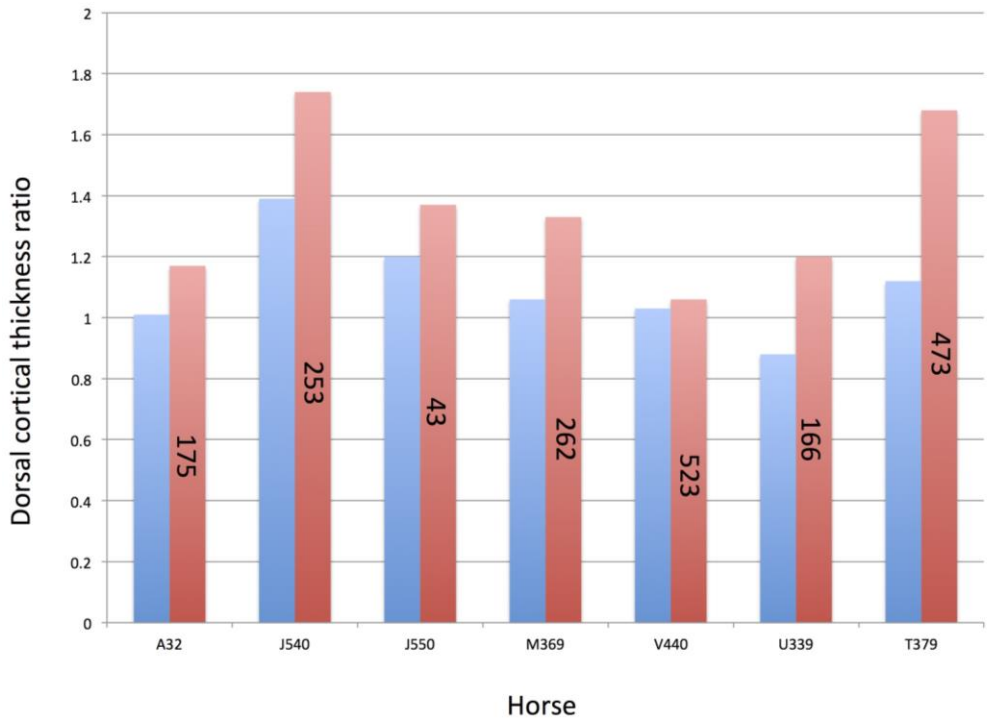

Fig 4.2: Bar graph displaying the dorsal cortical thickness of high-risk group horses (n=7) pre-fracture (blue bars) and post-fracture (red bars). The number of days between radiographs are displayed within the post-fracture (red) bars.

4.4.4 Metaphyseal angle measurement

4.4.4.1 Comparison between high and low risk groups

Lateromedial radiographs were available for high-risk horses (n=14) and low risk horses (n=15). The high risk and low risk groups had median ages of 4.95 (range 3.2-7.2 years) and 5.2 (range 3.3-7.0 years) respectively. There was no significant difference in age between groups (p=0.291).

The mean ± SD metaphyseal angle of the high and low risk groups were 9.65 ± 2.21 and 6.95 ± 1.65 respectively (Table 4.8, Fig 4.3). The metaphyseal angle was significantly greater in the high risk than the low risk group (p=0.000).

	Metaphyseal angle (°)				
Group	N	Mean	Std. Dev	Min.	Max.
High risk	14	9.65	2.21	6.80	15.23
Low risk	15	6.95	1.65	4.00	9.50

Table 4.8: Describing the metaphyseal angle measurements of the high and low risk groups of horses. The mean metaphyseal angle of the high-risk group was significantly greater than the low risk group (p=0.000).

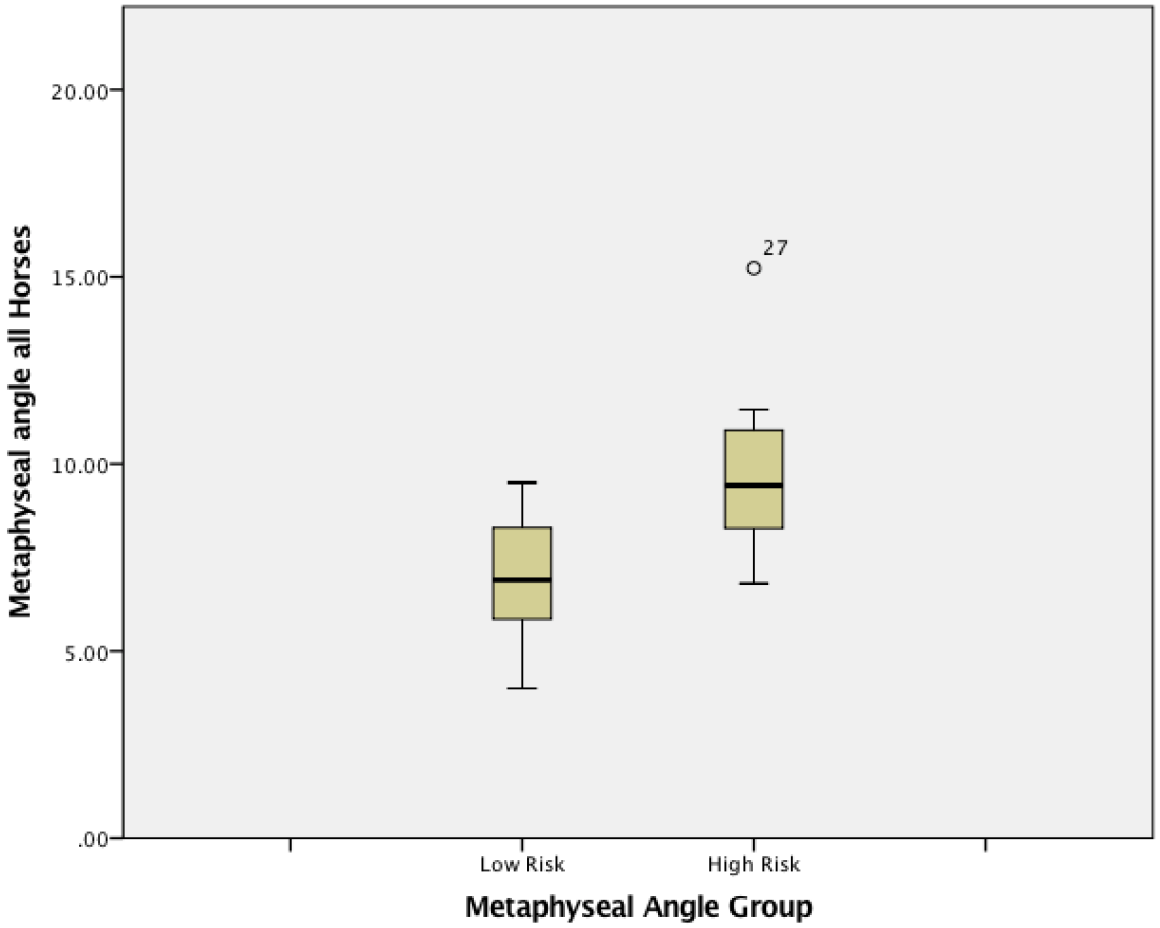

Figure 4.3: Box and whisker plot describing the distribution of the metaphyseal angle of the low and high-risk groups. The metaphyseal angle was significantly greater in the high-risk group than the low risk group (p=0.000).

In order to reduce the potential influence of age on metaphyseal angle, the analysis was repeated with six high-risk horses and six age-matched control low-risk horses. The mean ± SD metaphyseal angle of the age-matched high and low risk groups were 9.33 ± 1.32 and 6.57 ± 1.09 respectively (Table 4.9). The metaphyseal angle was significantly greater in the high risk than the low risk group (p=0.003).

	Metaphyseal angle (°)				
Age-matched Groups	N	Mean	Std. Dev	Min.	Max.
High risk	6	9.33	1.32	7.30	11.30
Low risk	6	6.57	1.09	5.40	8.10

Table 4.9: Describing the metaphyseal angle measurements of age-matched high and low risk groups of horses. The metaphyseal angle of the high-risk group was significantly greater than the low risk group (p=0.003).

4.4.4.2 Comparison pre- and post-fracture

Radiographs of the high-risk group horses acquired pre- and post- fracture were examined to determine whether the metaphyseal angle had changed over time. The pre-fracture radiographs were acquired a median of 253 days (range 43-523) prior to fracture.

The mean ± SD metaphyseal angle of the high risk group horses pre- and post-fracture were 8.33° ± 2.05° and 9.66° ± 2.21° respectively (Table 4.10). The metaphyseal angle was significantly greater in the post-fracture than the pre-fracture group (p=0.001).

	Metaphyseal angle (°)				
Group	N	Mean	Std. Dev	Min.	Max.
Pre-fracture	14	8.33	2.05	5.63	14.10
Post-fracture	14	9.66	2.21	6.80	15.23

Table 4.10: Describing the metaphyseal angle measurements of the high-risk group horse pre-and post-fracture (p=0.001).

4.5 Discussion

Previous studies have demonstrated that advanced diagnostic imaging modalities such as MRI and quantitative CT can distinguish between horses that have suffered a lateral condylar fracture and those that have not (Trope *et al.*, 2015). However, the clinical applicability of these studies is limited by the lack of availability of these technologies and validation in a population of racehorses. These studies are also limited by their control samples, which are taken from horses of unknown fracture risk. The purpose of this study was to investigate whether radiography, a widespread and economical diagnostic imaging modality could be used as a means of distinguishing between horses of low and high-risk of lateral condylar fracture. A previous chapter (Chapter 3) demonstrated that a radiopacity ratio that standardised the opacity of the parasagittal groove to an aluminium phantom, was able to distinguish between horses that suffered a lateral condylar fracture, and horses euthanized for other reasons. In the current study, no significant difference were found in the radiopacity ratios of horses that suffered a lateral condylar fracture (high risk) and those that did not. However, the retrospective nature of this current study meant that there were a number of limitations. Firstly, the aluminium phantom was not used during radiography and therefore the standardised ratio as previously described could not be obtained. Instead, to account for variation in radiopacity due to exposure factors the radiopacity of the diaphysis of the third metacarpal bone was used as a reference point. Similar techniques have been described previously in diagnostic imaging, for example in scintigraphy (Parker *et al.*, 2010). However, this may have been one reason that the results of the cadaver study were not replicated in this study. A second reason may be the different radiographic view used in this study. The current study used dorsoproximal-palmarodistal (20°) oblique radiographs to minimize the superimposition of the distal metacarpal condyle, and the proximal phalanx whereas the cadaver study used straight dorsal-palmar views. While superimposition was minimised, it could not always be completely eliminated and future investigation of alternative radiographic views e.g. flexed dorsal 125° distal palmaro-proximal oblique. Finally, the control group in the cadaver study was more than twice the size of the low risk group in this study. Based on the results of this chapter and Chapter 3, a large prospective study including the use of an aluminium phantom and standardised exposures to minimize variation would be necessary to determine if radiopacity ratios are truly clinically useful in predicting fracture.

In this chapter, dorsal cortical ratio was determined for horses at high and low-risk of fracture. Overall, the dorsal cortical ratio of horses at low-risk of fracture (1.08) was very

similar to that described in the previous chapter for control horses (1.04), and only slightly different from a previous report of racehorses free from shin soreness (1.15) (Davies, Gale, and Baker, 1999). Similar to a previous report, this study found that the dorsal cortical ratio increased significantly in racehorses from 1.09 to 1.36 over an average of 253 days in horses at high-risk of fracture. Modelling of the dorsal cortex of metacarpal III in response to the strain associated with exercise and racing has been previously described (Davies, Gale, and Baker (1999), Sherman *et al.*, 1995). However, it has not been associated with the risk of fracture. In the current study, the dorsal cortical ratio was significantly greater in horses at high-risk of fracture than those at low risk. This could be due to differences in the age or exercise history of the horses. However, there was no significant difference in age at the time of radiography between groups and an age-matched comparison was performed that supported this finding. Unfortunately, other than the number of races entered in Singapore there is no information on exercise history available. Therefore, it is possible that the greater dorsal cortical thickness in the horses at high-risk reflects greater exercise than the low-risk horses. This supports other research that links exercise history with risk of condylar fracture (Muir *et al.*, 2008). In the future, measurement of dorsal cortical thickness may provide a method of assessing the risk of condylar fracture in racehorses.

In Chapters 2 & 3, the relationship between the diaphysis and metaphysis was described using the metaphyseal angle, which has not previously been reported. Geometrical measurement of the relationship between the diaphysis, metaphysis and epiphysis of the femur in humans has been described as the femoral neck shaft angle (NSA) (Ripamonti, Lisi and Avella, 2014). The NSA changes during growth and development; initially it is approximately 150° and becomes more acute in the adult (120°) in response to loading, modelling and development (Dobbs and Morcuende, 1986). NSA has been linked to the risk of fracture in patients with osteoporosis as it affects the biomechanics of the hip; a more obtuse angle results in a higher bending moment at the femoral neck in the event of an impact on the femur (Ripamonti, Lisi and Avella, 2014). In the current study, the metaphyseal angle of the low-risk horses (6.95°) was very similar to the value reported in the horses in Chapter 2 (6.92°). Interestingly, in this study the metaphyseal angle was found to be significantly greater (9.33°) in the high-risk group when compared to the low risk group. In addition, the metaphyseal angle increased over time in horses in the high-risk group, from a median of 8.33° to 9.66° at the time of fracture. These findings are interesting as they suggest that the relationship between the metaphysis and diaphysis can change over time, as has been shown in the human. Similar to other changes in the metacarpal bone, this increase in the angle may be the result of loading and bone modelling and therefore reflects the exercise history of the

horse. The difference in metaphyseal angle between high and low-risk group horses may therefore reflect either a difference in exercise history. The relationship between metaphyseal angle and fracture risk may be biomechanical, or simply reflects other factors that influence fracture risk.

Chapter 5: Evaluation of the density of the palmar distal metacarpal III bone of Thoroughbred racehorses

5.1 Introduction

In Thoroughbred racehorses, exercise results in increased volume of trabecular bone mineral in the distal epiphysis of third metacarpal III. In contrast, there is only minimal increase in volumetric diaphyseal cortical bone mineral density in response to exercise (Firth *et al*,. 2005). Modelling is an adaptation phase during which bone adjusts itself to the current loading circumstances; however, this may contribute to increased bone density in the distal third metacarpal condyle leading to stress fracture (Whitton *et al.*, 2010). There is also evidence of microcracking, microfracture, and osteoclastic remodelling in the dense regions of the palmar aspect of the epiphysis of the third metacarpal bone (Stepnik *et al.*, 2004). Fractures typically occur in areas of high-density, remodelled bone (Whitton *et a.*, 2010). The regions of increased bone mineral density are associated with increased brittleness, and it is this fragility that may play a role in the development of condylar fractures (Les *et al*., 2002).

It was suggested by Riggs, Whitehouse and Boyde, (1999) that significant density gradients between the denser condyles and the subchondral bone of the sagittal groove could lead to stress concentration at the palmar/plantar aspect of the parasagittal grooves, which may predispose to fracture. On a similar stance, Loughridge *et al* (2017) have pointed out that an increase in bone heterogeneity is associated with lateral condylar fracture and marked increase in bone density tends to establish focal areas of stress and therefore predispose limbs to fracture.

A previous study compared bone mineral density of the distal condyle between metacarpal III bones with and without fracture. While no significant differences were found between groups, the CT images of the fracture group tended to have fewer voxels with low density and more voxels with high density in the region abaxial to the parasagittal groove suggesting that fracture is associated with high bone density (Bogers *et al.*, 2016). However, this previous study relied on a small population of young horses and one horse contributed two of the fractured limbs (Bogers *et al*., 2016).

Previous chapters have looked at radiographic methods of studying the metacarpal III bone of Thoroughbred racehorses. In this chapter, CT will be used to determine the maximum density of the distal condyle and examine whether this differs between horses that have suffered a condylar fracture, and horses euthanized for other reasons. In addition, the relationship between age and maximum density will be investigated and finally the relationship between maximum CT density and the previously described radiopacity ratio will be examined.

5.2 Aims and Objectives

The hypothesis for this work was that the maximum density of the condyles of the distal metacarpal III bone from Thoroughbred racehorses measured by computed tomography is greater in bones from horses with lateral condylar fracture compared to those without fracture. Furthermore, it was hypothesised that maximum density would be related to age, and therefore the duration of exercise a horse had experienced. Finally, we hypothesised that the maximum density measured using computed tomography (CT) would correlate with the maximum density (radiopacity) measured using radiography.

The principal aim of this study was to investigate the relationships between the density of the condyle and the risk of fracture, age, exercise history, and radiopacity of the condyle.

The following targeted objectives were set to accomplish this aim:

i. Determine the density of the condyle of the distal 3rd metacarpal bone in cadaver specimens from Thoroughbred racehorses using a computed tomography (CT) method.

ii. Compare the maximum density of bones with lateral condyle fracture, non-fractured bones from the contralateral limbs, and normal control bones (from horses euthanized for reasons unrelated to distal limb fracture).

iii. Compare the maximum density of the medial and lateral condyles.

iv. Determine whether there is a correlation between maximum density and the age of the horse.

v. Determine whether there is a correlation between the maximum density determined by CT and radiography.

5.3 Material and Methods

5.3.1 Horses

Cadaver metacarpal III bones (n=27) with the distal carpus but without soft tissues that were obtained from a previous study were used for this study (Parkin *et al.*, 2006). The bones were classified in to three groups based on the presence or absence of a lateral condylar fracture. Bones in the control group (n=10) were obtained from horses euthanized on racecourses as a result of injuries unrelated to fracture of the distal limb (including fracture of the neck or back and cardiovascular pathology); non-fractured group (n=8) bones were obtained from the contralateral limb of horses that sustained a lateral condylar fracture of the metacarpal bone III; fracture group (n=9) bones were obtained from the fractured limb of horses that sustained a lateral condylar fracture of the metacarpal III bone.

5.3.2 Computed Tomography

Quantitative CT of metacarpal bones was performed as previously described (Les *et al.*, 1994). Briefly, limb specimens were placed in a custom made Perspex support with a phantom consisting of five tubes containing distilled water and a solution of potassium phosphate (K_2HPO_4) at concentrations of 0, 50, 100, 200 and 300mg/mL (Fig 5.1). A computed tomography (CT) study of each limb was performed using a clinical CT machine (Somatom Spirit, Siemens) with settings of 130kV/30mAs, 2 x 1.5mm detector collimation and 0.5mm slice thickness. Field of view was 12cm, image matrix size was 512*512, and average voxel size was $0.24mm^3$ (0.28x0.28x3.0mm). The image included the distal metacarpal bone and the potassium phosphate phantoms. The images were stored as DICOM files for subsequent analysis using commercial software (Osirix Lite 2).

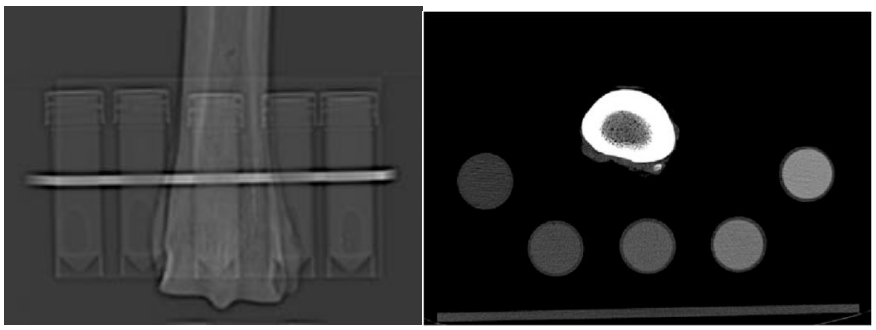

Figure 5.1: Pilot CT image (left) and transverse CT image (right) demonstrating arrangement of bone and phantom.

A 1cm^2 region of interest was placed over each phantom tube and the brightness was measured in Hounsfield units. Simple linear regression was performed to quantify the relationship between CT Hounsfield units and potassium phosphate concentration (mg/mL); the relationship between Hounsfield units and potassium phosphate equivalent was assumed to remain linear outwith the range of the phantom (0-300mg/mL) (Les *et al.*, 1994).

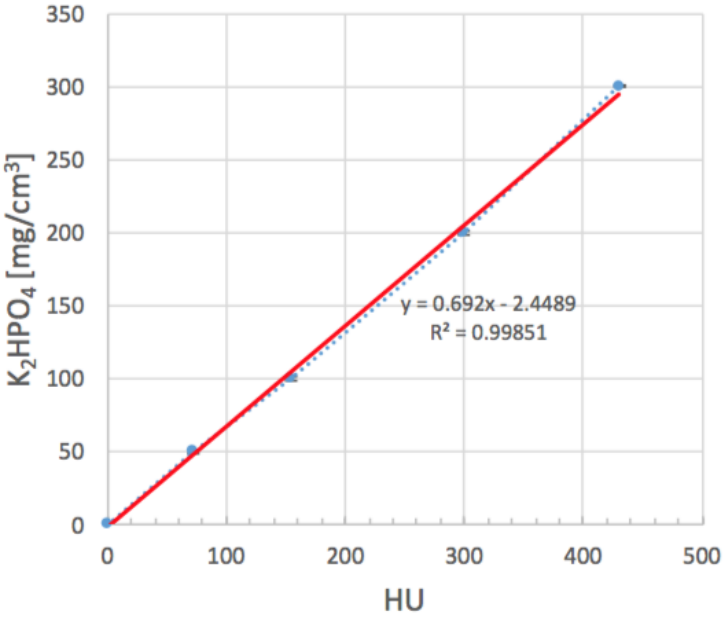

Figure 5.2: Linear regression analysis of the relationship between CT number (Hounsfield units, HU) and K_2PO_4 (mg/cm^3).

5.3.3 Radiography

The cadaveric bones were removed from -20°C storage and thawed at room temperature for 24 hours prior to radiography. Each limb was positioned on a radiographic cassette (AGFA, CR35-X, 3.0mm) so that the palmar surface was on the cassette and the long axis of the metacarpal III was parallel with the cassette and a 2mm aluminium radiographic phantom was placed laterally. The lateral side was identified using the anatomy of the carpus. Using a clamp for positioning, a dorsopalmar (DP) and a lateromedial (LM) projection were obtained for each specimen using exposure factors of 62kV/10mAs and 60kV/10mAs respectively. All radiography was performed using a film focus distance of 80 cm. The images were stored as DICOM files for subsequent analysis.

The standardised radiopacity of the distal metacarpal was described using a ratio of the bone radiopacity and the phantom radiopacity as previously described in Chapter 2. The dorsopalmar radiographs were used to calculate bone radiopacity ratios for each distal metacarpal III. Specifically, a square ROI of set size (8mm X 6.3mm) was drawn over the

subchondral bone of the lateral and the medial condyle. A further identical ROI was drawn over the phantom so that its boundaries were within the area of 2mm thick aluminium. The distal metacarpal III ROIs were positioned with their axial border aligned with the intersection of the sloping surface of the sagittal ridge and the more horizontal surface of the condyle and their distal border outlined the subchondral bone surface. These ROIs therefore included the parasagittal groove region of the condyles. The radiographic opacity of the condyle ROIs was determined from the opacity measurements made with Osirix Lite 2:

Condyle radiopacity ratio = lateral or medial condyle ROI opacity (X)/phantom ROI (Y) opacity

A single observer measured the condyle radiopacity ratio independently three times and the mean calculated.

5.3.4 Image analysis

CT images were converted from DICOM to metafile (.mhd) format using commercially available software (Osirix). The metafiles analysed to determine the maximum density of the medial and lateral palmar condyles using open-source image visualization and analysis software (Paraview, NTESS, Kitware Inc). Briefly, the .mhd file format images were opened (Fig 5.3A) and the thresholding tool was used to select the bone (Fig 5.3B). An ‘inside out’ spherical clip tool was used to select only the region of the condyle extending abaxially to the parasagittal groove and the density information was rescaled to the data range (Fig 5.3C). A spreadsheet of all data points within the clipped condyle region was created and sorted to determine the maximum density value (Fig 5.3D).

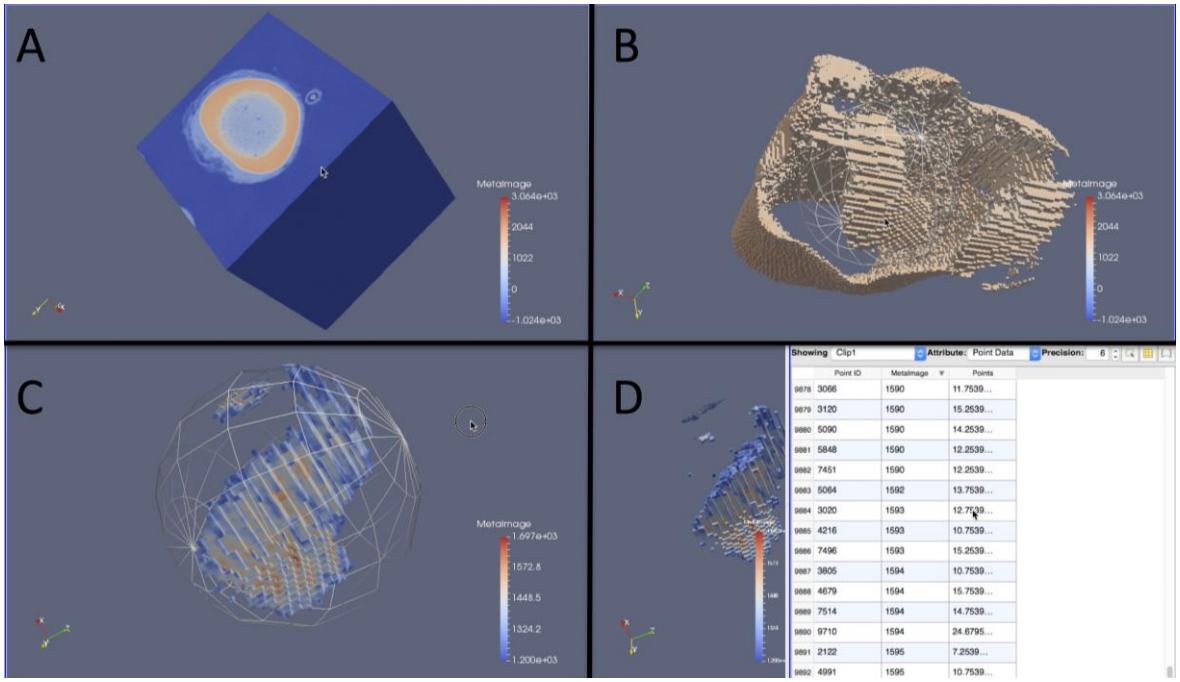

Figure 5.3: Analysis of CT images using Paraview software to determine the maximum density value of the condyles. Images were opened (A) and the thresholding tool was used to select the bone (B). An 'inside out' spherical clip tool was used to select only the region of the condyle and the density information was rescaled to the data range (C). A spreadsheet of all data points within the clipped condyle region was created and sorted to determine the maximum density value (D).

5.3.5 Data analysis and statistics

The maximum bone density determined by CT was expressed as Hounsfield units and K_2HPO_4 equivalent density. The mean maximum bone density was compared between groups and between the lateral and medial condyles using a two-way ANOVA with a Tukey's *post hoc* test. Statistical significance was set at $p<0.05$.

The correlation between the density of the condyle determined by CT and radiography was determined using Pearson's correlation coefficient. Statistical significance was set at $p<0.05$.

5.4 Results

The horses that were the source of the cadaver bones used in this study are described in Table 5.1.The mean ± SD age of all horses was 6.44 ± 2.25 years. There was no significant difference in age (p=0.326) or sex (p=0.287) between groups.

Group	No	Gelding	Female	Mean ± SD age (years)	Median age (years)
Control	10	10	0	7.00±2.71	7
Non Fractured	8	7	1	6.38±3.16	6
Fractured	9	7	2	6.44±2.30	7

Table 5.1: Describing the sex and age distribution of the horses from which the cadaver bones used in this study were collected (Parkin *et al.*, 2006). There was no significant difference in age or sex distribution between groups.

The mean ± SD maximum bone density (Hounsfield units) of the lateral condyle region of the control, non-fractured, and fractured groups were 1720 ± 54.23, 1695.88 ± 44.30, and 1726.78 ± 104.15 (Table 5.2). There was no significant difference in maximum bone density (Hounsfield units) of the lateral condyle region between groups.

The mean ± SD maximum bone density (Hounsfield units) of the medial condyle region of the control, non-fractured, and fractured groups were 1705 ± 82.58, 1710.38 ± 81.93, and 1695.22 ± 65.63 (Table 5.2). There was no significant difference in maximum bone density (Hounsfield units) of the medial condyle region between groups. There was no significant difference between the medial and lateral condyle regions.

Group	N	Condyle	Mean	Std. Dev	Min.	Max.
Control	10	Lateral	1720.00	54.23	1606.00	1797.00
		Medial	1705.10	82.58	1609.00	1863.00
Non Fractured	8	Lateral	1695.88	44.30	1632.00	1759.00
		Medial	1710.38	81.93	1620.00	1879.00
Fractured	9	Lateral	1726.78	104.15	1642.00	1980.00
		Medial	1695.22	65.63	1624.00	1829.00

Table 5.2: Describing the maximum density (Hounsfield units) of the medial and lateral condyle regions of the medial and lateral condyles of control, non-fractured, and fractured bones. There was no significant difference between groups.

The mean ± SD maximum bone density (K_2HPO_4 equivalent density) of the lateral condyle region of the control, non-fractured, and fractured groups were 1201.55 ± 37.96, 1184.66 ± 31.01, and 1206.29 ± 72.90 (Table 5.3). There was no significant difference in maximum bone density (K_2HPO_4 equivalent density) of the lateral condyle region between groups.

The mean ± SD maximum bone density (K_2HPO_4 equivalent density) of the medial condyle region of the control, non-fractured, and fractured groups were 1191.12 ± 57.80, 1194.81 ± 57.35, and 1184.21 ± 45.93 (Table 5.3). There was no significant difference in maximum bone density (K_2HPO_4 equivalent density) of the medial condyle region between groups. There was no significant difference between the medial and lateral condyle regions.

Group	N	Condyle	Mean	Std. Dev	Min.	Max.
Control	10	Lateral	1201.55	37.96	1255.45	1121.75
		Medial	1191.12	57.80	1301.65	1123.85
Non Fractured	8	Lateral	1184.66	31.01	1228.85	1139.95
		Medial	1194.81	57.35	1312.85	1131.55
Fractured	9	Lateral	1206.29	72.90	1383.55	1146.95
		Medial	1184.21	45.93	1277.85	1134.35

Table 5.3:Describing the maximum density (K_2HPO_4 equivalent density) of the medial and lateral condyle regions of the medial and lateral condyles of control, non-fractured, and fractured bones. There was no significant difference between groups.

There was a significant correlation between age and both maximum lateral condyle density (r=0.44, p=0.019) and maximum medial condyle density (r=0.54, p=0.003) (Fig 5.4). There was no significant correlation between radiopacity ratio and CT measurement of maximum density for any group.

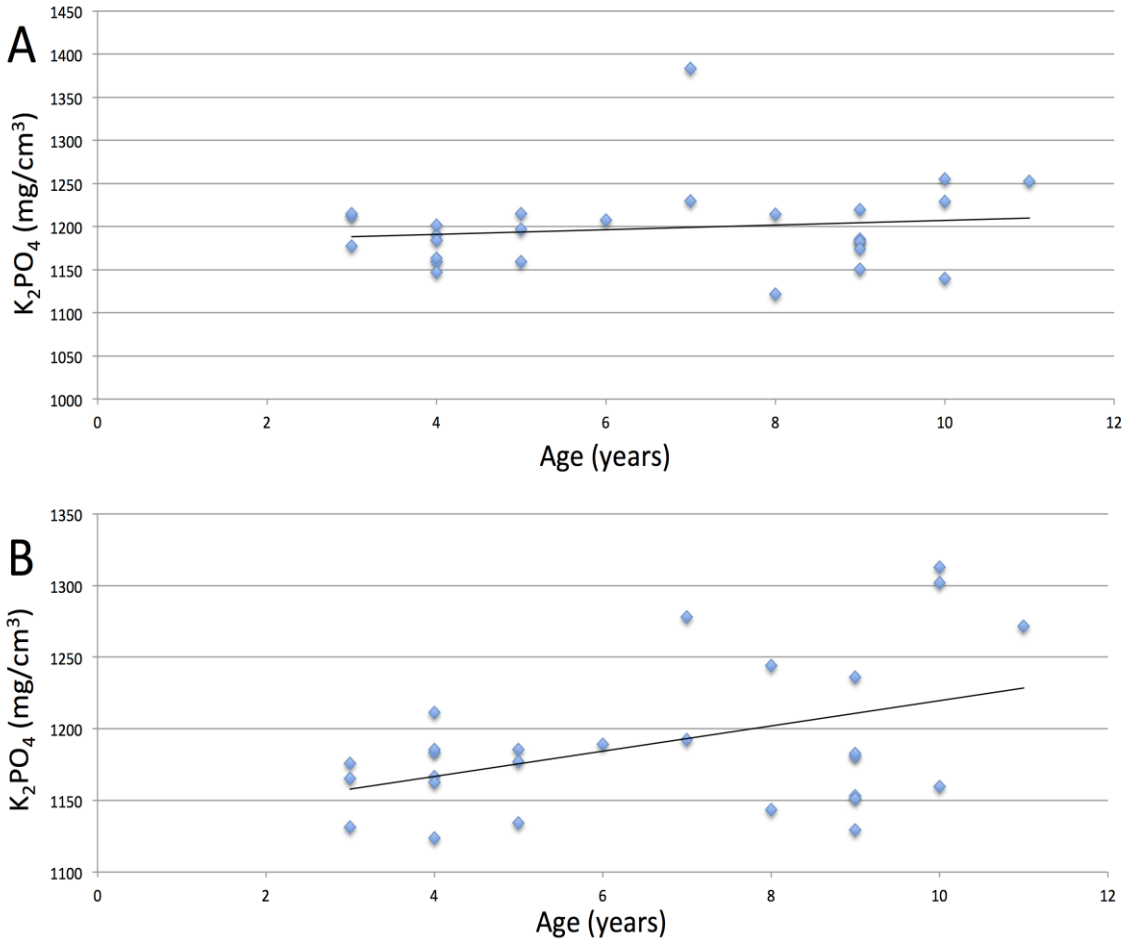

Figure 5.4:Scatter plots displaying the age and K_2HPO_4 equivalent density of the lateral (A) and medial (B) condyle regions for all horses. There was a significant correlation between age and both maximum lateral condyle density (A, r=0.44, p=0.019) and maximum medial condyle density (B, r=0.54, p=0.003)

5.5 Discussion

In this study, condyle density was examined with quantitative computed tomography using an open-source image visualization and analysis software (Paraview, NTESS, Kitware Inc) and a potassium phosphate phantom (K_2PO_4) using a method similar to that previously described by Les *et al*, (1994). The K_2PO_4 equivalent density determined using CT has previously been shown to have excellent correlation with wet, dry and ash density of equine bone (Les *et al*, 1994).

The current study compared the maximum density in the region of the medial and lateral condyles between groups of horses that had suffered a condylar fracture, or were euthanized for other reasons. Compared to a previous study, a greater number of horses of a wider range of ages were examined in this study (Bogers *et al.,* 2016). However, similar to the previous study no significant difference was found in the maximum bone density of the palmar condyle between groups (Bogers *et al.*, 2016).

It has been shown that significant changes in bone density are associated with age and training (Firth *et al.,* 2005). To determine whether there was an effect of age among horses and groups on the analysis, the age of horses was compared between groups and no significant difference was identified; the groups had similar mean and median ages. Unfortunately, information regarding the training and racing histories of the horses were not available and therefore these factors could not be taken into account. Further evidence for the effect of age and training was found in the regression analyses of bone density. Significant, moderate levels of correlation were found between the age of the horse and the maximum density of both the lateral and medial condyles.

In Chapter 3, significant differences were found in the radiopacity of the lateral condyle between groups. The region of interest analysed in the current study should have incorporated the same area examined in the radiography study. In the current study no significant difference was found between groups using CT and no correlation was identified between CT density data and radiopacity. This may reflect the differences between these two methods of evaluating bone density. While radiography represents the ‘average’ bone density of the three-dimensional bone measured over a region of interest, the CT method employed in this study simply identified the single highest pixel density value. While, the CT method employed in this study was simplistic, the results are in agreement with a previous study that used more complex analyses (Boger *et al.*, 2016).

Chapter 6: Overall Discussion and Conclusion

6.1 Overall Discussion

The purpose of this study was to investigate the potential of novel and existing radiographic measurements to detect Thoroughbred racehorses at risk of lateral condyle fracture. Condylar fracture is usually preceded by pathological fatigue damage, and therefore an opportunity may exist to evaluate these pre-existing changes before the fracture occurs using a diagnostic imaging modality (Morgan *et al.*, 2006). Radiography is a diagnostic imaging technique that could potentially be used to examine the premonitory changes that occur in the distal metacarpal III of Thoroughbred racehorses and determining whether these changes may be used to identify horses at increased risk of fracture. While radiography is a long established technique with well-recognized limitations, it remains the most frequently used diagnostic imaging modality in equine practice. Radiographs are economical and easily acquired compared with more recently developed techniques such as MRI and CT.

The first study described in chapter two validated three methods to quantify radiopacity and bone geometry including condyle opacity, cortical thickness and metaphyseal angle using cadaver bones. In this chapter, radiographic findings were compared with computed tomography to determine the correlation between them. In chapter three, the study focused to identify differences in condylar radiopacity, dorsal cortical thickness and metaphyseal angle of the distal metacarpal III cadaver bone between horses that sustained a lateral condylar fracture and horses that were euthanized for other reasons. In chapter four, the previously described novel measurements including condyle opacity, cortical thickness and metaphyseal angle were applied to a series of clinical radiographs obtained over a period of years from Thoroughbred race horses trained and raced under similar conditions. These radiographs were taken both prior to and post fracture from horses that sustained a condylar fracture, and from horses that raced for a minimum of 2-years and did not sustain a fracture. This allowed comparison between horses that were at high risk (fractured) with horses at low risk (control) of lateral condylar fracture. The final chapter (chapter 5), examined the relationship between the maximum bone density as determined by CT and radiography and investigated further the impact of age on condyle maximum density.

The results presented in the second chapter, describe the validation of the three proposed novel measurements (condyle opacity, cortical thickness and metaphyseal angle) by radiography. Firstly, these measurements were performed in triplicate by a single observer, and it was found that there was no significant difference between these repeated measurements. Secondly the correlation between radiography measurements and CT, a golden standard modality was determined. Examination of bone mineral density has been applied to the assessment of fracture risk in human subjects. Bone mineral density (BMD) measurement of the hip is the strongest predictor of hip fracture (Gnudi, Sitta and Pignotti, 2012). Both radiography and CT identified the existence of mineralisation (density) along the distal III metacarpal bone and this significantly lower in the lateral condyle than the medial condyle. However, radiopacity measurements by radiography and CT were poorly correlated. This is in agreement with a previous study, in which there were no significant correlations for erosion, cracking, and sclerosis of the subchondral plate, as detected by both CT, MRI and radiography in equine third metacarpal bone (O'Brien *et al.*, 2011). Other reasons for the difference between methods may relate to fundamental differences in techniques. A previous study found that pathologic features such as linear defects in the mineralized articular cartilage and subchondral bone which precede development of a condylar fracture were presented differently by radiography and CT, and standard radiography yields incomplete information about condylar fractures, but cross sectional imaging modalities like CT are more comprehensive (Morgan *et al.*, 2006). In summary, despite of weak correlation between radiography and CT for condyle opacity assessment, both modalities identified greater opacity or sclerosis in the medial condyle.

Cortical thickness measurement was investigated because it has been shown to change with exercise and training (Davies, Gale, and Baker,1999), factors that play a role in condylar fracture (Parkin *et al*., 2004). Cortical thickness measurements performed using radiography and CT were strongly correlated, in agreement with the findings of a previous study (Yamada *et al.*, 2016). In the human field, a study comparing proximal humeral cortical thickness measurement between radiography and dual-energy x-ray absorptiometry (DXA) found a strong correlation (Mather *et al.*, 2013). Radiography cortical thickness measurement in Thoroughbred horses was compared with that of ultrasound and it was found that a significant linear relationship exists between ultrasound speed and radiographic bone size and shape measurements (Davies, 2002). Thus, there is evidence to support radiography as a potential method of monitoring cortical thickness variation in Thoroughbred racehorses at risk of condyle fracture.

A strong correlation was found between radiographic and CT measurements of metaphyseal angle. This suggests that although radiography has the limitations of variation in positioning and superimposition, it is possible to accurately measure the relationship between the diaphysis and metaphysis on a radiograph.

In chapter three, radiography was used to examine condyle opacity (sclerosis), cortical thickness and metaphyseal angle between control, non fractured and fractured cadaver bones that were collected from euthanized racing Thoroughbred horses. In respect to condyle opacity measured by radiography, it was significantly greater in both the fracture and non-fracture groups than the control group. This is an agreement with a previous study that pointed out that subchondral sclerosis was significantly different between the control and fracture groups as determined by a range of imaging modalities including radiography, CT and MRI (O'Brien *et al.,* 2011). This trend was observed in both the lateral and medial condyles. The findings of this study are in agreement with a previous study that used CT to demonstrates higher bone volume in the lateral condyle of horses that suffered a lateral condylar fracture compared to non fractured and control bones (Loughridge *et al*. 2017). This is contrary to De Lasalle *et al.*, (2016) who observed less density in osteoarthritic medial condyle femur of horses imaged by CT, but these changes were the result of chronic stifle disease and active condyle bone resorption. Interestingly, this is the case in human severe chronic femorotibial osteoarthritis too (Buckland, *et al.*,2007). The variation in subchondral bone density between fractured and non fractured and control racing Thoroughbreds is attributed to suppression of remodelling (bone repairing phase) as a result of rapid fatigue cyclic loading by modelling process (bone adaptation phase). Fatigue fractures and subchondral bone injuries occur when micro damage accumulates by modelling (bone formation) faster than can be repaired by remodelling (bone resorption). This coincides with less bone resorption and more bone formation in the subchondral bone of highly loaded areas of the distal metacarpus limiting the replacement of fatigued bone (Holmes *et al.*, 2014). This results in a decrease in subchondral bone porosity and subsequent transfer the mechanical force to trabecular bone, which induces thickening of bone trabecular leading to brittle bone and fracture (Whitton *et al.*, 2010). Bones that are involved in galloping or racing in addition to the third metacarpal, include the first phalanx that has a rotary movement between its parasagittal groove proximally and the distal metacarpal III sagittal ridge. This induces compressive and torsional forces and this bone is reported to develop regions of dense bone at the parasagittal groove, which is greater in fractured racing Thoroughbred relative to control (Noble, Singer and Jeffery, 2016).

In human athletics it was shown by Liu *et al.*, (2003) that young female athletes who engage in impact loading sports, such as volleyball and gymnastics, have a greater bone mineral density at a majority of skeletal sites.

The density of the medial condyle of non fractured and fractured horses had greater density when compared to contrast when measured by both radiography and computed tomography. A previous study found that the density of the medial condyle of horses in training was greater than in those not in training, and suggested that this is likely due to a response to microfracture (Bani Hassan *et al.*, 2017). This is supported by Young *et al.*, (2007) who claimed that the distal metacarpal III palmaromedial zone was significantly more dense than the palmarolateral. The medial condyle has been shown to sustain more load than the lateral compartment in the Thoroughbred femoral condyle (Walker, Kawcak and Hill, 2013). This has also been reported in healthy and osteoarthritic human knees and this unbalance has been reported to increase with medial knee osteoarthritis (Omoumi *et al.*, 2017). The results of this study suggest that the lateral and medial distal condyles are more sclerotic, and therefore denser in those horses at risk of fracture. Both the lateral and medial condyle radiopacity ratios were found to be good diagnostic tests, with areas under the curve of 0.83 and 0.91. The sensitivity and specificity of measurement of the lateral condyle radiopacity ratio were reasonable at 75% and 83% respectively; the sensitivity and specificity of measurement of the medial condyle radiopacity ratio were greater at 83% and 80% respectively.

Changes in thickness of the dorsal cortex of the third metacarpal bone have been studied, especially in young Thoroughbreds (Beccati *et al.*, 2011). Dorsal cortical thickness ratio measurements were performed in chapter three on cadaver bones, similarly to those previously described in horses undergoing exercise (Davies, Gale, and Baker, 1999). Exercise has been shown to result in reduction in cortical bone remodelling and expansion in cortical bone width (McCarthy and Jeffcott, 1992). The mean of the dorsal cortical ratio observed on the current study (1.1) was similar to that previously reported in group of race of Thoroughbred horses (1.18) by Davies, Gale, and Baker (1999) who have reported the dorsal cortex thickness increases in response to training speed and duration. Horses included in this study all had racing careers, but unfortunately there is a lack of available information about training and type of exercise that might influence the cortical thickness between groups. It is likely that all horses encountered similar exercise conditions, potentially explaining the similar cortical thickness ratios across groups.

It was suggested by McCarthy and Jeffcott, (1992) that dorsal cortical thickness in the adult Thoroughbred is relatively larger than in the adult Standardbred and the enlargement of the dorsal cortex is a result of galloping exercise.

In the fourth chapter, a database of clinical radiographs was developed including serial flexed dorsopalmar and lateromedial radiographs were taken at different time points and limited horse and racing data. This database included Thoroughbred horses that sustained a lateral condylar fracture and were therefore catagorised as 'high risk' and control non-fractured horses that raced for a minimum of two years following radiography and did not sustain a fracture. The control group was therefore considered to be at 'low risk' of fracture. The current study compared the condyle opacity, cortical thickness and metaphyseal angle between these high and low risk groups. There was no significant difference in condyle opacity ratio between high and low risk group horses. This finding is not consistent with the finding in cadaver bones of Thoroughbred race horses in chapter three. Chapter 3 evaluated condyle opacity for control, and fractured horses using a 2mm step wedge aluminium phantom as a standard reference to all radiographs. Fakhar *et al.,* (2016) supported measuring pixel intensity on digital images of conventional films by using an aluminium step wedge as the reference for density. The absence of a phantom possibly explains the difference in these results, but the retrospective nature of the clinical study obviously did not allow the use of a phantom. Radio-densitometry was first used to assess bone structures by Morgan *et al.*, in 1967. Yang *et al.*, (1994), investigated the accuracy of radiographic absorptiometry (RA) for examining the bone mineral density of phalanges and metacarpals in their cadaveric study and reported that the radiographic absorptiometry method is precise and accurate for bone mineral assessment of the peripheral appendicular skeleton. Moreover, radiographic absorptiometry in which a standardized hand radiograph is taken with an aluminium step wedge placed on the film. Then bone mineral density is determined by comparing it with the defined density of the aluminium step wedge (Pekkan, Aktas and Pekkan, 2012). Therefore, probably lack of phantom in the longitudinal clinical radiographs had implications on the condyle opacity ratio findings.

An interesting finding of this study was the substantial difference between high risk (fractured) and low risk (control) horses in relation to cortical thickness ratio; high risk horses were demonstrated to have higher cortical thickness. Increased thickness of the dorsal cortex in exercised horses means that the bone is better able to withstand loading of this cortex where very high compressive strains can occur during locomotion (McCarthy and Jeffcott, 1992). This expansion of dorsal thickness is likely due to minimal bone remodelling

in the exercised horses, but extensive modelling as evidenced by the large amount of subperiosteal bone formation and it is lower in unexercised horses (McCarthy and Jeffcott, 1992). The findings of chapter four are in contrast to the findings in cadaver bones, which were reported in chapter three where no significant difference between fractured and control was observed. While the dorsal cortical thickness ratios of both control groups were similar, the dorsal cortical thickness ratio measured in fractured clinical radiographs was greater than that of cadaver bone radiographs. It may be that there may be unknown differences in exercise history, as racing and training increase the diameter of medial and lateral cortices as well as the width of dorsopalmar and lateromedial cortices and these changes can be measured via radiography, allowing assessment of functional adaptation to exercise in the equine skeleton (Beccati *et al.*, 2011). It was reported by Davies and Watson, (2005) that this dorsal thickness of midshaft of metacarpal III has a linear relationship to exercise speed and is thought to be associated with bending magnitude of the bone during each step and consequently leading to fracture. This is supported by a later study of humans that stated that the proximal tibia diaphysis in athletic runners responds to exercise with increases in cortical mass, thickness, diameter, suggesting a progressive adaptation of the bone to additional stresses caused by bending and/or torsion (Feldman *et al.*, 2012). On this theme another study found that thickness of cortical bone in the tibia of jumpers was greater than those of swimmers and controls, suggesting stronger bone against compressive and bending strains (Liu *et al.*, 2003). These observations are consistent with a notion that impact loading (such as jumping) expands periosteal area, whereas active loading (such as swimming) expands endocortical area. In the current study, cortical thickness was evaluated for high risk horses between pre-fracture and post fracture radiographs, and a significant increase over time was identified.

Another aspect of bone geometry that was examined in this study was the metaphyseal angle, referring to the deviation of distal condyle relative to its own diaphysis. This investigation examined whether the angle of the distal condyle of third metacarpal bone is related to the risk of lateral condylar fracture. Unt *et al.*, (2010) reported that conformation in horses is often considered an indicator of athletic ability, performance and resistance to orthopaedic disease. The conformation and alignment of the dorsal hoof wall and metacarpophalangeal joint was investigated by Anderson, McIlwraith and Douay (2004) who reported that for every degree of increase in hind dorsal hoof angle, the risk of effusion in the hind fetlock increased 1.19 times and the risk of hind fetlock problems increased by a factor of 1.14.

In the current study, the distal third metacarpal bone geometry was investigated to evaluate the angle formed by the diaphysis and metaphysis of third distal metacarpal bone. This was inspired by clinical observation (J. Marshall, personal communication) and proximal femur geometry studies describing the prediction of hip fracture risk in humans, where neck–shaft angle between the femoral neck and shaft axes (NSA) was examined by (Gnudi, Sitta and Pignotti, 2012). It was shown that wider femoral neck shaft axes and hip axis length were significant risk factors for hip fractures and correlated with age. The current findings of metaphyseal angle analysis were similar to cortical thickness measurement in Chapters two and three. Firstly, in Chapter two a significant correlation between measurements of metaphyseal angle by radiography and computed tomography ($r=0.73$, $p=0.004$) was found, validating the use of the radiographic measurement technique. Secondly, in Chapter three no significant differences in metaphyseal angle were found between Thoroughbred racehorses which were categorised as control, non fractured and fractured. This finding in cadaver bones suggests that the geometry conformation of distal metacarpal III is not a risk factor for fracture. Increase in joint angulation is observed in horses between standing and walking, walking and trotting, and is more pronounced in high speed (Unt *et al.*, 2010). As the current study examined the geometry of the third metacarpal bone only with absence of the entire metacarpophalangeal joint structures such as sesamoid bones and proximal phalanx, further investigation of the overall geometry of the fetlock and fracture risk may be worthwhile. Finally, in Chapter four measurement of the metaphyseal angle was applied to clinical radiography of the entire metacarpophalangeal joint structure; similar to cortical thickness a significant difference between fractured and control horses was demonstrated. Fractured, high-risk horses had a greater angle than low risk, control horses. This is an agreement with the human literature, that has revealed that neck shaft angle is wider in males with hip fracture than in the controls (Ripamonti, Lisi and Avella, 2014). Alteration in joint angulation has been implicated in osteoarthritis related conditions. In man, knee malalignment is a risk factor for the progression of knee osteoarthritis and cartilage loss or meniscal degeneration, may render the joint less able to handle the forces imposed by a given alignment (Cerejo *et al*. 2002) and increases in knee valgus of 1° have been associated with the risk of lateral compartment cartilage defects in subjects with radiographic changes of osteoarthritis (Felson *et al.*, 2014). Anderson *et al*. (2005) identified several conformation parameters associated with the risk of sustaining a fracture and suffering from joint effusion in the racing Thoroughbred. Increasing metacarpophalangeal joint angle with carpus valgus conformation has been shown to predispose to superficial digital flexor tendon injury (Weller *et al.*, 2006). This may be due to the fact that the forces acting on the musculoskeletal

system during locomotion are not evenly distributed across the limb in the lateromedial direction. Joints angulation appears to play an important role in osteoarthritis progression; varus and valgus malalignment were shown to increase the risk of subsequent medial and lateral knee osteoarthritis development (Cerejo *et al., 2002).* Another aspect of this study was the use of serial radiographs taken prior to and post lateral condylar fracture in Thoroughbred racehorses. Comparison between pre fractured and post fractured metaphyseal angle indicated a significant increase between pre and post fracture. This result does suggest that the metaphyseal angle is dynamic and changes over time, and is an agreement with a 5 years study of post menopausal women where femoral neck shaft angle was investigated, and found to change over the examination period till fracture occurred; widening of femoral neck angle was a significant risk factor for hip fracture (Gnudi, Sitta and Pignotti, 2012). Thus, quantification of musculoskeletal conformation may be an useful tool in selection and management of the racing Thoroughbred (Anderson, McIlwraith and Douay, 2004) in order to reduce injury and subsequent fractures.

In Chapter five, a quantitative CT method was used to determine the maximum density of the distal condyles for control, non-fractured and fractured cadaver metacarpal III bones. A potassium phosphate phantom ($K2HPO_4$)was used to convert Hounsfield units measured using CT images into K_2HPO_4-equivalent bone mineral density values (mg/ml) according to a linear regression line as previously documented in equine metacarpal bones (Les *et al*. 1994). Analysis was performed by first converting DICOM images to mhd format before further examination using the open-source image visualization program known as "Paraview". The density of the lateral and medial parasagittal groove regions was examined because this is the site from which condylar fracture lines originate (Riggs, Whitehouse and Boydet, 1999b). The distal epiphysis of metacarpal III reacts actively to exercise in Thoroughbreds, with significant increases in the volume of trabecular bone resulting in increased condylar density, with only minor effect on cortical bone (Bogers *et al.*, 2016). Increased bone density occurs on the palmar aspect of the condyles and minimally at the sagittal ridge, creating the possibility for development of shear along planes of different densities (Bogers *et al.*, 2014). The results of the current study found no difference between the maximum bone density in the region of the parasagittal groove and adjacent condyle between groups of control, non-fractured and fractured cadaver bones. However, the gradient of change in bone density was not measured. The lack of a significant difference between groups might reflect the prevalence of bone disease; it was suggested that 80% of racing Thoroughbreds presented with osteochondral disease even in the absence of clinical signs (Bani Hassan *et al.*, 2017). The horses in the present study were all over 3 years of age

and had all trained and raced, and this likely yielded bone density distribution in the regions that had been under compression from the sesamoid bones. This finding is similarly observed by Bogers *et al.*, (2014) who examined fractured and non fractured Thoroughbred third metacarpal bones by computed tomography with no significant difference between groups. In a similar finding, a previous study found that horses that are exercising at racing speed, with no history of significant (clinical) shin soreness, may have a similar total bone mass (size x density) in the midshaft of the third metacarpal to those with clinical signs. Another study investigated the differences in subchondral bone volume for training and resting horses with no significant difference found; it was suggested that this was because examinations were confined to only a small proportion of the epiphysis (Holmes *et al.*, 2014) . Therefore, the lack of a detectable difference when measuring the maximum density of a specific region is perhaps not surprising.

In order to determine whether there is a correlation between radiographic and computed tomographic measurement of bone density, the maximum density values were compared to the radiopacity ratios. Poor correlation between maximum density and radiopacity was found for all groups and for both the lateral and medial condyles. This is consistent with the finding of Chapter two, which revealed significant differences in terms of condyle radiopacity and computed tomography measurements. The results of Chapter five likely reflect the difference between methods, with the maximum density representing a single pixel value while the radiograph represents the average of a region of interest. Furthermore, radiography is a two-dimensional representation of a three-dimensional bone and is therefore more representative of the bone overall than a single pixel in a CT image. Subchondral bone sclerosis is considered to be of limited discriminatory capacity in respect to a radiographic diagnosis of osteoarthritis (De Lasalle *et al.*, 2016). Furthermore, Gaschen and Burba (2012) indicated that poor agreement was achieved for detection of proximal phalanx osteochondral fractures and condylar small cracks and lucencies between radiography and CT. Another study examined distal pathology of metacarpal III including subchondral bone sclerosis for age matched Thoroughbreds that sustained catastrophic fracture and controls (O'Brien *et al.*, 2011). This study highlighted that with radiography and CT, articular cartilage pathology does not correlate with visual assessment of subchondral bone. An interesting finding of the current study was the association between maximum condylar density and age. This likely represents the association between age and longer exercise history in Thoroughbred racehorses in training and racing. As training increases, adaptation of the subchondral bone plate leads to sclerosis of trabecular bone in the palmar/plantar aspect of distal metacarpal III or metatarsal III (Dubois *et al.*, 2014).

6.2 Overall Conclusion

The overall conclusion of this thesis focuses on whether radiography can effectively detect early stress changes in the distal metacarpus of Thoroughbred racehorses to potentially identify horses at risk of condylar fracture. The results of the cadaver study suggested that standardised measurement of radiopacity has the potential to differentiate between horses that have suffered a fracture and those that have not. The longitudinal study in Chapter four revealed considerable differences between pre and post fracture measures of bone geometry, namely cortical thickness and metaphyseal angle. However, limitation in the study methodology meant that no differences in radiopacity were found. To sum up, objective measurement of cortical thickness, metaphyseal angle and radiopacity could be performed quickly and easily using radiography and the results of this study suggest that they could be useful in monitoring the response to bone to exercise, and potentially the risk of fracture. Further evaluation of these methods in clinical radiography is therefore warranted to develop methods of predicting and preventing lateral condyle fracture.

6.3 Limitations

A single observer performed the analyses described in this thesis, and no inter-observer validation was performed, In addition, blinding evaluation of specimens and imaging was limited by the obvious differences between groups, e.g. control and fractured horses. However, every effort was made to evaluate radiographs anonymously wherever possible. Exercise plays a important role by inducing stress loading on metacarpal III. Unfortunately, in these studies only very limited information regarding the history of training, exercise and racing of the horses was available and therefore groups could not be not standardised. Moreover, these cadaver bones were permitted to perform only one shoot, due to no previous racing event data images for such bones or horses to compare with against advance in time on exercise or racing . In Chapter four the radiopacity measurements were performed without a radiographic phantom, as a consequence of the retrospective nature of the project. The number of horses limbs adopted in the various parts of this study was relatively low, presenting another limitation that could affect the validity of the results. It may have been useful to perform radiography and physical testing of bone sections, however the bones used in this study were preserved for use in future studies and could not be destroyed.

6.4 Future Work

The results of this study suggest that further work including a prospective study of Thoroughbred racehorses using a dorsoproximal-palmarodistal (20°) oblique radiographic projection including the validated aluminium phantom to determine radiopacity ratio over time is warranted. A prospective study would allow appropriate radiographs to be acquired at regular intervals, and training and medical histories to be acquired for analyses. This would allow for a complete study of the geometry and radiopacity of the third metacarpal bone, and the relationship between exercise, bone morphology, and fracture risk.

Other diagnostic techniques that could be applied to the study of fracture risk include dual- energy X-ray absorptiometry (DEXA) and gadolinium dual photon absorptiometry (DPA). Bone mineral density has been calculated in healthy equine stifles using dual- energy X-ray absorptiometry (DEXA) by De Lasalle *et al.*,(2016), and it might be beneficial to use this technique to examine the third metacarpal bone. However, it could not be performed on standing or conscious horses (Yamada *et al.*, 2016). Adopting gadolinium dual photon absorptiometry for study of the equine metacarpal III mineral density could yield novel information. However, unlike radiography this approach is costly and requires special equipment and knowledge that limits its availability.

List of references

Allen, S. E. *et al.* (2017) 'Description of veterinary events and risk factors for fatality in National Hunt flat racing Thoroughbreds in Great Britain (2000–2013)', *Equine Veterinary Journal*, 49(6), pp. 700–705. doi: 10.1111/evj.12676.

Anderson, T. M., McIlwraith, C. W. and Douay, P. (2004) 'The role of conformation in musculoskeletal problems in the racing Thoroughbred', *Equine Veterinary Journal*, 36 (7), pp. 571–575. doi: 10.2746/0425164044864462.

Baker, W. T. *et al.* (2015) 'Improvement in bilateral carpal valgus deviation in 9 foals after unilateral distolateral radial periosteal transection and elevation', *Veterinary Surgery*, 44(1), pp. 547–550. doi: 10.1111/vsu.12322.

Bani Hassan, E. *et al.* (2017) 'Prevalence of subchondral bone pathological changes in the distal metacarpi/metatarsi of racing Thoroughbred horses', *Australian Veterinary Journal*, 95(10), pp. 362–369. doi: 10.1111/avj.12628.

Bassage, L. H. and Richardson, D. W. (1998) 'Longitudinal fractures of the condyles of the third metacarpal and metatarsal bones in racehorses: 224 cases (1986-1995)', *Journal of American Veterinary Medicine Association*, 212(11), pp. 1757–1764.

Beccati, F. *et al.* (2011) 'Radiographic evaluation of changes in the proximal phalanx of Thoroughbreds in race training', *American Journal of Veterinary Research*, 72(11), pp. 1–7. doi: 10.2460/ajvr.72.11.1482.

Bland, J. and Altman, D. (1999) 'Measuring agreement in method comparison studies', *Statistical Methods in Medical Research*, 8, pp. 135–160.

Boden, L.A. *et al*. (2006) 'Risk of fatality and causes of death of Thoroughbred horses associated with racing in Victoria, Australia: 1989-2004`, *Equine Veterinary Journal*, 38(4), 312–318. https://doi.org/10.2746/042516406777749182.

Bogers, S. H. *et al.* (2014) 'Impact of race training on volumetric bone mineral density and its spatial distribution in the distal epiphysis of the third metatarsal bone of 2-year-old horses', *The Veterinary Journal*, 201(3), pp. 353–358. doi: 10.1016/j.tvjl.2014.06.018.

Bogers, S. H. *et al.* (2016) 'Quantitative comparison of bone mineral density characteristics of the distal epiphysis of third metacarpal bones from Thoroughbred racehorses with or without condylar fracture', *American Journal of Veterinary Research*, 77(1), pp. 32–38. doi: 10.2460/ajvr.77.1.32

Buckland, J. *et al.* (2007) `A 2 year longitudinal radiographic study examining the effect of a bisphosphonate (risedronate) upon subchondral bone loss in osteoarthritic knee patients`, *Rheumatology*, 46(2), pp:257–264.

Butler, J. *et al.* (2011) 'The metacarpal and metatarsal regions', in *Clinical radiology of the horse*, 3rd edn, John Wiley & Sons, Oxford, pp. 189–232.

Carrier, T. K. *et al.* (1998) 'Association between long periods without high-speed workouts and risk of complete humeral or pelvic fracture in Thoroughbred racehorses: 54 cases (1991-1994)', *Journal of American Veterinary Medicine Association*, 212(10), pp. 1582–1587.

Cerejo,R. *et al.* (2002) 'The influence of alignment on risk of knee osteoarthritis progression according to baseline stage of disease', *Arthritis and Rheumatism Journal*, 46, (10), pp 2632–2636, doi: 10.1002/art.10530

Clayton, H. M. *et al.* (1998) 'Net joint moments and powers in the equine forelimb during the stance phase of the trot', *Equine Veterinary Journal*, 30(5), pp. 384–389. doi: 10.1111/j.2042-3306.1998.tb04505.x.

Cogger, N. *et al.* (2008) 'Incidence rate of musculoskeletal injuries and determinants of time to recovery in young Australian Thoroughbred racehorses', *Australian Veterinary Journal*, 86(12), pp. 473–480. doi: 10.1111/j.1751-0813.2008.00359.x.

Cohen, N. D. *et al.* (1999) 'Results of physical inspection before races and race-related characteristics and there association with musculoskeletal injuries in Thoroughbreds during races', *Journal of American Veterinary Medicine Association*, 215(5), pp. 654–661.

Cruz, A. M. *et al.* (2007) 'Epidemiologic characteristics of catastrophic musculoskeletal injuries in Thoroughbred racehorses', *American Journal of Veterinary Research*, 68(12), pp. 1370–1375. doi: 10.2460/ajvr.68.12.1370.

Currey, J. D. (2003) ‘How well are bones designed to resist fracture?’, *Journal of Bone and Mineral Research*, 18(4), pp. 591–598. doi: 10.1359/jbmr.2003.18.4.591.Davies, H., Gale, S. and Baker, I. (1999) ‘Radiographic measures of bone shape in young thoroughbreds during training for racing’, *Equine Veterinary Journal, 30, Supplement*, 31, pp. 262–265. doi: 10.1111/j.2042-3306.1999.tb05231.x.

Davies, H. M. S. (2002) ‘Dorsal metacarpal cortex ultrasound speed and bone size and shape’, *Equine Veterinary Journal, 34, Supplement*, 34, pp. 337–339.

Davies, H. M. S. and Watson, K. M. (2005) ‘Third metacarpal bone laterality asymmetry and midshaft dimensions in Thoroughbred racehorses’, *Australian Veterinary Journal*, 83(4), pp. 224–226. doi: 10.1111/j.1751-0813.2005.tb11657.x.

Dinçel, V. E. *et al.* (2008) ‘The association of proximal femur geometry with hip fracture risk’, *Clinical Anatomy*, 21(6), pp. 575–580. doi: 10.1002/ca.20680.

Dobbs, M. and Morcuende, J. (1986) ‘Other conditions of the hip’ (2), in Lowell, W. W. and Winter, R. B. (eds), *Pediatric Orthopedics*, J. B. Lippincott Company, Philadelphia, pp. 1222-1260.

Dubois, M.S. *et al.* (2014) ‘Computed tomographic imaging of subchondral fatigue cracks in the distal end of the third metacarpal bone in the thoroughbred racehorse can predict crack micromotion in an ex-vivo model’, *PloS one*, 9(7), pp. e101230. doi: 10.1371/journal.pone.0101230.

Dymock, D. C. and Pauwels, F. E. T. (2012) ‘Investigation into the morphology of the third metacarpal bone in the horse’, *New Zealand Veterinary Journal*, 60(4), pp. 223–227. doi: 10.1080/00480169.2011.651056.

Dyson, P. K. *et al.* (2008) ‘Days lost from training by two and three year old Thoroughbred horses: A survey of seven UK training yards’, *Equine Veterinary Journal*, 40(7), pp. 650–657. doi: 10.2746/042516408X363242.

Ellis, D. R. (1994) ‘Some observations on condylar fractures of the third metacarpus and third metatarsus in young thoroughbreds’, *Equine Veterinary Journal*, 26(3), pp. 178–183. doi: 10.1111/j.2042-3306.1994.tb04365.x.

Fakhar, H. B. *et al.* (2016) 'A comparison of radiographic film densitometry using a new computerized tool with a digital densitometer', *Journal of Dentistry*, 13(4), pp. 252–260.

Feldman, S. *et al.* (2012) 'Site and sex effects on tibia structure in distance runners and untrained people', *Medicine and Science in Sports and Exercise*, 44(8), pp. 1580–1588. doi: 10.1249/MSS.0b013e31824e10b6.

Felson, D. T. *et al.* (2014) 'Valgus malalignment is a risk factor for lateral knee osteoarthritis incidence and progression: findings from most and the osteoarthritic Initiative', *Arthritis and Rheumatology*, 65(2), pp. 355-362. doi: 10.1002/art.37726

Firth, E. C. *et al.* (2005) 'Musculoskeletal response of 2-year-old Thoroughbred horses to early training. Conclusions', *New Zealand Veterinary Journal*, 53(6), pp. 377–383.

Firth, E. C. *et al.* (2011) 'Mild exercise early in life produces changes in bone size and strength but not density in proximal phalangeal, third metacarpal and third carpal bones of foals', *The Veterinary Journal*, 190(3), pp. 383-389. doi: 10.1016/j.tvjl.2010.11.016.

Gaschen, L. and Burba, D. J. (2012) 'Musculoskeletal injury in Thoroughbred racehorses. correlation of findings using multiple imaging modalities', *Veterinary Clinics of North America - Equine Practice*, 28(3), pp. 539–561. doi: 10.1016/j.cveq.2012.09.005.

Gnudi, S. *et al.* (2004) 'Differences in proximal femur geometry distinguish vertebral from femoral neck fractures in osteoporotic women', *British Journal of Radiology*, 77(915), pp. 219–223. doi: 10.1259/bjr/79551075.

Gnudi, S., Sitta, E. and Pignotti, E. (2012) 'Prediction of incident hip fracture by femoral neck bone mineral density and neck-shaft angle: A 5-year longitudinal study in post-menopausal females', *British Journal of Radiology*, 85(1016), pp. 467–473. doi: 10.1259/bjr/57130600.

Harrison, S. M. *et al.* (2014) 'Evaluation of a subject-specific finite-element model of the equine metacarpophalangeal joint under physiological load', *Journal of Biomechanics*. 47(1), pp. 65–73. doi: 10.1016/j.jbiomech.2013.10.001.

Hill, A. E. *et al.* (2015) 'Non-fatal injury occurrence in Southern California Thoroughbred racehorses 2009-2010', *The Veterinary Journal*, 205(1), pp. 98–100. doi: 10.1016/j.tvjl.2015.04.001.

Hill, A. E. *et al.* (2016) 'Prevalence, location and symmetry of noncatastrophic ligamentous suspensory apparatus lesions in California Thoroughbred racehorses, and association of these lesions with catastrophic injuries', *Equine Veterinary Journal*, 48(1), pp. 27–32. doi: 10.1111/evj.12367.

Holmes, J. M. *et al.* (2014) 'Thoroughbred horses in race training have lower levels of subchondral bone remodelling in highly loaded regions of the distal metacarpus compared to horses resting from training', *The Veterinary Journal*. 202(3), pp. 443–447. doi: 10.1016/j.tvjl.2014.09.010.

Jacklin, B. D. and Wright, I. M. (2012) 'Frequency distributions of 174 fractures of the distal condyles of the third metacarpal and metatarsal bones in 167 Thoroughbred racehorses (1999-2009)', *Equine Veterinary Journal*, 44(6), pp. 707–713. doi: 10.1111/j.2042-3306.2012.00558.x.

Johnson, B. J. *et al.* (1994) 'Causes of death in racehorses over a 2 year period', *Equine Veterinary Journal*, 26(4), pp. 327–330. doi: 10.1111/j.2042-3306.1994.tb04395.x.

Kane, A. J. *et al.* (1996) 'Horseshoe characteristics as possible risk factors for fatal musculoskeletal injury of Thoroughbred racehorses', *American Journal of Veterinary Research*, 57(8), pp. 1147–1152.

Kawcak, C. E. *et al.* (1999) 'Effects of third metacarpal geometry on the incidence of condylar fractures in Thoroughbred racehorses', in *Proceedings of 55th Annual Convention of the American Association of Equine Practitioners*, p. 197.

De Lasalle, J. *et al.* (2016) 'Comparisons among radiography, ultrasonography and computed tomography for ex vivo characterization of stifle osteoarthritis in the horse', *Veterinary Radiology and Ultrasound*, 57(5), pp. 489–501. doi: 10.1111/vru.12370.

Le Jeune, S. S. *et al.* (2003) 'Biomechanical investigation of the association between suspensory ligament injury and lateral condylar fracture in thoroughbred racehorses', *Veterinary Surgery*, 32(6), pp. 585–597. doi: 10.1053/jvet.2003.50071.

Les, L.M., *et al.* (1994) 'Estimation of material properties in the equine metacarpus with use of quantitative computed tomography', *Journal of Orthopaedic Research*, 12(6), pp. 822-833.

Les, L.M. *et al.* (2002) 'Stiff and strong compressive properties are associated with brittle post yield behavior in equine conipact bone material', *Journal of Orthopaedic Research*, 20(3), pp. 607-614.

Liu, L. *et al.* (2003) 'Effects of physical training on cortical bone at midtibia assessed by peripheral quantitative computed tomography', *Journal of Applied Physiology*, 95(1), pp. 219–224. doi: 10.1152/japplphysiol.01055.2002.

Loughridge, A. *et al.* (2017) 'Qualitative assessment of bone density at the distal articulating surface of the third metacarpal in Thoroughbred racehorses with and without condylar fracture', *Equine Veterinary Journal*, 49(2), pp. 172-177. doi: 10.1111/evj.12544.

Maeda, Y. *et al.* (2011) 'Comparison of femoral morphology and bone mineral density between femoral neck fractures and trochanteric fractures', *Clinical Orthopaedics and Related Research*, 469(3), pp. 884–889. doi: 10.1007/s11999-010-1529-8..

Maeda, Y., Hanada, M., and Oikawa M. (2016) 'Epidemiology of racing injuries in Thoroughbred racehorses with special reference to bone fractures: Japanese experience from the 1980s to 2000s', *Journal of Equine Science*, 27(3), pp. 81–97. doi: 10.1294/jes.27.81.

Martig, S. *et al.* (2014) 'Bone fatigue and its implications for injuries in racehorses', *Equine Veterinary Journal*, 46(4), pp. 408–415. doi: 10.1111/evj.12241.

Mather, J. *et al.* (2013) 'Proximal humerus cortical bone thickness correlates with bone mineral density and can clinically rule out osteoporosis', *Journal of Shoulder and Elbow Surgery*, 22(6), pp. 732–738. doi: 10.1016/j.jse.2012.08.018.

McCarthy, R. N. and Jeffcott, L. B. (1992) ‘Effects of treadmill exercise on cortical bone in the third metacarpus of young horses’, *Research in Veterinary Science*, 52(1), pp. 28–37. doi: 10.1016/0034-5288(92)90054-6.

Merritt, J. S. *et al.* (2010) ‘Mechanical loading of the distal end of the metacarpal bone in horses during walking and trotting’, *American Journal of Veterinary Research*, 71(5), pp. 508–514. doi: 10.2460/ajvr.71.5.508

Merritt, J.S. and Davies, H.M. (2010) ‘Metacarpal geometry changes during Thoroughbred race training are compatible with sagittal plane cantilever bending’, *Equine Veterinary Journal, 42, Supplement* 38, pp.407-411. doi: 10.1111/j.2042-3306.2010.00209.x

Mohammed, H. O., Hill, T. and Lowe, J. (1991) ‘Risk-factors associated with injuries in Thoroughbred horses’, *Equine Veterinary Journal*, 23(6), pp. 445–448.

Morgan, D.B, *et al,*.(1967) ‘The amount of bone in the metacarpal and the phalanx according to age and sex’, *Clinical Radiology*, 18(1), pp. 101-108.

Morgan, J. W. *et al.* (2006) ‘Comparison of radiography and computed tomography to evaluate metacarpo/metatarsophalangeal joint pathology of paired limbs of thoroughbred racehorses with severe condylar fracture’, *Veterinary Surgery*, 35(7), pp. 611–617. doi: 10.1111/j.1532-950X.2006.00198.x.

Muir, P. *et al.* (2006) ‘Role of endochondral ossification of articular cartilage and functional adaptation of the subchondral plate in the development of fatigue microcracking of joints’, *Bone*, 38(3), pp. 342–349. doi: 10.1016/j.bone.2005.08.020.

Muir, P. *et al.* (2008) ‘Exercise-induced metacarpophalangeal joint adaptation in the Thoroughbred racehorse’, *Journal of Anatomy*, 213(6), pp. 706–717. doi: 10.1111/j.1469-7580.2008.00996.x.

Noble, P., Singer, E. R. and Jeffery, N. S. (2016) ‘Does subchondral bone of the equine proximal phalanx adapt to race training?’, *Journal of Anatomy*, 229(1), pp. 104–113. doi: 10.1111/joa.12478.

O'Brien, T., *et al.* (2011) 'Detection of articular pathology of the distal aspect of the third metacarpal bone in Thoroughbred racehorses: comparison of radiography, computed tomography and magnetic resonance imaging', *Veterinary Surgery*, 40(8), p. n/a-n/a. doi: 10.1111/j.1532-950X.2011.00881.x..

Omoumi, P. *et al.* (2017) 'Quantitative regional and sub-regional analysis of femoral and tibial subchondral bone mineral density (sBMD) using computed tomography (CT): Comparison of non-osteoarthritic (OA) and severe OA knees', *Osteoarthritis and Cartilage*, 25(11), pp. 1850–1857. doi: 10.1016/j.joca.2017.07.014.

Parker, R. A. *et al.* (2010) 'Quantitative evaluation of subchondral bone injury of the plantaro-lateral condyles of the third metatarsal bone in Thoroughbred horses identified using nuclear scintigraphy: 48 cases', *Equine Veterinary Journal*, 42(6), pp. 552–557. doi: 10.1111/j.2042-3306.2010.00088.x.

Parkin, T. D. *et al.* (2004a) 'Race- and course-level risk factors for fatal distal limb fracture in racing Thoroughbreds', *Equine Veterinary Journal*, 36(6), pp. 521–526.

Parkin, T. D. *et al*.(2004b) 'Risk of fatal distal limb fractures among Thoroughbreds involved in the five types of racing in the United Kingdom', *The Veterinary Record*, 154(16), pp. 493–497. doi: 10.1136/vr.154.16.493.

Parkin, T. D. *et al.* (2005) 'Risk factors for fatal lateral condylar fracture of the third metacarpus/metatarsus in UK racing', *Equine Veterinary Journal*, 37(3), pp. 192–199. doi: DOI: 10.2746/0425164054530641.

Parkin, T. D. *et al.* (2006) 'Catastrophic fracture of the lateral condyle of the third metacarpus/metatarsus in UK racehorses - fracture descriptions and pre-existing pathology', *The Veterinary Journal*, 171(1), pp. 157–165. doi: 10.1016/j.tvjl.2004.10.009.

Pekkan, G., Aktas, A. and Pekkan, K. (2012) 'Comparative radiopacity of bone graft materials', *Journal of Cranio-Maxillofacial Surgery*, 40(1), pp. e1–e4. doi: 10.1016/j.jcms.2011.01.018.

Peloso, J. G., Mundy, G. D. and Cohen, N. D. (1994) 'Prevalence of and factors associated with musculoskeletal racing injuries of Thoroughbreds', *Journal of American Veterinary Medical Association*, 204 (4), pp. 620-626.

Peloso, J. G. et al, (2015) 'Association of catastrophic biaxial fracture of the proximal sesamoid bones with bony changes of the metacarpophalangeal joint identified by standing magnetic resonance imaging in cadaveric forelimbs of Thoroughbred racehorses', *Journal of American Veterinary Medical Association*, 246(6), pp. 661-673. doi: 10.2460/javma.246.6.661

Radtke, C. L. *et al.* (2003) 'Macroscopic changes in the distal ends of the third metacarpal and metatarsal bones of Thoroughbred racehorses with condylar fractures', *American Journal of Veterinary Research*, 64 (9), pp. 1110-1116.

Ramzan, P. H. and Palmer, L. (2011) 'Musculoskeletal injuries in Thoroughbred racehorses: a study of three large training yards in Newmarket, UK (2005-2007)', *The Veterinary Journal*, 187(3), pp. 325–329. doi: 10.1016/j.tvjl.2009.12.019.

Ramzan, P. H., Palmer, L. and Powell, S. E. (2015) 'Unicortical condylar fracture of the Thoroughbred fetlock: 45 cases (2006-2013)', *Equine Veterinary J*ournal 47(6), pp. 680–683. doi: 10.1111/evj.12349.

Reed, S. R. *et al.* (2013) 'Exercise affects joint injury risk in young Thoroughbreds in training', *The Veterinary Journal*, 196(3), pp. 339–344. doi: 10.1016/j.tvjl.2012.11.014.

Richardson, D. W. (2012) 'Third metacarpal and metatarsal bones', in Auer, J. A. and Stick, J. A. (eds), *Equine Surgery*, 4th edition, Elsevier, St Lous, pp. 1325–1338.

Rick, M. *et al.* (1983) 'Condylar fractures of the third metacarpal and third metatarsal bone in 75 horses: Radiographic features, treatments, and outcome', *Journal of American Veterinary Medicine Association*, 183(3), pp. 287–296.

Riggs, C. M. (1999) 'Aetiopathogenesis of parasagittal fractures of the distal condyles of the third metacarpal and third metatarsal bones- review of the literature', *Equine Veterinary Journal*, 31(2) pp. 116–120.

Riggs, C. M., Whitehouse, G. H. and Boyde, A. (1999a) 'Structural variation of the distal condyles of the third metacarpal and third metatarsal bones in the horse', *Equine Veterinary Journal*, 31(2), pp. 130–139.

Riggs, C. M., Whitehouse, G. H. and Boyde, A. (1999b) 'Pathology of the distal condyles of the third metacarpal and third metatarsal bones of the horse', *Equine Veterinary Journal*, 31(2), pp. 140–148. doi: 10.1111/j.2042-3306.1999.tb03807.x.

Ripamonti, C., Lisi, L. and Avella, M. (2014) 'Femoral neck shaft angle width is associated with hip-fracture risk in males but not independently of femoral neck bone density', *British Journal of Radiology*, 87, 20130358. doi: 10.1259/bjr.20130358.

Rosanowski, S. M. *et al.* (2017) 'Descriptive epidemiology of veterinary events in flat racing Thoroughbreds in Great Britain (2000 to 2013)', *Equine Veterinary Journal*, 49(3), pp. 275–281. doi: 10.1111/evj.12592.

Santschi, E. M. (2008) 'Articular fetlock injuries in exercising horses', *Veterinary Clinics of North America - Equine Practice*, 24(1), pp. 539–561. doi: 10.1016/j.cveq.2007.11.011

Sherman K.M *et al.* (1995) 'The effect of training on equine metacarpal bone breaking strength', *Equine Veterinary Journal*, 27(2), pp.135–139.

Smith, R. K. W. *et al.* (2002) 'The influence of ageing and exercise on tendon growth and degeneration - Hypotheses for the initiation and prevention of strain-induced tendinopathies', *Comparative Biochemistry and Physiology - A Molecular and Integrative Physiology*, 133(4), pp. 1039–1050. doi: 10.1016/S1095-6433(02)00148-4.

Stepnik, M. W. *et al.* (2004) 'Scanning electron microscopic examination of third metacarpal/third metatarsal bone failure surfaces in Thoroughbred racehorses with condylar fracture', *Veterinary Surgery*, 33(1), pp. 2–10. doi: 10.1111/j.1532-950x.2004.04007.x.

Tranquille, C. A., Parkin, T. D. and Murray, R. C. (2012) 'Magnetic resonance imaging-detected adaptation and pathology in the distal condyles of the third metacarpus, associated with lateral condylar fracture in Thoroughbred racehorses', *Equine Veterinary Journal*, 44(6), pp. 699–706. doi: 10.1111/j.2042-3306.2011.00535.x.

Trope, G. D., Anderson, G. A. and Whitton, R. C. (2011) 'Patterns of scintigraphic uptake in the fetlock joint of Thoroughbred racehorses and the effect of increased radiopharmaceutical uptake in the distal metacarpal/tarsal condyle on performance', *Equine Veterinary Journal*, 43(5), pp. 509–15. doi: 10.1111/j.2042-3306.2010.00316.x.

Trope, G. D. *et al.* (2015) 'Can high-resolution peripheral quantitative computed tomography imaging of subchondral and cortical bone predict condylar fracture in Thoroughbred racehorses?', *Equine Veterinary Journal*, 47(4), pp. 428-432. doi: 10.1111/evj.12312

Unt, V. E. *et al.* (2010) 'Variation in frontal plane joint angles in horses', *Equine Veterinary Journal*, 42, Supplement 38, pp. 444–450. doi: 10.1111/j.2042-3306.2010.00192.x.

Verheyen, K. *et al.* (2006) 'Exercise distance and speed affect the risk of fracture in racehorses', *Bone*, 39(6), pp. 1322–1330. doi: 10.1016/j.bone.2006.05.025.

Waite, K. L. and Nielsen, B. D. and Rosenstein, D.S. (2000) 'Computed tomography as a method of estimating bone mineral content in horses', *Equine Veterinary Journal*,. 20(1), pp. 49–52.

Walker, W. T., Kawcak, C. E. and Hill, A. E. (2013) 'Medial femoral condyle morphometrics and subchondral bone density patterns in Thoroughbred racehorses' *American Journal of Veterinary Research*,74(5), pp. 691–699.

Weller, R. *et al.* (2006) 'The effect of conformation on orthopaedic health and performance in a cohort of National Hunt racehorses: preliminary results', *Equine Veterinary Journal*, 38(7), pp. 622–627. doi: 10.2746/042516406X159034.

Whitton, R. C. *et al.* (2010) 'Third metacarpal condylar fatigue fractures in equine athletes occur within previously modelled subchondral bone', *Bone*, 47(4), pp. 826–31. doi: 10.1016/j.bone.2010.07.019.

Yamada, K. *et al.* (2016) 'Experimental investigation of bone mineral density in Thoroughbreds using quantitative computed tomography Experimental investigation of bone mineral density in Thoroughbreds using quantitative computed tomography', *Journal of Equine Science*, 26(3), pp. 81–87.doi: 10.1294/jes.26.81.

Yang, S.O *et al*. (1994) ‘Radiographic absorptiometry for bone mineral measurement of the phalanges: precision and accuracy study’, *Radiology*, 192(3), pp. 857-859.

Young, B. D. *et al.* (2007) ‘Subchondral bone density and cartilage degeneration patterns in osteoarthritic metacarpal condyles of horses’, *American Journal of Veterinary Research*, 68(8), pp. 841-849.

Zekas, L. J. *et al.* (1999) ‘Results of treatment of 145 fractures of the third metacarpal/metatarsal condyles in 135 horses (1986-1994)’, *Equine Veterinary Journal*, 31(4), pp. 309–313. doi: 10.1111/j.2042-3306.1999.tb03822.x.